Theresa Ebner, BSc

Fracture Toughness of Paper

Master Thesis

to achieve the university degree of

Diplom-Ingenieur

Master's Degree Program: Chemical and Process Engineering

submitted to **Graz University of Technology**

Supervisor:

Univ.-Prof. Dipl.-Ing. Dr.techn. Ulrich Hirn

Institute of Biobased Products and Paper Technology

Graz, August 2023

AFFIDAVIT

I declare that I have authored this thesis independently, that I have not used other than the declared sources/resources, and that I have explicitly indicated all material which has been quoted either literally or by content from the sources used. The text document uploaded to TUGRAZonline is identical to the present master‘s thesis.

22.08.2023 .....

(date)

.....

(signature)

Acknowledgment

I would first like to thank my supervisor Ulrich for the support throughout the master thesis and my advisors from Mercer and Omya GmbH Frank and Johannes for the guidance. Their expertise and encouragement helped me to complete this research and write this thesis.

I also want to thank the laboratory staff at the Institute of Paper, Pulp and Fiber Technology, especially Heidi for supporting me during the trials and always have an answer to my questions.

I would also like to thank my colleagues at the Institute for their support and making my time at the Institute enjoyable.

Finally, I am deeply thankful to my friends and family for their love and support during my studies. Without their encouragement and motivation, I would not have been able to complete this journey.

Abstract

The ambition for this master thesis was to understand how the mechanical properties fracture toughness, tensile strength and tear behave different in reference to refining and filler content. The research question was: Can fracture toughness be compared to tensile strength or tear, or is it a completely different parameter? To answer that, two main-trials were performed. In the first main-trial the impact of refining was analyzed. For this, pulp was refined with two lab refiners, to simulate an industrial refining at different specific refining energies, and with a PFI mill at different revolutions. For the second main-trial a variation of filler content and a constant amount of retention agent were added to the pulp. The filler content was increased up to 30 % during the trial. For every experimental point handsheets were made and a tensile test, a notched tensile test and a tearing resistance test Elmendorf were performed. The analysis show, that fracture toughness, tensile strength and tear in fact are different parameter. However, the notched tensile strength from the notched tensile test and the tensile strength from the tensile test correlates almost perfectly. Because of the duplication of effort for the notched tensile test an addition of fracture toughness to the standard paper parameter is not required.

Contents

1 Motivation

Motivation of the master thesis was the understanding of how the mechanical property fracture toughness behaves differently from tear and tensile strength. This should be observed in relation to the impact of refining and the impact of filler. Another question was to get to understand the measuring method and to evaluate in detail how fracture toughness can be determined. For this, the reproducibility and handling of the measuring instrument must be investigated.

2 Introduction

2.1 Fracture toughness definition [J/m]

Fracture toughness is a fundamental mechanical property of the material and is described as the ability to resist propagation of a pre-existing crack. [1]

The stresses and strain appearing close to the crack tip can be characterized by J. This can be seen in Figure 2-1: Stress and strain at the crack tip. To start a crack growth, the fracture criterium J_{cr} must be smaller or equal to J. The fracture criterium is called fracture toughness and has the unit J/m² (Equation (2.1)). [2] [3]

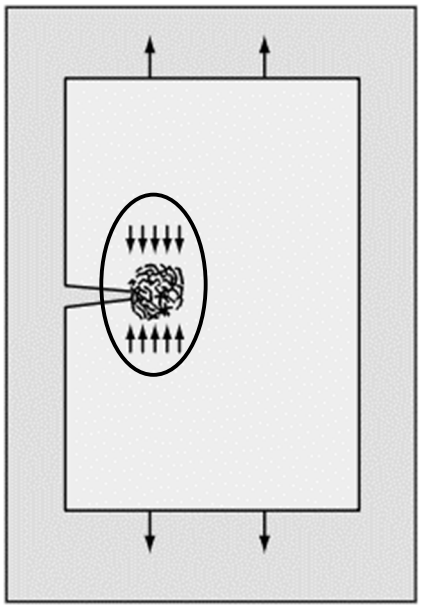

Figure 2-1: Stress and strain at the crack tip [2]

$$J_{cr} \leq J \qquad (2\text{-}1)$$

Fracture toughness can then be described as the needed fracture energy dU [J] to receive the fracture crack area dA [m²] (Figure 2-2: Fracture area dA received during fracture., Equation (2-2)). According to the standard ISO test method for paper fracture toughness has the unit

J/m. This is simply achieved by multiplying fracture toughness with the paper thickness t, which leads to a new definition for fracture toughness. It can now be described as the needed fracture energy *dU* to receive the fracture length *da* (Figure 2-3, Equation (2-3)). [1]

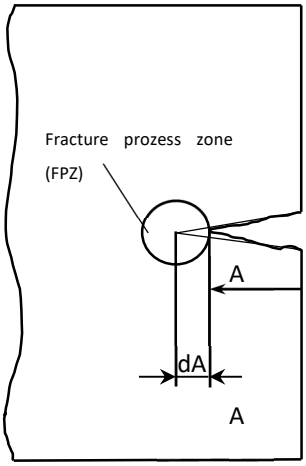

Figure 2-2: Fracture area dA received during fracture.

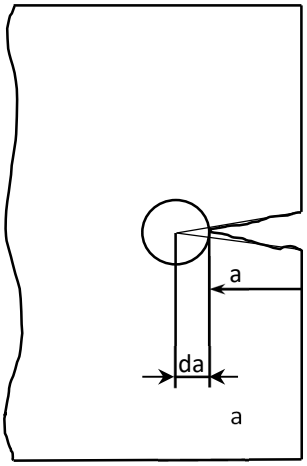

Figure 2-3: Fracture length da received during fracture.

$$J_{cr} = -\frac{dU}{dA} \qquad (2\text{-}2)$$

$$J_c = -\frac{dU}{da} \qquad (2\text{-}3)$$

When comparing the three mechanical properties fracture toughness, tear, and tensile strength, two different tearing modes are used. The in-plane tearing force, which is used for the tensile test and the notched tensile test, and the out-of-plane tearing force, which is used for the tearing resistance test Elmendorf. This makes clear, that the loading modes for the tear test and the fracture toughness are different and, hence, these tests are expected to quantify rather different material properties.

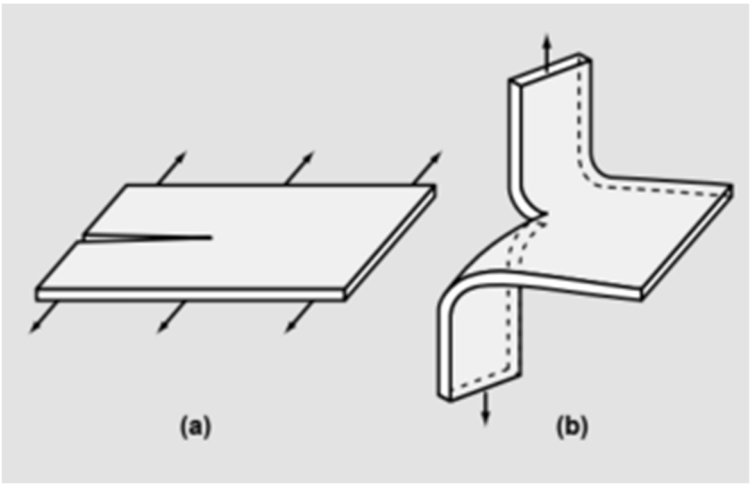

Figure 2-4: Tearing modes used for comparison of facture toughness (a), tensile strength (a), and tearing resistance test (b) [2]

2.2 Fracture toughness determination according to ISO/TS 17958

Fracture toughness is here determined in three steps:

- Step (1): standard tensile test where the material tensile behavior without pre-damage (crack) is evaluated. The tensile test is performed according to ISO 1924-3 with test pieces of 15 mm in width and 100 mm in length.
- Step (2): notched tensile test where the material tensile behavior with pre-damage (crack) is evaluated. It is performed according to the same ISO standard as the tensile test (50 mm in width, 100 mm in length) with one difference. The test pieces also have a center notch with a length of 20 mm.(Figure 4-3)
- Step (3): Calculation of the fracture toughness from the material behavior of step (1) and step (2). The determination occurs according to ISO/TS 17958.

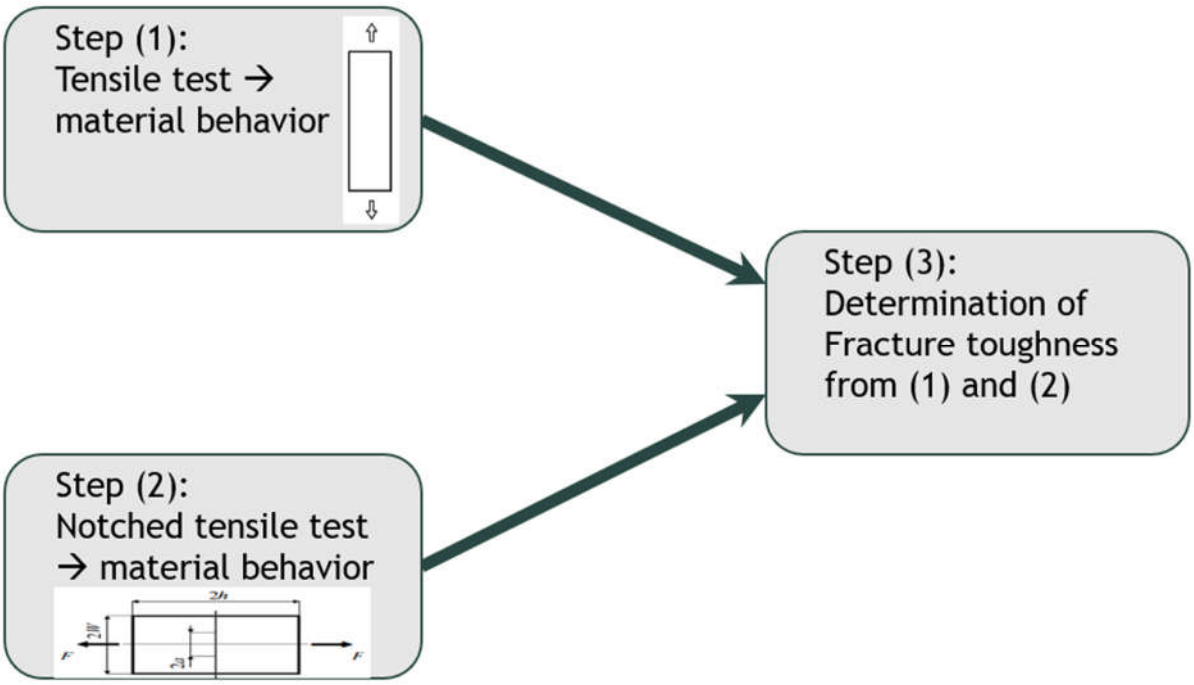

Figure 2-5: Determination of fracture toughness in three steps

3 Theoretical background

3.1 Fracture mechanics

Within solid mechanics the discipline of dealing with strength of structures containing defects is called fracture mechanics. It is of fundamental interest for preventing failures of paper in converting and end-use, as well as in designing material properties for applications where controlled failure is needed (e.g., creasing, and folding operations in paper converting). The strength of a notched structure is influenced by the three principal factors: the loading situation,

the geometry of the structure and the fracture toughness (Figure 3-1). Here, the geometry of the structure includes the size and shape of defects. Fracture mechanics describe the relation of these three factors and if two of them are known, the third can be calculated. [4] [5]

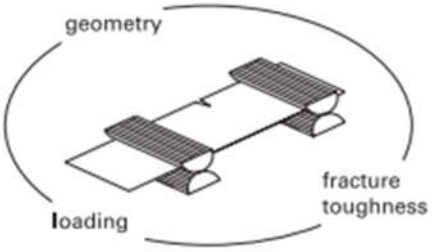

Figure 3-1: Influencing factors of strength of a notched structure [5]

3.1.1 Paper failure

In technical language, the word failure means “failure to perform the intended function”. For example, a curled sheet that jams in a photocopier has failed its function. If a material separates in two or more pieces this particular mode of failure is called fracture. As efforts to lower costs by decreasing basis weight or using more filler material, the issue of sheet fracture will remain a key factor in paper design. There are four places in which a fracture can occur:

- On the paper machine (wet end failure): in the first open draw, in the press section, in the dryer section and in the winding/rewinding operations.
- During converting (pressroom runnability): in the printing press, in box-making operations, in operations such as folding and slitting.
- During filling and transportation of sack paper.
- In service, i.e., during utilization of the paper product: directory, sack kraft, tissue, etc.

To predict and prevent fracture a correlation between the fracture, material properties, applied load and displacements must be found. [6] [2]

Back in the 1920s it was already known that the strength of a cracked paper structure was a property not necessarily connected directly to other mechanical properties. This knowledge led to the development of the out-of-plane tear tests Elmendorf and Brecht-Imset. Nowadays we know that defects influence the integrity of structures primarily under tensile loading, which is the main focus in the discipline of fracture mechanics. For example, a 10 mm long cut on the edge of a typical office paper sheet reduces the failure load to one-half and the failure elongation to one-third of the original. To avoid macroscopical breaks of the structure the external stress must be small enough, then the defect is stable. If the external stress is increasing, damage will accumulate mostly around the defect and can lead to rupture of the structure. These defects can also affect the performance of the paper products. [4] [5]

The deformation of a defect under loading is defined in the general deformation and the relative deformation. The general deformation is described by the displacements of two crack surfaces relative to one another. The relative displacement can be described as the crack propagation in different modes. Mode I is in-plane and mode III are out-of-plane tearing, and mode II is transverse shear as shown in Figure 3-2. An example for an out-of-plane tearing force is the Elmendorf tear test. Notched tensile tests and tensile strength tests are typical examples for in-plane tearing forces. [4] [2]

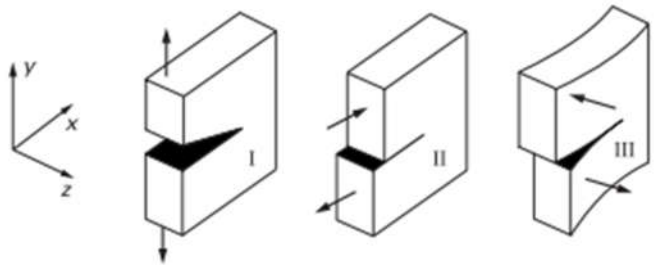

Figure 3-2: Different crack propagation in paper under mode I in-plane, mode II transverse shear and mode III out-of-plane tearing forces [5]

3.1.2 Web breaks

Even though web breaks are a rare event with a break rate of 1-2 %, i.e., 1 to 2 breaks per 100 paper rolls, they are a major runnability issue in many pressrooms. Web breaks are mostly caused by defects, which function as weak spots in the paper web or the sources of stress concentration. Normally defects are classified into two categories. The macroscopically visible defects or macro defects, such as holes, cuts, thin/thick spots, burst, wrinkles and shives, and the natural disorder of paper, such as formation and local fiber orientation. [7]

To research the first category, macro defects, Uesaka and Ferahi [8] were using a fracture mechanics model for typical newsprint rolls, where they assumed that each roll contains a single crack in CD either in the center or on the edge of the roll. In this work they used a length from about 40 mm for the edge crack and about 80 mm for the center crack length. The press room tension is kept constant. Figure 3-3 shows the damaging effect on web breaks of the differently located cracks. The edge cracks have a more damaging effect than the center cracks, which sometimes are snapped off at the roll edge, and can cause a web break. The constant press room tension and the very large critical crack length (40 mm and 80 mm), predicts that it is rare to have such macro defect-driven web breaks. [7]

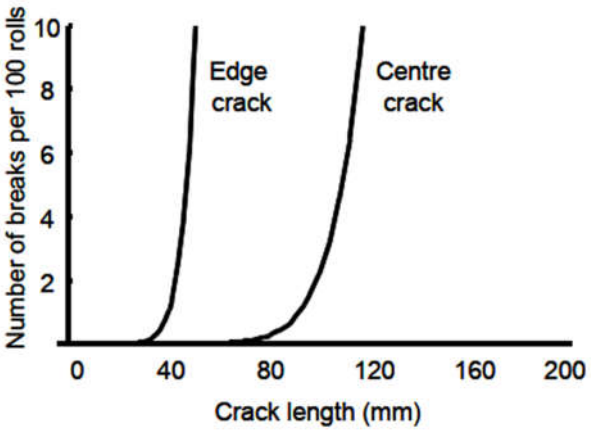

Figure 3-3: Number of breaks per 100 rolls as a function of crack length [7] [8]

Another macro defect, which was not considered in the model above, are shives. In an experiment Sears et al. [9] found evidence that 98,5 % of more than 3200 breaks are due to shives. Especially shives longer than 4 mm with a thickness equal to a considerable fraction of the web thickness are the weak spots which lead to web breaks. Most problematic are hard shives after calendering creating cracks and cuts in the web. It should be noted, that over the last 40 years the shive content in mechanical printing grades has been reduced dramatically, which results in rare observations of shive-induced breaks in the pressroom. [7]

Due to the rare macro defect-driven web breaks the cause of tension variations have been investigated. Larsson [10] indicated a web tension variation from 200 N/m to 600 N/m at different sections of a press unit and variations as a function of time. The tension variations a paper web undergoes moving in the press room is described by the maximum tension T_{max} [N/m] and is given in Equation (3-1). The maximum tension T_{max} equals the set tension T_0 [N/m] in the press room plus the maximum of the deviation of tension ΔT_{max} [N/m] from the mean value. Equivalently this is the elastic modulus in MD ε_{MD} [%] multiplied by the maximum of the strain deviation $\Delta\varepsilon_{max}$ [%]. ΔT_{max} and $\Delta\varepsilon_{max}$ depends on where in the press room it is measured.

$$T_{max} = T_0 + \Delta T_{max} = T_0 + E_{MD}\Delta\varepsilon_{max} \tag{3-1}$$

$$n_{100} = 100\ ln2\ \frac{A_{roll}}{A_{ref}}\left[\left(\frac{T_0}{T_{MD}} + \frac{\Delta\varepsilon_{max}(L)}{\varepsilon_{MD}}\right)^m\right]_L \tag{3-2}$$

The break rate n_{100} [%] is given in Equation (3-2) withFrac the total area of a paper roll A_{roll} [m], the area of the specimen A_{ref} [m], which is used to determine the average strength T_{MD} [N/m], and the strength uniformity parameter m [-]. The strength uniformity parameter m is the Weibull modulus, which represents the uniformity of the tensile strength distribution of the test specimen. The higher the strength uniformity parameter m is, the more uniform is the tensile strength. The strain to failure ε_{MD} [%] or elastic stretch can also be described as T_{MD}/E_{MD}. With

the operator $[\ ]_L$ the averaging for the random variable $\Delta\varepsilon_{max}(L)$ [%] over the length L can be denoted.

In Figure 3-4 the Equation (3-2) for the break rate is plotted, with the assumption that $\Delta\varepsilon_{max}$ = 0 and follows a normal distribution. Virtually, the break rate is zero until the strain deviation increases to 0,08 %. At the standard deviation 0,1 % a very realistic level of break rate can be seen.

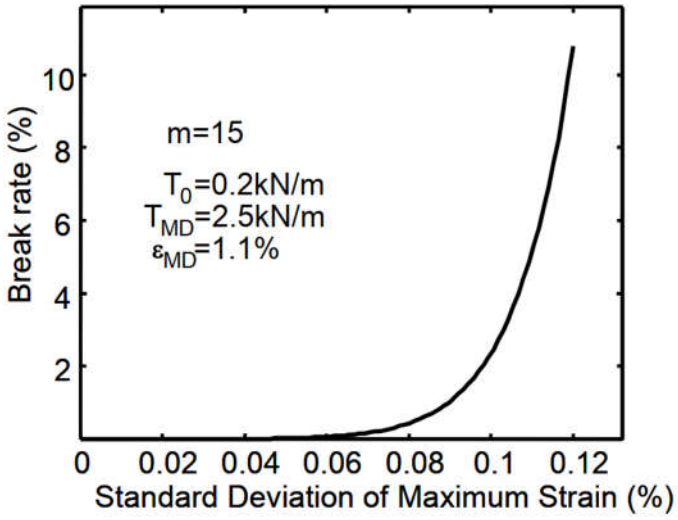

Figure 3-4: Break rate as function of standard deviation of maximum strain deviation [7]

Controlling factors leading to breaks in press rooms are the average tensile strength, the strain to failure and the strength uniformity parameter. Tensile strength is the most consistent predictor of web breaks among the routinely measured strength properties of paper. For reducing the break rate, the most effective way is to reduce the tension variation, which is not only caused by press room operations but also by paper factors like paper splices, out of roundness, and web tension non-uniformity. By reducing the break rate, the uniformity and therefore the formation of the paper can be improved. [7]

3.1.3 Practical applications of fracture mechanics

With fracture mechanics the effects of crack propagations are analyzed. The web strength can be improved by increasing the insensitivity of paper grade against defects. In many paper applications the in-plane crack propagation is the dominating mode of failure. A paper web break can be caused by macroscopic defects, such as rigid fiber bundles, holes in the web or edge cuts wreaked by careless handling of paper rolls. Defects in the paper structures are of such a small size that non-linear effects must be considered. The integrity of paper web can be valued if the crack tip stress, depending on the crack length, crack position and web tension, and the fracture toughness of the material, is known (Figure 3-5). The schematic definition of the fracture mechanics problem of web breaks contains several simplifying assumptions including out-of-plane deformation, loading perpendicular to the plane of the web and skew

web tension. These simplifying assumptions should be quantified to accurately predict the real performance of a paper web. [5] [11]

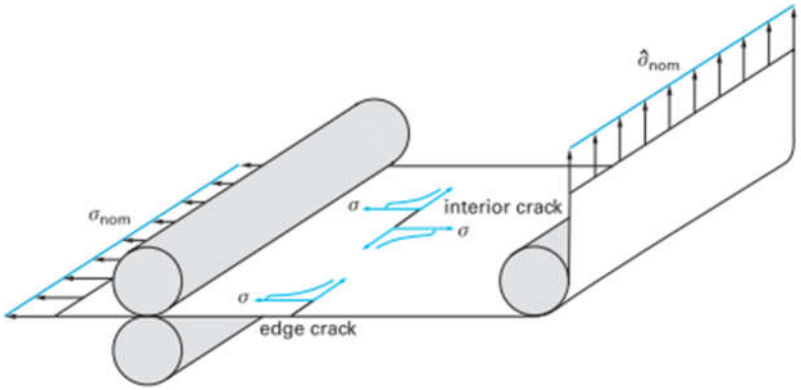

Figure 3-5: Fracture mechanics problem of web breaks caused by defects [5]

The stress state of a web in the crack tip region is affected by (a) tensile-induced buckling and (b) bulging over a pressurized turner (Figure 3-6). In general, a web is not flat. Is a crack oriented in cross-machine (CD) the cracks are primarily loaded in mode I, if it is not exactly oriented in CD the crack tip can be loaded in mode I and mode II (Figure 3-2). By passing a pressurized turner bar, the crack tip is loaded to the plane of the web by the air pressure and is bulging. A nonuniform web tension profile can arise from misaligned turner bars, frictional effects and web tension profiles created on the paper machine. This can severely affect crack tip loading. [5]

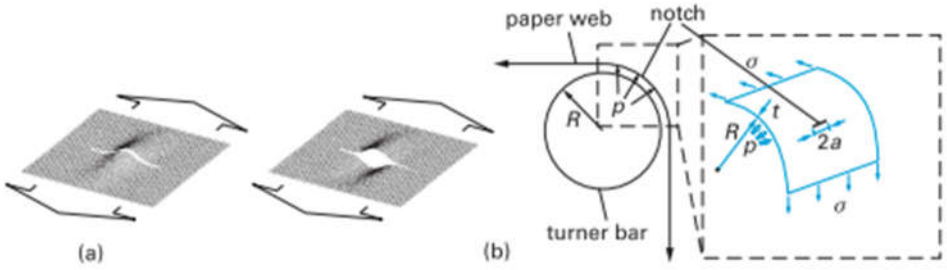

Figure 3-6: Effects on crack tip stresses in a paper web: (a) tension-induced buckling and (b) bulging over a pressurized turner [5]

In the work of Wellmar et al. [11] the aim of the work was to solve the problem of crack growth initiation in large paper structures containing small defects. For the tests performed, two different test pieces were designed. The first test piece contained a center notch Figure 3-8 *a)* and the second test piece an edge notch Figure 3-8 *b)*. For both, the center notched, and the edge notched the proportions were chosen to be twice the height (*2h*), twice the width (*2W*) and the center notch (*2a*) is also twice the length of the edge notch (*a*). The dimensions and the clamping arrangement of the test pieces are shown in Figure 3-7. To avoid buckling an anti-buckling guide was installed on the clamping arrangement. The variable dimension was the crack length with a variation from 2-50 mm for both configurations and the critical force and

critical displacement were calculated and experimentally evaluated. The work shows that the critical displacement as well as the critical force decrease with increasing crack length. This means a bigger crack reduces the critical force and the critical displacement of paper. [11]

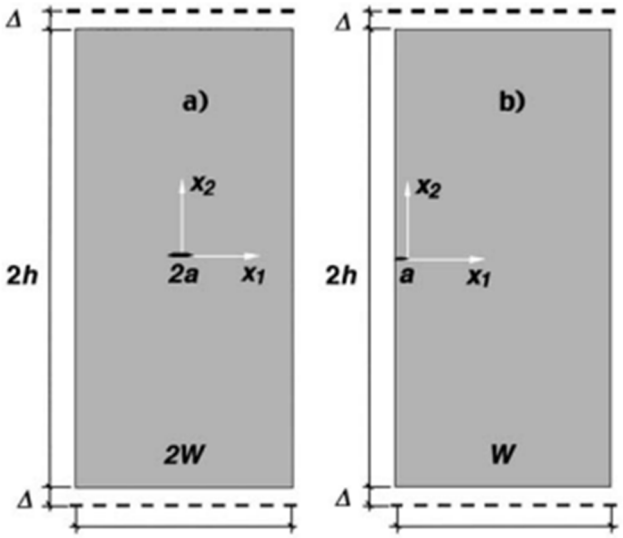

Figure 3-8: Test pieces for the fracture toughness experiment. [4]

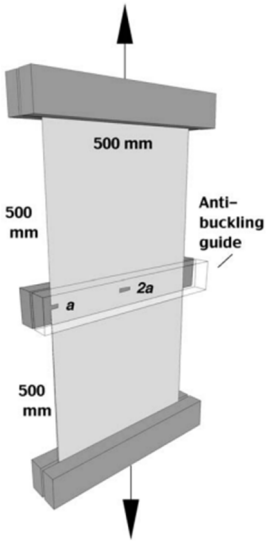

Figure 3-7: Clamping arrangement of the test pieces [4]

In a previous work Wellmar et al. [3] the variable was the relative notch length *a/W*. Test pieces were cut with a length of *2h* = 100 mm and a width of *2W* = 50 mm. The relative notch length varied from 0,1<*a/W*<0,7. The fracture toughness was determined for six test pieces for each notch length with a finite element analysis.

Purpose of the tests was the determination of a consistent notch length *2a* to be used in the fracture toughness measurement. Figure 3-10 and Figure 3-9 show the results of the test with a kraftliner in MD 200 g/m² and a fine paper in MD with 80 g/m². The best results were achieved with a relative notch length *a/W* between 0,3 and 0,5. Which leads to the appropriate choice of a relative notch length *a/W* = 0,4 and further, with the dimensions of a test piece from *2h* = 100 mm and *2W* = 50 mm to a notch length of *2a* = 20 mm. [3]

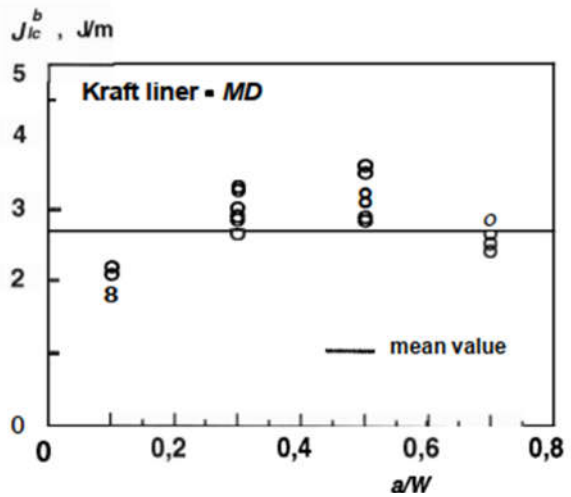

Figure 3-9: Fracture toughness measurement on kraft liner in MD [3]

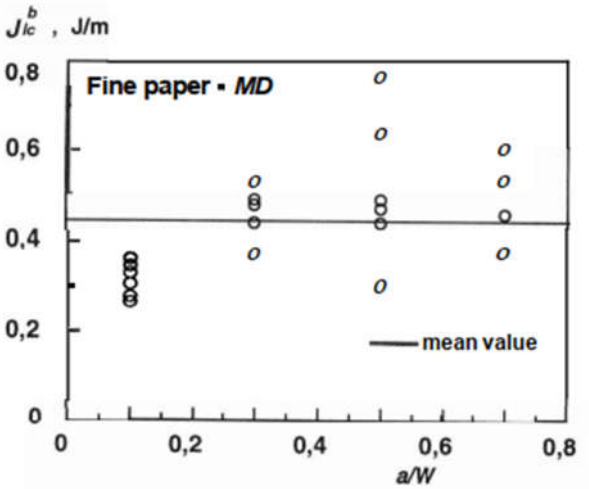

Figure 3-10: Fracture toughness measurement on fine paper in MD [3]

3.1.4 Crack tip modeling

The nature of cracks depends on microscopic fracture mechanisms of the paper, where inter-fiber bond failure, related fiber pull-out and fiber breakage dominate. To release a fiber, tens of bonds must fail, and the order of hundreds of fibers must either be released or broken perpendicular to paper plane propagated by one fiber length. Consequently, one single microscopic event cannot trigger a failure of paper. Microscopic damage is typically accumulated across several millimeters, comparable to fiber length, which surrounds the crack tip where stress concentration results in irreversible deformation and damage. Figure 3-11 shows the distribution of microscopic bond failures in a laboratory sheet just before crack propagation starts. To see the damage, it is made visible with silicone oil impregnation. In fracture mechanics this area is known as fracture process zone (*FPZ*). Most of the fracture mechanical models used are depending on the problem and objectives of the analysis. It is best to use the simplest possible model that has predictive capability. With the size of FPZ in comparison to characteristic dimension (e.g., crack length) the choice of model is determined, which is usually not known. Therefore, the accuracy of the chosen crack tip modeling approach must be verified by comparing the predictions with experiments or with a more advanced model that has already been proven reliable. [5]

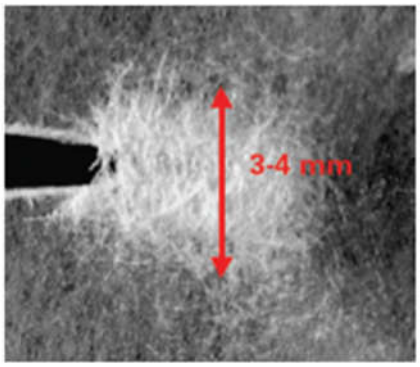

Figure 3-11: Microscopic bond failures in a laboratory sheet [5]

3.1.5 Linear elastic fracture mechanics

An elastic fracture occurs when all irreversible deformations are contained within the small FPZ of the material and the remaining deformations in the rest of the material are below the yield strain of the material. This fracture can be described as the work consumed in the FPZ, is provided by the strain energy of the elastic material surrounding the crack and is given as the strain energy release rate G [J/m²] where it reaches the critical value G_c [J/m²]:

$$G = -\frac{dU}{dA} \qquad (3\text{-}3)$$

The strain energy release rate *G* is the relation between the strain energy in the material *U* [J] and the crack area *A* [m²]. It is a function of the specimen size, the crack geometry, the elastic properties of the material and the loading conditions.

For a linear elastic material, the stress-strain curve follows the same path for material loads and unloads (Figure 3-13). With a load-displacement curve the crack growth can be described. It is shown in Figure 3-12. To the point of crack propagation, the curve *c* is linear from zero, where the material is unloaded. The reversible work follows the same path back to zero, and the irreversible work follows the crack area after propagation *(A+dA)* [m²]. The area encircling the curve shows the work of fracture. [1]

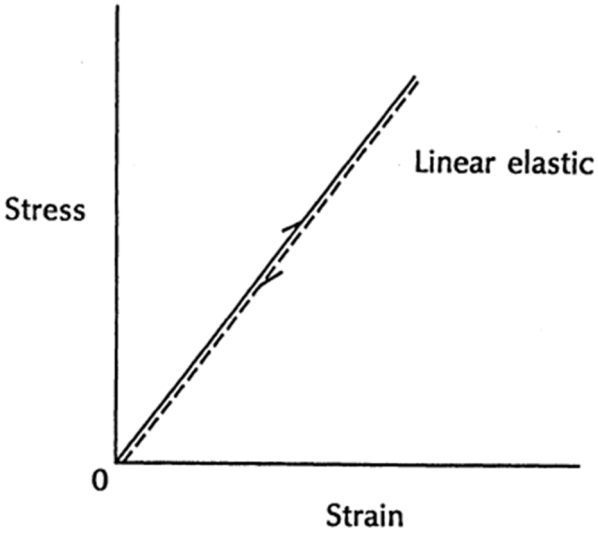

Figure 3-13: Stress-strain curve for a linear elastic material [1]

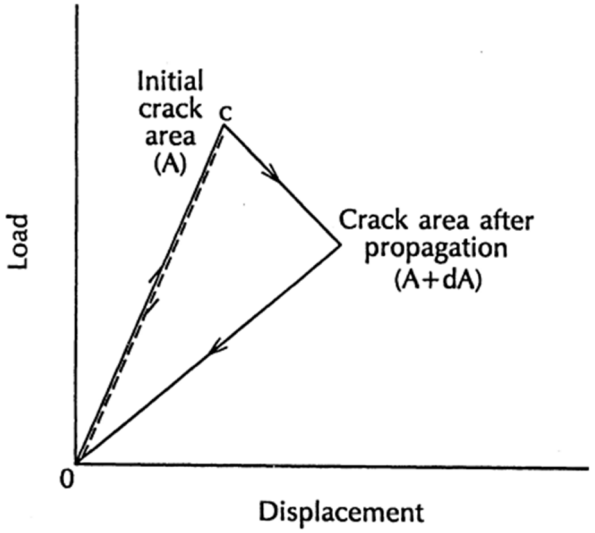

Figure 3-12: Load-displacement curve for crack growth [1]

In the theory of linear elastic fracture mechanics (LEFM) the FPZ is mathematically treated as a point. This is known as small-scale yielding, and with these assumptions the crack tip stress field can be determined by using the LEFM. If the paper sheet is loaded in mode I, the multi-axial stress and strain field close to the crack tip can be characterized by one single parameter. This parameter is the stress intensity factor *K* [-], and with this the nonzero stress component σ_{ij} [N/m²] (3-4) can be determined. For this, the crack tip coordinates *r* [m] and φ [rad] are defined in the x- and y-axes relative to the crack orientation and not in MD and CD of paper (Figure 3-14). With the angular function $f_{ij}(\varphi)$ the displacement, the strain fields, and the effects of orthotropic material properties are described. [5]

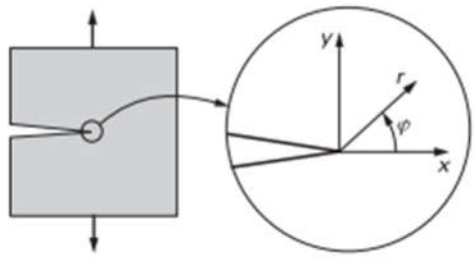

Figure 3-14: Crack tip coordinates used for the nonzero stress component [5]

The validity of Equation (3-4) is restricted to the singularity-dominated zone near the crack tip. For the zone further away from the crack tip, higher order terms should be included. Equation (3-4) is invalid in the FPZ, because no real material can carry infinite loads, which means singular stresses do not exist. Even though the equation is invalid the stress intensity factor *K* [-] is useful because it can be determined from measurements with notched specimens and for some simple geometries and loading modes solutions are available. The values of K from experiments can be used to evaluate at which crack growth begins and are the critical value K_c [-] in the LEFM. This critical value K_c is taken to be a material property and is called fracture toughness. For finite specimens the expression of the relation between K and external stresses is given in Equation (3-5), where σ [N/m²] is the remote stress, *a* [m] the crack size and *f(C)* the function of a geometry and characteristic dimension of the structure *C*. Macroscopic fracture begins when *K* reaches K_c (3-6). [5]

$$\sigma_{ij} = \frac{K}{\sqrt{2\pi r}} f_{ij}(\varphi) \qquad (3\text{-}4)$$

$$K = \sigma\sqrt{\pi a} f(C) \qquad (3\text{-}5)$$

$$K = K_c \qquad (3\text{-}6)$$

As paper is not linear elastic and shows plastic deformation when strained to failure a correction for the elastic stress analysis must be made. For this, a plastic zone of the size r_y [m] to the initial crack length *a* [m] is added to the yield stress σ_y [N/m²]. This addition is given by adding r_y:

$$r_y = \frac{1}{2\pi}\left(\frac{K_c}{\sigma_y}\right)^2 \qquad (3\text{-}7)$$

The crack length is now longer than the original one and with this a stress field identical to the elastic field, shifted ahead by r_y is created. The crack tip is now in the center of the plastic zone with a diameter of $2r_y$ (Figure 3-15). [1]

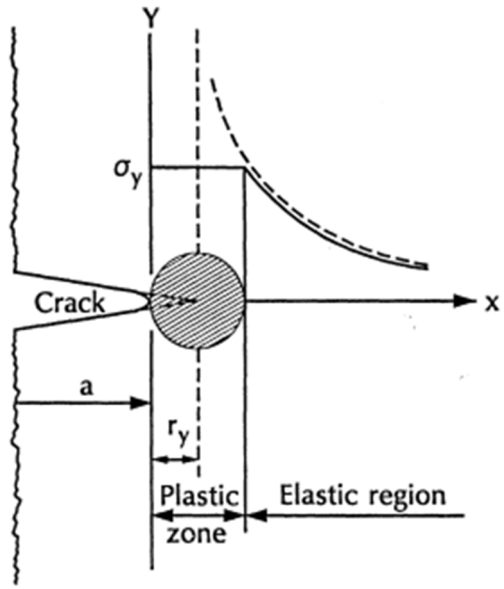

Figure 3-15: Crack tip fracture process zone (FPZ) [1]

The criterion for a valid application of elastic fracture mechanics is that the critical failure stress σ_c [N/m²] should be much less than the yield stress σ_y of the material. The net stress is applied over the uncracked region of the material at failure (Equation (3-8)).

$$\sigma_c \left(\frac{W}{W-a}\right) \ll \sigma_y \qquad (3\text{-}8)$$

This criterion also specifies large enough specimen dimensions, so that the specimen boundaries do not interfere with the crack tip stress distribution. [1]

$$r_y \ll a \ll (W-a) \qquad (3\text{-}9)$$

3.1.6 Nonlinear fracture mechanics

Paper normally leaves the paper machine as an anisotropic nonlinear material. This means for paper a more complex fracture mechanics model is needed. Even small adjustments of the paper machine have a great influence on the material properties, which according to some authors, means that an enormous potential in optimizing the material properties for different end-use situations can be achieved. [4]

Equation (3-10) is the base for most crack tip models and the uniaxial version of the stress-strain expression. Here, the linear elastic relation σ/E is extended with the strain-hardening exponent N and the strain-hardening modulus E_0.

$$\varepsilon = \frac{\sigma}{E} + \left(\frac{\sigma}{E_0}\right)^N \qquad (3\text{-}10)$$

The linear elastic part (dashed line) and the non-linear elastic part (continuous line) of Equation (3-9) are shown in Figure 3-16. The deviation of the dashed line and the continuous line can be described with the strain-hardening components E_0 and N.

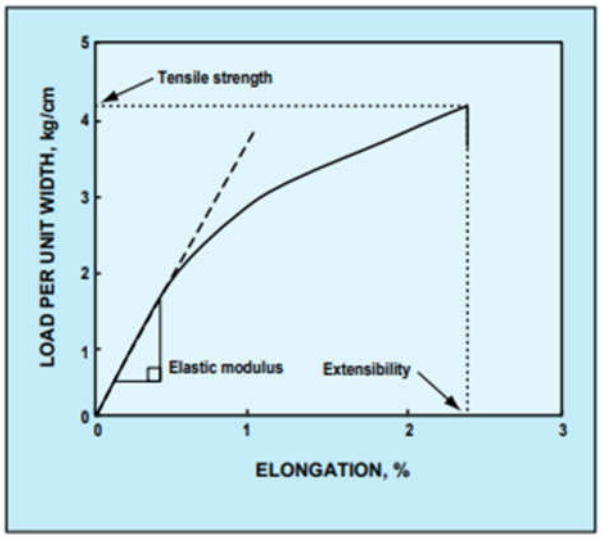

Figure 3-16: Load-Elongation curve of a typical paper sheet [2]

With Equation (3-10) the stress field in the vicinity of the crack tip, known as the HRR-field, can be determined:

$$\sigma_{ij} = \alpha \left(\frac{J}{r}\right)^{\frac{1}{N+1}} f_{ij}(n, \varphi) \qquad (3\text{-}11)$$

The material and stress state, if it is plane strain or plane stress, describes the dependence of the scalar multiplier α. In the HRR-field the crack tip conditions of a nonlinear elastic material are characterized by the J-integral. It predicts that the stresses in the vicinity of a crack tip are singular and governed by the stress-strain behavior of the material and have a uniform distribution. The J-integral determines the amplitude of the stresses. In analogy with K of the LEFM the stresses close to a crack tip are characterized by J. For a linear elastic material where plane stress conditions apply J can be described as followed:

$$J = \frac{K^2}{E} \qquad (3\text{-}12)$$

Figure 3-17 shows the schematic illustration of the relation of Equation (3-12). The HRR-field points out that single-parameter characterizations of the crack tip stress field which uses a J- integral are possible. For the J-dominated zone the stresses and strain scales are distributed uniformly inside this zone. [5]

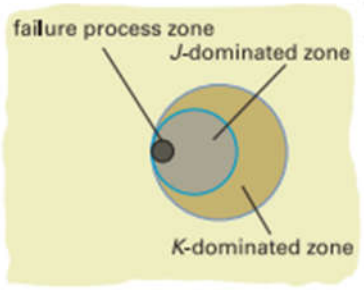

Figure 3-17: Crack opening stress σ_{yy} in a nonlinear elastic material [5]

Analog to the LEFM, the critical value, or nonlinear fracture toughness J_c is needed to start the crack growth. With the fracture criterion for in-plane mode I (3-13) the crack starts to grow and should hold for any arbitrary geometry of structure. [5] [11]

$$J \geq J_c \qquad (3\text{-}13)$$

The external loading, J and the critical value J_c are depending on the material behavior N and E_0. To analyze the nonlinear fracture mechanics, numerical methods such as the J-integral evaluation, is needed. The unique relationship between strain and stress of a nonlinear elastic material can be seen in Figure 3-16. To evaluate the defect sensitivity of paper grades the determination of the material behavior via a tensile test is the first step. Basically Equation (3-9) is fitted to the stress strain curve by finding the parameters E, E_0, and N, thus describing the material behavior. The next step would be the determination of nonlinear fracture toughness J_c from tensile test of a notched test piece. With the help of finite element analysis J can be calculated and is used to predict failure. This procedure is schematically shown in Figure 3-18. [5] [1]

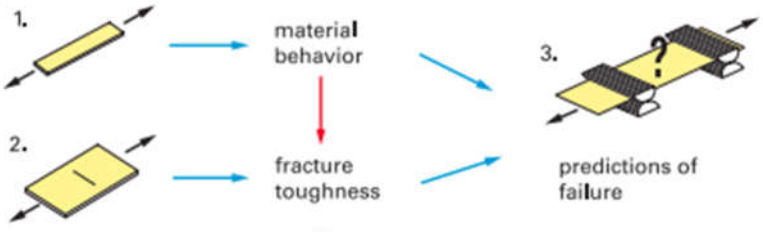

Figure 3-18: Practical use of nonlinear fracture mechanics [5]

Here the approach of the determination of the J-integral is to idealize an irreversible plastic material with a crack as a reversible non-linear elastic material.

The loading and unloading of a non-linear elastic material are occurring along the same path. The load-elongation curve is shown in Figure 3-16. The non-linear response can be described with J [J/m²] by a power-law relationship between stress σ [N/m²] and strain ε [%]:

$$J = \sigma \varepsilon^N \quad (3\text{-}14)$$

For paper this relationship is not valid, because the strain is not zero at zero stress, which means fracture is difficult to analyze. For this, *J* can be described by a path-independent contour integral around the crack tip. For a non-linear elastic material at crack extension the critical strain energy release rate or fracture toughness J_{cr} [J/m²] is given by:

$$J_{cr} = -\frac{dU^*}{dA} \quad (3\text{-}15)$$

It is a relation of the potential energy *U** [J] in the non-linear elastic material to the crack area *A* [m²]. [1]

If fracture toughness would be calculated with Equation (3-15) or finite element analysis the unit for fracture toughness would result in J/m². According to the calculation methods used in this thesis, fracture toughness has the unit J/m. For this, Equation (3-15) can simply be multiplied with the thickness of the paper grade (Equation (3-16)). [4] [11]

$$J_c^b = J_c \cdot t \quad (3\text{-}16)$$

3.2 Fracture toughness calculation methods

In this thesis three different calculation methods were analyzed. The choices made for these three methods were 1) the used notched tensile tester is working with the SCAN-P 77:95 method, 2) during the research the method of Seth was discovered and 3) the use of the standardized method ISO/TS 17958:2013 is international approved and is the main calculation method of this thesis. All three methods are described in the following sections.

As we know fracture toughness is a fundamental mechanical property of the material and is described as the ability to resist propagation of a pre-existing crack. [1]

By the current state of scientific knowledge many different methods are known to calculate fracture toughness. Each method is based on the same scientific facts but uses different procedures for calculation. While Seth [1] analyzes two sets of results for softwood pulps and shows the relationship between fracture toughness, tensile strength, and extensibility, in the SCAN norm and in the ISO norm fracture toughness is analyzed with the help of FE-analyses. Hence the calculation in the SCAN norm and the ISO norm is more complex than the method of Seth.

3.2.1 Fracture toughness SCAN-P 77:95

The SCAN-test method is based on ISO 1924-3 which is a method for determination of tensile properties. It is performed on a tensile testing machine with a test span length of 100 mm, and

a rate of elongation of 1,7 mm/s. The test piece has measurements of 15 mm in width for the tensile test and 50 mm in width for the notched tensile test. The 50 mm test piece is center notched with a 20 mm notch. This method benefits from the high testing rate and the high calculation capacity of modern computerized tensile testing machines. [12]

The procedure and evaluation of fracture toughness takes place in two steps. In the first step a tensile test in MD and CD is performed. It has the purpose to construct a representative mean force-elongation curve. From this, the material parameters nominal elongation, nominal force and the maximum slope can be calculated. In the second step a notched tensile test is performed, and the tensile stiffness is reported. With the material parameters from the tensile test and the tensile stiffness of the notched tensile test the fracture toughness can be determined for MD and CD. The calculation of fracture toughness must be computerized and is not further discussed in this work. It is described in detail in the work of Wellmar P. et al. [4]. [12]

This calculation method uses different equations to determine the required parameters for MD and CD. It is also necessary to perform the tensile test and the notched tensile test in MD and CD to be able to determine the fracture toughness and the required parameter. This means with this method fracture toughness of handsheets cannot be calculated correctly.

3.2.2 Fracture toughness R.S. Seth

Fracture always involves the creation of new surfaces at the expense of work. The fracture toughness is the work consumed in the FPZ per unit crack area and depends on the strain energy and the applied external forces. It is assumed that the FPZ provides a high opposing stress that prevents the crack propagation, shown in Figure 3-19. It is also assumed that the strain associated with this stress is high too, which leads to a high resistance for the crack propagation. With these assumptions it can be said that the in-plane fracture toughness will be high if the in-plane tensile strength and extensibility are high. The strength of the fibers and the extent of bonding between them are the factors that are important for the tensile strength. High extensibility means a high breaking strain of the paper. [2]

In his work Seth [2] used two sets of softwood pulps including commercial and laboratory-made, bleached, and unbleached kraft. The first set contains 93 different handsheet samples. For the second set 123 samples were measured. By analyzing these two sets two different relationships between fracture toughness, tensile strength and extensibility were formulated. Equation (3-17) gives the relationship for the first set, and Equation (3-18) for the second set. The fact that a high tensile strength is more important than a high extensibility can be seen in both equations, where the exponent of the tensile strength is higher than the exponent of the extensibility. [2]

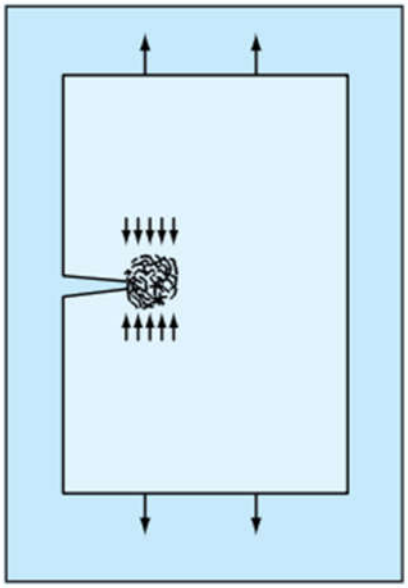

Figure 3-19: Stress at the FPZ opposing crack propagation [2]

$$J_c = 1{,}08(Tensile(N)^{0{,}63} \cdot Stretch(\%)^{0{,}52}) \quad (3\text{-}17)$$

$$J_c = 0{,}60(Tensile(N)^{0{,}74} \cdot Stretch(\%)^{0{,}58}) \quad (3\text{-}18)$$

3.2.3 Fracture toughness ISO/TS 17958:2013

The standard test method is based on the work of Mäkelä et al. [13], [14], [15]. In his work he performed the tensile test for paper webs and the tensile test and the notched tensile test according to ISO 1924-3 for large web-wide paper samples. The results of the tests of six different paper grades were compared: medium weight coated paper, testliner board, fluting paper, sack paper, newspaper, and supercalendered paper.

The test of edge-notched paper webs was performed on the Wide Web Tensile Tester (Figure 3-20) at Norwegian University of Science and Technology (NTNU), which can handle web widths up to 1 m. [14]

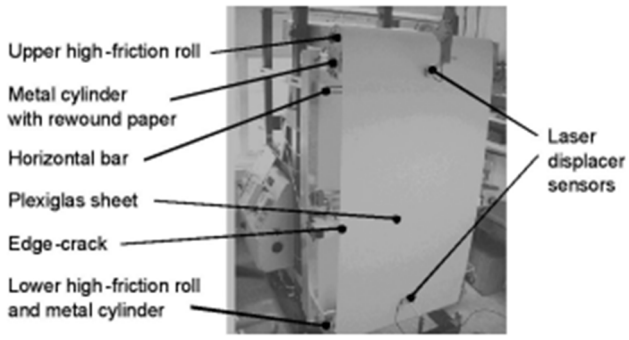

Figure 3-20: Wide Web Tensile Tester at the NTNU [14]

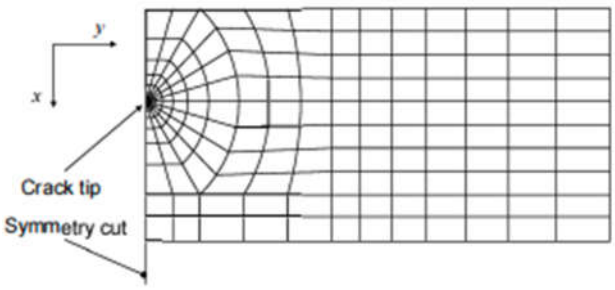

Figure 3-21: Illustration of the used finite element mesh [14]

The relevant tests were the tensile test and the notched tensile test according to ISO 1924-3. For this, paper samples of the different paper grades were cut out of the paper webs and cut into test pieces for the tensile and notched tensile test. With the data of the laboratory notched tensile test and predictions of ultimate failure of edge-notched paper webs a fracture mechanics analysis was performed. This was realized with a finite element analysis (code ABAQUS/Standard), with symmetry considerations for geometry and loading of the notched tensile test and the tensile test of the edge-notched paper webs. At the nodes along the clamped edge, right edge in Figure 3-21, the loading was applied by prescribing the monotonically increasing displacement. [13]

As described above (Figure 3-18) the determination of the fracture toughness is consisting of two steps. In step 1 first a normal tensile test is carried out. The parameters E, E_0 and N of Equation (3-9) are fitted to the measured stress strain curve, thus describing the material behavior. In step 2 a notched tensile test is carried out, and the fracture toughness is calculated.

Step 1:

First the tensile stiffness E [N/m] is determined as the maximum slope in the stress strain curve. With the development of analytic expressions, the evaluation of tensile material properties, the strain-hardening exponent N [-], and the strain-hardening modulus E_0 [N/m], can be described with the help of the tensile energy absorption W_T [J/m²] [15]:

$$W_T = \int_0^{\varepsilon_T} \sigma \, d\varepsilon \qquad (3\text{-}19)$$

It can be re-formulated as:

$$W_T = \sigma_T \varepsilon_T - \int_0^{\sigma_T} \varepsilon \, d\sigma \qquad (3\text{-}20)$$

With the equation for the uniaxial strain ε [%] (3-10), described in chapter 3.1.6, the integrand in Equation (3-20) can be replaced:

$$W_T = \sigma_T \varepsilon_T - \frac{(\sigma_T)^2}{2E} - \frac{(\sigma_T)^{N+1}}{(N+1)(E_0)^N} \qquad (3\text{-}21)$$

With the re-expressed Equation (3-10) the strain-hardening modulus can be substituted.

$$E_0^N = \frac{(\sigma_T)^N}{\left(\varepsilon_T - \frac{\sigma_T}{E}\right)} \qquad (3\text{-}22)$$

$$W_T = \sigma_T \varepsilon_T - \frac{\sigma_T^2}{2E} - \frac{\sigma_T \left(\varepsilon_T - \frac{\sigma_T}{E}\right)}{(N+1)} \qquad (3\text{-}23)$$

Re-formulating Equation (3-23) the strain-hardening exponent N and re-formulating Equation (3-22) the strain-hardening modulus E_0 can be expressed:

$$N = \frac{\left(\sigma_T^b\right)^2 - 2E^b W_T^b}{\left(\sigma_T^b\right)^2 + 2E^b\left(W_T^b - \sigma_T^b \varepsilon_T\right)} \tag{3-24}$$

$$E_0 = \frac{\sigma_T^b}{\left(\varepsilon_T - \frac{\sigma_T^b}{E^b}\right)^{\frac{1}{N}}} \tag{3-25}$$

Both, the strain-hardening exponent, and the strain-hardening modulus, are based on the tensile stiffness E [N/m], tensile strength σ_T^b [N/m], strain at break ε_T [%] and tensile energy absorption W_T^b [J/m²]. These tensile material parameters are obtained from the tensile test following ISO 1924-3. [15]

Step 2:

With the J-integral theory the principal form of a semi-analytic expression for the J-integral of a notched rectangular piece exhibiting mode I fracture can be utilized. For linear elastic material this form is expressed in Equation (3-26) and for the non-linear material it is expressed in Equation (3-27). For both equations Σ [N/m] is a stress measure which characterizes the severity of the loading. The two geometry functions f_{el} [-] and f_{nl} [-] for the linear elastic part and the non-linear part are depending on the characteristic dimensions of the test piece a [m], W [m] and h [m], and f_{nl} [-] also on the strain-hardening exponent N [-]. [15]

$$J_{el} = \frac{a\Sigma^2}{E} f_{el}\left(\frac{a}{W}; \frac{h}{W}\right) \tag{3-26}$$

$$J_{nl} = \frac{a\Sigma^{N+1}}{(E_0)^N} f_{nl}\left(\frac{a}{W}; \frac{h}{W}; N\right) \tag{3-27}$$

Combining the two parts for the linear elastic material, Equation (3-26), and the non-linear material, Equation (3-27), an approximate semi-analytic expression for the J-integral of a notched rectangular piece, obeying the isotropic deformation theory of plasticity model, Equation (3-10) chapter 3.1.6, can be formulated (3-28). It correlates the J-integral to the material behavior, the structural geometry, and the applied loading.

$$J = \frac{a\Sigma^2}{E} f_{el}\left(\frac{a}{W}; \frac{h}{W}\right) + \frac{a\Sigma^{N+1}}{(E_0)^N} f_{nl}\left(\frac{a}{W}; \frac{h}{W}; N\right) \tag{3-28}$$

To determine the fracture toughness from the expression in Equation (3-28), the structural geometry and the applied loading must be considered. For the notched tensile tests, a test piece with a width of 50 mm, a clamping length of 100 mm and a center notch with a length of 20 mm were used, shown in Figure 3-22. That will lead to the characteristic dimensions used

in the determination with *a*=10 mm, *W*=25 mm and *h*=50 mm and further to *a/W* = 0,4 and *h/W* = 2. [14]

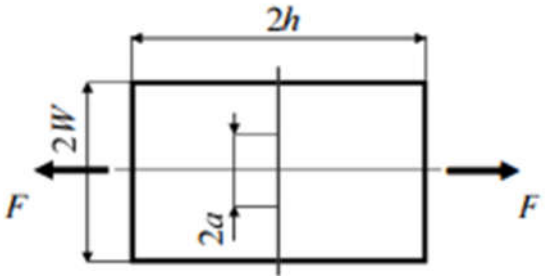

Figure 3-22: Illustration of the in-plane characteristic dimensions of a center-notched test piece [14]

During the notched tensile test, the apparent tensile strength σ_{cr}^{b} [N/m] is measured, which leads to the consideration of the applied loading. It is given in Equation (3-29), where the critical net- section stress $\sigma_{ns,cr}^{b}$ [N/m] is determined. [14]

$$\sigma_{ns,cr}^{b} = \frac{\sigma_{cr}^{b}}{1-\frac{a}{W}} = \frac{\sigma_{cr}^{b}}{0{,}6} \tag{3-29}$$

$$\varepsilon_{ij} = S_{ij,kl}\sigma_{ij} + \frac{3}{2}\left(\frac{\sigma_e}{E_0^b}\right)^N \frac{s_{ij}}{\sigma_e} \tag{3-30}$$

$$f_{el} = 1{,}4096 \tag{3-31}$$

With the commercial finite element code ABAQUS/Standard an isotropic deformation theory of plasticity model was used to describe the material behavior. This model established a one- to- one relation between the strain tensor component, ε_{ij} [%], and the stress tensor component σ_{ij} [N/m]. In Equation (3-30) this relation is expressed, where S_{ijkl} [-] describes the linear elastic compliance tensor components, σ_e [N/m] the von Mises effective stress and s_{ij} [-] the deviatoric stress tensor component. By setting the second term on the right-hand side to zero only the linear elastic part of the material model was used in the analysis. To get the numerically obtained relation between the J-integral and the net-section stress, the linear elastic part of Equation (3-28) was fitted. The linear elastic geometry function is used as a free parameter, which results in Equation (3-31). [14] [15]

For the non-linear geometry function the evaluation occurred similarly. Therefore, the complete J-integral expression, Equation (3-28), with Equation (3-31) inserted, was used. The non-linear geometry function was also determined for different values of the strain-hardening exponent N, and the following equation was developed:

$$f_{nl} = \frac{N^{0{,}5494}}{0{,}2459N + 0{,}4612} \tag{3-32}$$

Inserting the critical net-section stress and both geometry functions the obtained expression of the J-integral, Equation (3-28), will predict the corresponding critical value J_{cr}^{b} [J/m], the fracture toughness:

$$J_{cr}^{b} = \frac{a\left(\sigma_{ns,cr}^{b}\right)^{2}}{E^{b}} f_{el} + \frac{a\left(\sigma_{ns,cr}^{b}\right)^{N+1}}{\left(E_{0}^{b}\right)^{N}} f_{nl} \qquad (3\text{-}33)$$

With this calculation method the fracture toughness can be calculated independent from MD and CD, which means the laboratory handsheets can be measured without other precautions. [14] [16]

3.3 Example calculation of fracture toughness

As a calculation example a data set in MD from the office paper is used. From the tensile test the mean values of the material behavior tensile stiffness E^{b} [kN/m], tensile force F_T [N], tensile energy absorption W_T^{b} [J/m²] and elongation δ_T [mm] are received.

Table 3-1: Constant values used for the calculation

Constant values for fracture toughness calculation		
Strip length l	100	mm
Strip width tensile test b	15	mm
Strip width notched tensile test 2W	50	mm
Center notch length 2a	20	mm

Table 3-2: Material behavior from tensile test

Material behavior from tensile test		
Tensile stiffness E^{b}	625,68	kN/m
Tensile force F_T	74,04	N
Tensile energy absorption W_T^{b}	47,99	J/m²
Elongation δ_T	1,47	mm

With these values tensile strength σ_T^{b} [N/m] (Equation (4-7)) and strain at break ε_T [%] (Equation (4-8)) can be determined:

$$\sigma_T^{b} = \frac{\bar{F}_T}{b} = \frac{74{,}04}{15} = 4935{,}89\ \frac{N}{m}$$

$$\varepsilon_T = \frac{1000\bar{\delta}_T}{l} = \frac{1000 * 1{,}47}{100} = 1{,}47\ \%$$

From these values the strain-hardening exponent *N* [-] (Equation (3-24)) and the strain- hardening modulus E_0 [N/m] (Equation (3-25)) can be determined:

$$N = \frac{\left(\sigma_T^b\right)^2 - 2E^b W_T^b}{\left(\sigma_T^b\right)^2 + 2E^b\left(W_T^b - \sigma_T^b \varepsilon_T\right)} = \frac{4935{,}89^2 - 2 * 625{,}68 * 47{,}99}{4935{,}89^2 + 2 * 625{,}68 * (47{,}99 - 4935{,}89 * 1{,}47)} = 5{,}65$$

$$E_0^b = \frac{\sigma_T^b}{\left(\varepsilon_T - \frac{\sigma_T^b}{E^b}\right)^{\frac{1}{N}}} = \frac{4935{,}89}{\left(1{,}47 - \frac{4935{,}89}{625{,}68}\right)^{\frac{1}{5{,}65}}} = 11932{,}8\ \frac{N}{m}$$

After performing the notched tensile test, where the apparent tensile strength σ_{cr}^b=*2320,0* [N/m] is measured, the critical net-section stress $\sigma_{ns,cr}^b$ [N/m] (Equation (3-29)), the non-linear geometry function f_{nl} [-] (Equation (3-32)) and finale the fracture toughness J_{cr}^b (Equation (3-33)) can be determined. The linear elastic geometry function f_{el}=*1,4096* [-] is an absolute term.

$$\sigma_{ns,cr}^b = \frac{\sigma_{cr}^b}{0{,}6} = \frac{2320{,}0}{0{,}6} = 3866{,}67\ \frac{N}{m}$$

$$f_{nl} = \frac{N^{0{,}5494}}{0{,}2459N + 0{,}4612} = \frac{5{,}65^{0{,}5494}}{0{,}2459 * 5{,}65 + 0{,}4612} = 1{,}4$$

$$J_{cr}^b = \frac{a\left(\sigma_{ns,cr}^b\right)^2}{E^b} f_{el} + \frac{a\left(\sigma_{ns,cr}^b\right)^{N+1}}{\left(E_0^b\right)^N} f_{nl} = \frac{10 * 3866{,}67^2}{625{,}68} 1{,}4096 + \frac{10 * 3866{,}67^{5{,}65+1}}{11932{,}8^{5{,}65}} 1{,}4 = 0{,}454\ \frac{J}{m}$$

3.4 Reproducibility of fracture toughness

To find possible outliers a box plot was performed. The first step is the determination of the median *x* from the data set. The median is the datapoint of the dataset, where one half of the dataset is higher, and the other half is lower than this datapoint. It can be determined with Equation (3-34), where *p* is 0,5 for 50 % of the dataset and *n* is the number of all data points. The second step is to determine the upper quartile also with Equation (3-34), where *p* is 0,75 for 75 % of the dataset and *n* is the number of datapoints in this quartile. The determination of the lower quartile is the same only with *p*=0,25 for 25 % and *n* is the number of datapoints in the lower quartile. For an even number of datapoints the upper equation is used and for an uneven number of datapoints the lower equation is used. With $x_{0,25}$ and $x_{0,75}$ the interquartile range *IQR* can be determined, Equation (3-35). To get the limits for major outliers the *IQR* is simply multiplied with 3 and either summated or subtracted to the upper and lower quartile, Equation (3-36). [17]

$$x_i \begin{cases} p\left(x_{\frac{n}{2}} + x_{\frac{n}{2}+1}\right) \\ x_{\frac{n+1}{2}} \end{cases} \quad (3\text{-}34)$$

$$IQR = x_{0,75} - x_{0,25} \quad (3\text{-}35)$$

$$major\ outlier = x_i \pm IQR \cdot 3 \quad (3\text{-}36)$$

The measurement datapoints which came out as outlier were then left out of the further analysis of the test series.

A better way to calculate outliers would be a outlier test by Grubbs [18]. This test would be more accurate.

To get the confidence interval width the arithmetic mean $\bar{x}$, Equation (3-37), and the standard deviation σ, Equation (3-38) must be determined. Both, the arithmetic mean, and the standard deviation have the unit of fracture toughness index [Jm/kg]. [19]

$$\bar{x} = \frac{\sum_{i=1}^{n} x_i}{n} \quad (3\text{-}37)$$

$$\sigma = \sqrt{\frac{\sum_{i=1}^{n}(x_i - \bar{x})^2}{n}} \quad (3\text{-}38)$$

With these two parameters the coefficient of variation *CV,* Equation (3-39), and the confidence interval width *CIW*, Equation (3-40), can be determined.

$$CV = \frac{\sigma}{\bar{x}} \quad (3\text{-}39)$$

$$CIW = 2 \cdot z_0 \frac{CV}{\sqrt{n}} \quad (3\text{-}40)$$

The coefficient of variation is a measure of dispersion relative to the standard deviation at the mean value. With a defined confidence interval of 95 % the probability that population parameters are in this area, which can be considered as “producer” for an empirical determined sample value, is due to 95 %. This means in the standard normal distribution 95 % of the total area are between -1,96 and 1,96. This leads to the used confidence level value z_0 = ± 1,96. With the confidence level value, the arithmetical mean, and the standard deviation the upper and lower limits of the confidence interval can be determined:

$$upper\ limit = \bar{x} + 1{,}96 \cdot \sigma \quad (3\text{-}41)$$

$$lower\ limit = \bar{x} - 1{,}96 \cdot \sigma \qquad (3\text{-}42)$$

By using the coefficient of variation to determine the confidence interval width it can be given in percentage, and the different paper grades can be compared to each other. [19]

4 Materials and methods

4.1 Pulp used in the experiments

The pulp for this work was provided from Mercer Stendal as dry pulp boards for the lab PFI refining or as refined and extracted wet pulp after industrial refining. For long fibers, a bleached hardwood kraft pulp (BHKP, Eucalyptus) and for the short fibers a bleached softwood kraft pulp (BSKP, Referenz) was used. The BHKP is a TCF bleached eucalyptus pulp from South America (Brazil). The BSKP consists of 40-70 % pine and 30-60 % spruce and is ECF bleached. Before starting the trials, the dry content was measured according to EN ISO 638 (2008 10):

Table 4-1: Dry content of pulp after industrial refining

Industrial refining	BSKP				BHKP
Refining energy [kWh/t]	**0**	**40**	**80**	**120**	**60**
Dry content [%]	15,9	19,1	15,2	18,0	14,6

Table 4-2: Dry content of pulp for the lab PFI refining

Lab PFI refining	BSKP	BHKP
Dry content [%]	94,574	*94,591*

Table 4-3: Dry content of pulp after industrial refining for filler material impact

Industrial refining	BSKP	BHKP
Refining energy [kWh/t]	**80**	**60**
Dry content [%]	19,168	15,105

For the analysis of the pulp the following standardizations were used:

- Wet disintegration: DIN EN 20638
- SR freeness: EN ISO 5267-1 (2000 07)
- Water retention value: ISO 23714

The tests were performed according to these standards for the pre-trials and the main-trials, they are not further described here.

4.2 Filler material

As filler (HC 60), a ground calcium carbonate (GCC) with the median particle size of 1,5 µm from Omya GmbH was used. HC 60 means that 60 % of the particle have a size under 2 µm. The filler is a refined calcium carbonate and was provided as a high concentrated pigment slurry.

Table 4-4: Dry content of filler slurry HC 60

Filler slurry	*HC 60*
Dry content [%]	*77,98*

The filler must be cooled after preparation and stirred during handsheet forming to avoid agglomeration of the filler. The container with filler is stirred with a magnetic stirrer and the amount used for a single handsheet is measured shortly before it is put in the pulp.

The handsheets with filler and retention agent were made different to the handsheets without. For every handsheet the filler and retention agent were added separately to the pulp. The amount of pulp and filler were determined before the test series to obtain a handsheet with a weight of 2,4 g:

Table 4-5: Filler amount per handsheet

Pulp	[%]	95	90	80	75	70
	[g oven dry]	2,28	2,16	1,92	1,8	1,68
Filler	[%]	5	10	20	25	30
	[g oven dry]	0,12	0,24	0,48	0,60	0,72

Assuming a retention of 50 % leads to higher filler amounts needed in the pulp suspension. The higher the filler content gets the higher the amount of filler needed for a handsheet is. The used filler amount for the varied filler content is given in the table below.

Table 4-6: Actual filler amount per handsheet

Filler	[%]	5	10	20	25	30
	[g oven dry]	0,15	0,28	0,65	0,8	1,2

For the final handsheets the ash content [%] was determined, according to ISO 1762. The handsheets were first dried at 105 °C then they were weighed before they were put into the oven for 5 h by a temperature of 575 ± 25 °C. After 5 h the rest was weight and the ash content was determined, Equation (4-2). The ash content of the slurry was determined the same way.

The loss on ignition *LOI* [%] can be determined with the ash content of the slurry, Equation (4-1). With the output weight and the *LOI* of the filler the filler amount [%] in the ash can be calculated, Equation (4-3). The filler content [g] can then be determined with the filler amount divided by the initial weight, Equation (4-4).

Table 4-7: Ash content and loss on ignition of slurry

Filler slurry	*HC 60*
Ash content slurry [%]	*97,8*
Loss on ignition [%]	*2,2*

$$LOI = 100 - ash\ content\ slurry \quad (4\text{-}1)$$

$$Ash\ content = \frac{output\ weight}{initial\ weight} \quad (4\text{-}2)$$

$$Filler\ amount = \frac{output\ weight}{(100 - LOI)} \quad (4\text{-}3)$$

$$Filler\ content = \frac{filler\ amount}{initial\ weight} \quad (4\text{-}4)$$

4.3 Retention agent

The retention agent Percol from BASF SE is a cationic polyacrylamide and was provided as a dry chemical from Omya GmbH. For the right preparation of the retention agent an Excel file from Omya GmbH with the equations was used. An example is shown in Table 4-8. The stock solution of 150 g was calculated for a sheet weight of 2,4 g (Equation (4-5), (4-6)). The retention agent per handsheet in percentage, the dosage [ml] per handsheet as well as the amount of stock solution [g] are predetermined. The pulverized Percol was measured exactly to receive the desired properties. The retention agent was then dissolved in the deionized water to get a stock solution of 150 g. To get a smooth stock solution the retention agent was stirred with a magnetic stirrer until it was completely dissolved.

$$retention\ agent\ [g] = sheet\ weight\ [g] * \frac{retention\ agent\ [\%]}{100} \quad (4\text{-}5)$$

$$weight\ of\ sample\ [g] = \frac{retention\ agent\ [g] * stock\ solution\ [g]}{dosages\ [ml]} \quad (4\text{-}6)$$

Table 4-8: Sample of retention agent preparation

Stock solution		
Retention agent per sheet	0,075	%
Retention agent per sheet	0,0018	g
Dosages	1,875	ml
Weight of sample taken	0,144	g
Deionized water	149,856	g

The retention agent was prepared three times overall. It was never stored overnight to avoid a change in behavior of the retention agent.

4.4 Industrial refining

The refining was performed in the internal laboratory at Mercer Stendal. A lab refiner (LR40) with a conical refiner from Voith Paper was used to simulate the industrial refining. Before refining the pulp consistency, the output weight and the specific refining energy can be adjusted. The modular design of the lab refiner enables the use of disc and cone refiner plates and can be installed easily. The sampling at various specific refining energy takes place automatically. [20]

For both short fibers and long fibers a consistency of 4 % was adjusted. The specific edge load for long fibers was 1,5 J/m and for short fibers 0,5 J/m.

The refining procedure was carried out as follows and a scheme of the refiner is shown in Figure 4-1. The pulp was added to the pulper and weighed on the integrated scales. Water is then added to reach the required consistency. To warm up the pulp to the operating temperature of 30 °C it is pumped without load through the refiner back to the pulper. After it reaches the operating temperature the refining process starts. The samples were taken automatically when the required specific refining energy is reached. [21]

For long fibers 3 l of pulp was carried out at the specific refining energy at 0, 40, 80 and 120 kWh/t, while short fibers were refined at 60 kWh/t.

At Mercer Stendal for each specific refining energy SR freeness, and water retention value were performed. Afterwards, the pulp was subsequently extracted and transported to Graz.

For the main trial to see the impact of refining and beating on fracture toughness, for each specific refining energy a mixture of 30 % long fiber pulp and 70 % short fiber pulp was put into the distributor. A mixture of 30 % of the long fiber pulp at the specific work at 80 kWh/t and 70 % of the short fiber pulp at 60 kWh/t was used for the main trial to see the impact of filler material on fracture toughness.

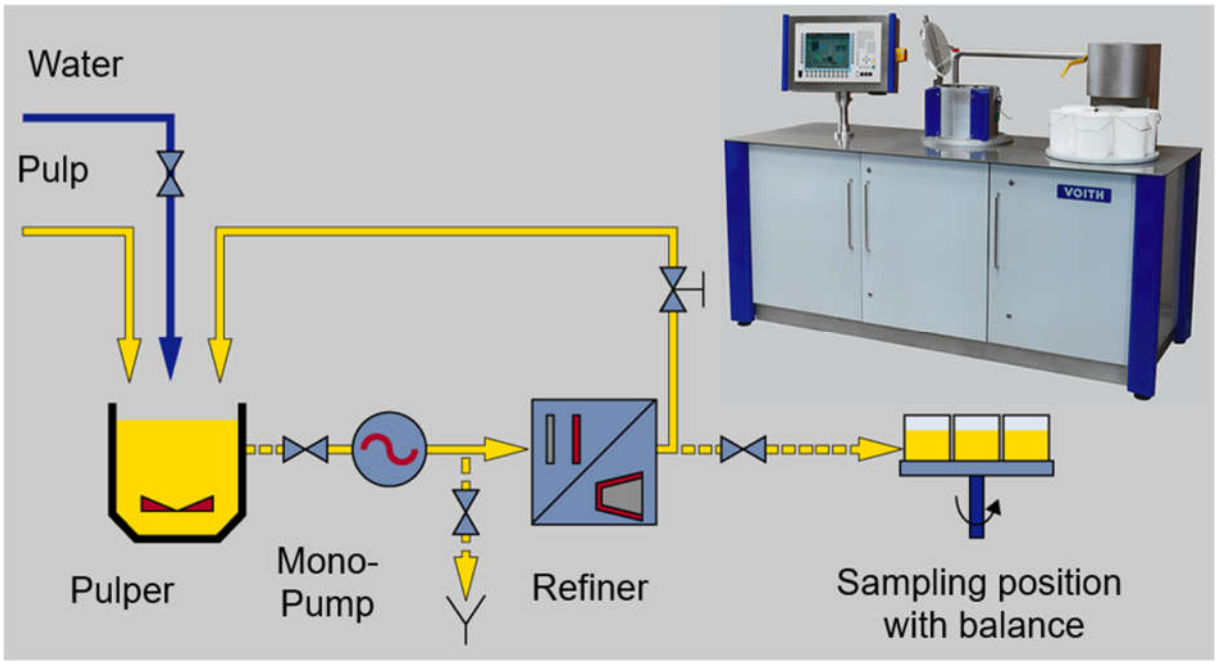

Figure 4-1: Scheme of industrial refiner at Mercer Stendal. [20]

4.5 Lab PFI refining

The lab PFI refining was performed with the PFI mill from Hamjern Maskin A.G. at the technical university Graz. The PFI mill is of the type: MARK IV and follows the standard ÖNORM EN ISO 5264/2.

During the beating process of the PFI mill three primary effects appear:

- Internal fibrillation: by crushing the fibers the internal fiber structure is broken off and the flexibility of the fibers is increasing.
- External fibrillation: with the occurring shear stresses the fiber surface is roughened and fibrils are increasing protruding from the fiber wall.
- Fiber cutting and production of fines.

For each beating 30 g oven-dry pulp were soaked in water for a minimum time of 4 hours and afterwards disintegrated for 10 min and then filtered on a glass frit, until the filtrate is transparent. The resulting filter cake is weighed and filled up with distilled water to 300 ± 5 g. Then it is put against the wall of the housing of the PFI mill. While beating the roll containing the bars is pushed to one side of the housing and the pulp transported through the beating gap between housing and bar. Roll and housing are rotating with different speed. The forces taking effect on the fibers are shear and compression forces in the beating zone. A sketch of a PFI mill and the movement of the housing and roll is shown in Figure 4-2. [22] [23]

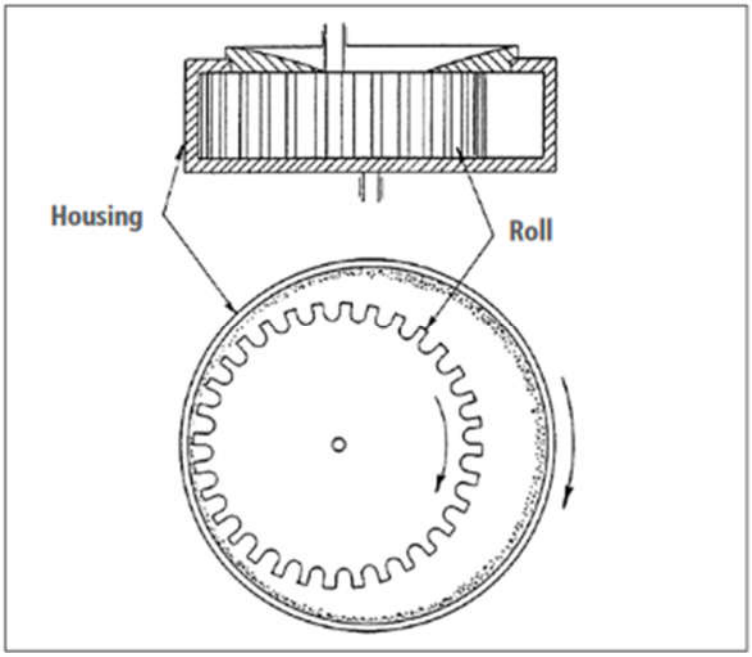

Figure 4-2: Beating element of a PFI mill. [22]

For the lab PFI refining a pre-trial was necessary. The purpose of the pre-trial was to achieve the same tensile strength index for the pulp mixture like the industrial refining. It was performed for long fibers at 400, 700, 1000, 2000 and 3000 revolutions and for short fibers at 400, 700, 1000, 1300 and 1400 revolutions. This is further described in chapter 5.5. The beating for the main trial was performed for the short fibers at 700 revolutions and for the long fibers at 600, 1200 and 1700 revolutions.

Afterwards the pulp was mixed, disintegrated again for 933 revolutions, and then put into the distributor. The mixture of the long fibers and the short fibers was the same as for the industrial refining. 70 % of the short fibers, which were beaten by 700 revolutions, were mixed with 30 % of long fibers beaten at 0, 600, 1200 and 1700 revolutions. For each rotation the SR freeness, and water retention value were measured.

4.6 Pulp recipes for the different trials

For the main-trials (industrial refining, lab refining and filler content) the following pulp mixtures, filler content and retention agents were used.

For the industrial refining two distributor for each specific refining energy were charged. In the first distributor 30 g oven dry pulp was dissolved in 10 l fresh water. For the second distributor 40 g oven dry pulp were dissolved in 10 l fresh water. For both distributors, a pulp mixture of 30 % long fibers and 70 % short fibers was used. The short fibers were refined at 60 kWh/t and the long fibers at 0, 40, 80 and 120 kWh/t.

Table 4-9: First distributor for industrial refining

LF 0 kWh/t **9 g oven dry**		**LF 40 kWh/t** **9 g oven dry**		**LF 80 kWh/t** **9 g oven dry**	
Dry content [%]	15,95	Dry content [%]	19,10	Dry content [%]	15,21
Initial weight [g]	56,43	Initial weight [g]	47,13	Initial weight [g]	59,17
LF 120 kWh/t **9 g oven dry**		**SF 60 kWh/t** **21 g oven dry**			
Dry content [%]	17,97	Dry content [%]	14,56		
Initial weight [g]	50,09	Initial weight [g]	144,23		

Table 4-10: Second distributor for industrial refining

LF 0 kWh/t **12 g oven dry**		**LF 40 kWh/t** **12 g oven dry**		**LF 80 kWh/t** **12 g oven dry**	
Dry content [%]	15,95	Dry content [%]	19,10	Dry content [%]	15,21
Initial weight [g]	75,25	Initial weight [g]	62,83	Initial weight [g]	78,90
LF 120 kWh/t **12 g oven dry**		**SF 60 kWh/t** **28 g oven dry**			
Dry content [%]	17,97	Dry content [%]	14,56		
Initial weight [g]	66,79	Initial weight [g]	192,31		

For the lab PFI refining two distributors for every revolution were charged. For this 40 g oven dry pulp were dissolved in 10 l fresh water. Also, a pulp mixture of 30 % long fibers and 70 % short fibers was used. The short fibers were refined at 700 revolutions and the long fibers at 0, 600, 1200 and 1700 revolutions. For every revolution 30 g oven dry pulp was weighed. For the 0 revolutions of long fibers 12 g oven dry pulp was weighed. After refining the pulp mixture of 40 g oven dry pulp was mixed, which leads to an initial weight for short fibers of 280 g and for long fibers 120 g.

Table 4-11:Pulp used for lab PFI refining

LF 600, 1200, 1700 rev. **12 g oven dry**		**LF 0 rev.** **12 g oven dry**		**SF 700 U** **28 g oven dry**	
Dry content [%]	94,57	Dry content [%]	94,57	Dry content [%]	94,59
Initial weight [g]	31,72	Initial weight [g]	12,69	Initial weight [g]	31,72

For the filler content campaign also a pulp mixture of 70 % short fibers refined in 60 kWh/t and 30 % long fibers refined at 80 kWh/t was used. In the distributor 50 g oven dry pulp are dissolved in 10 l fresh water.

Table 4-12: Pulp used for filler content campaign

LF 80 kWh/t 15 g oven dry		**SF 60 kWh/t 35 g oven dry**	
Dry content [%]	15,11	Dry content [%]	19,17
Initial weight [g]	231,64	Initial weight [g]	78,25

The filler as well as the retention agent are put in the pulp after measuring the amount of pulp suspension for one handsheet. The retention agent dosage was 1,875 ml per handsheet.

Table 4-13: Filler content used per handsheet

0 % Filler	**5 % Filler**	**10 % Filler**	**20 % Filler**	**25 % Filler**	**30 % Filler**
0 g	0,192 g	0,357 g	0,834 g	1,026 g	1,539 g

4.7 Sheetformer

For the handsheet forming the sheetformer Rapid-Köthen (Type: RK4-KWT; EN ISO 5269-2 (2004 12)) was used. The sheetformer automatically runs every sequence and the pulp with or without filler and retention agent was put into the cylinder at about 4 l water level. Before starting the test series, a test sheet was made to get the desired mass of 2,4 g. The test sheet was put in the drying chamber and weighed after a minimum of 10 min with the built in weighting system. The right pulp amount was then calculated, and the test series started.

In the distributors a pulp mixture of 70 % BHKP and 30 % BSKP was used. The BHKP was refined at constant specific refining energy or revolution and the BSKP was refined at varied specific refining energy or revolution. The grammage of the handsheets were expected to be about 80 g/m².

After the test series the handsheets were stored in the climate room for at least 24 h. In the climate room the following tests were performed:

- Grammage: EN ISO 536 (2020 05)
- Thickness: EN ISO 534 (2011 11)
- Air permeability Gurley: EN ISO 5636-5
- Opacity: EN ISO 2471 (2008-12)
- Brightness: ISO 2470 (R457 C)

These tests again were performed for every test series. The grammage and the thickness were then further used in the tensile test and the notched tensile test.

4.8 Determination of Tensile Strength ISO 1924-3

Before the tensile test was performed the test pieces were stored in a controlled climate. The tensile test was conducted following the procedures outlined in ISO 1924-3. Specifically, test pieces measuring 15 ± 0,1 mm in width and a minimum length of 100 ± 2 mm were cut for testing. The tensile properties were then determined with a constant rate of elongation of 100 mm/min.

The outputs of the measuring instrument, which are important for the fracture toughness calculation, include the following material parameters:

Table 4-14: Parameters for the fracture toughness calculation

F_T [N]	tensile force
δ_T [mm]	elongation
W_T^b [J/m²]	tensile energy absorption TEA
E^b [kN/m]	tensile stiffness

The mean values of each output were calculated and from these, the tensile strength σ_T^b [N/m] and strain at break ε_T [%] were determined. The width of the test piece is given with *b* in mm and the length with *l* in mm.

$$\sigma_T^b = \frac{\bar{F}_T}{b} \qquad (4\text{-}7)$$

$$\varepsilon_T = \frac{100\bar{\delta}_T}{l} \qquad (4\text{-}8)$$

The tensile strength, strain at break, tensile energy absorption and tensile stiffness is then further used for the fracture toughness determination.

Because of the different grammages *w* [g/m²] of the used paper grades the tensile strength index σ_T^w [Nm/kg] is used to can compare the paper grades. The tensile strength is simply divided by the grammage.

$$\sigma_T^w = \frac{1000\sigma_T^b}{w} \qquad (4\text{-}9)$$

4.9 Determination of Fracture toughness ISO/TS 17958:2013

To determine the fracture toughness according to ISO/TS 17958:2013, it is necessary to first perform a tensile test of each paper grade. Then a notched tensile test is conducted. Based

on the results of the tensile test and the notched tensile test, the fracture toughness of each strip can be calculated.

The preparation of test pieces for the notched tensile test is described in ISO 1924-3. The difference between notched tensile test and tensile test are the measurements of the test piece and the center notch. For the notched tensile test, the measurements of the test pieces are 50 mm in width, a minimum length of 100 mm and have a center notch of 20 mm. These dimensions of a test strip are shown in Figure 4-3. The center notch is made automatically in the measuring instrument with a built-in notch punch.

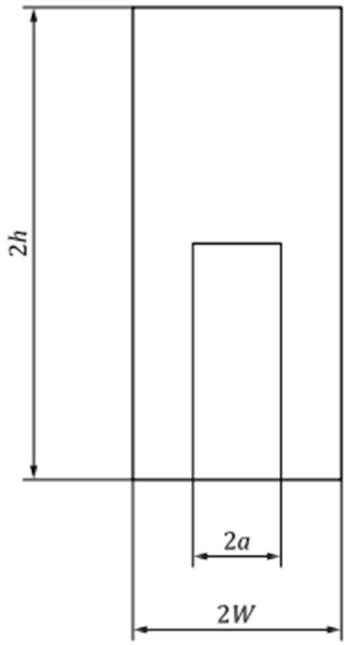

Figure 4-3: Test piece for notched tensile test: 2h=100 mm test piece length between clamps, 2a=20 mm notch length, 2W=50 mm test piece width [16]

The notched tensile test is performed according to ISO 1924-3 with the exception that out-of-plane buckling of the test pieces is prevented in the notched region of the test pieces by anti-buckling guides. The outputs of the measuring instrument are the apparent tensile strength σ_{cr}^{b} [N/m] and the apparent strain at break ε_{cr} [-], both of which are determined without considering that the notched tensile test pieces contain a center notch. Consequently, the apparent tensile strength and the apparent strain at break are lower than the actual tensile strength and strain at break of the material, as the presence of the center notch weakens the test piece. [13] [14] [15]

Before the tensile test was performed the test pieces were stored in a controlled climate. The tensile test was conducted following the procedures outlined in ISO 1924-3. Specifically, test pieces measuring 15 ± 0,1 mm in width and a minimum length of 100 ± 2 mm were cut for testing. The tensile properties were then determined with a constant rate of elongation of 100 mm/min.

The outputs of the measuring instrument, which are important for the fracture toughness calculation, include the material parameters from Table 4-14, chapter 4.8. The strain hardening exponent N [-] (Equation (3-24)) and the strain hardening modulus E_0^b [N/m] (Equation (3-25)), developed in chapter 3.2.3, can then be determined, both parameters represent the material parameters from the tensile test.

The derivation for the calculation of the fracture toughness J_{cr}^b [J/m] (3-33) is described in chapter 3.2.3. The critical net-section stress $\sigma_{ns,cr}^b$ [N/m] (3-29) is determined for every single test piece and the linear elastic geometry parameter f_{el} (3-31) as well as the non-linear geometry parameter f_{nl} (3-32) are determined for one testing series. For a detailed example how fracture toughness is calculated see chapter 3.3.

To compare fracture toughness of the used paper grades the fracture toughness index J_{cr}^w [Jm/kg] is used. It is determined by dividing fracture toughness with the grammage w [g/m²].

$$J_{cr}^w = \frac{1000 J_{cr}^b}{w} \qquad (4\text{-}10)$$

The determination of the fracture toughness of each paper grade was implemented in Excel, which ensured uniformity of the procedure across all measurements and facilitated analysis of the resultant datasets.

4.9.1 Notched tensile tester L&W

During the time of the master thesis a measuring instrument, shown in Figure 4-4, was rented from L&W and installed in the climate room at TU Graz. The instrument is designed to perform both the tensile test as well as the notched tensile test. For this, the measuring instrument features a built-in cutting mechanism for cutting center notches on test pieces. The center notch is made automatically before the test piece is pulled apart. To avoid out-of-plane buckling an anti-buckling guide is installed to the measuring instrument which locks the test piece before the center notch is made.

Figure 4-4: Measuring instrument from L&W for the notched tensile test.

The measuring program utilized for both the tensile test and the notched tensile test is the same. The fracture toughness cannot be measured without a tensile test before. Also, the grammage as well as the thickness of the paper grade must be indicated before measuring. The output is then sent to a laptop connected to the measuring instrument.

4.10 Tearing resistance test Elmendorf EN ISO 1974 (2012 05)

The tearing resistance test by Elmendorf was performed according to ISO 1974 at TU Graz with the A/4 pendulum. The test pieces were cut to sizes of 62 mm in length and 50 mm in width. The test was only performed for the handsheets made at TU Graz.

Before testing the pendulum factor *p* must be identified. For this, the pendulum is put into starting position and the needle to the 0-point of the scale. After releasing the pendulum detent, the deviation to the 0-point can be read. This should not pass the additional tolerance limit. For this work the pendulum factor *p* equals 8.

After the pendulum was caught the reading from the test should be within 20-80 % of the scale-end-value. From one test series the mean value $\bar{x}$ from the readings was constituted. Multiplied with the pendulum factor *p* and divided by the number of sheets tested simultaneously *n* the tear value can be determined:

$$Tear = \frac{\bar{x} \cdot p}{n} \qquad (4\text{-}11)$$

Only for the handsheets with a filler content of 30 % the reading was not in 20-80 % of the scale-end value. For this, the number *n* of sheets tested simultaneously was raised to 2 for the 30 % filler sheets. All other sheets were tested at *n*=1.

5 Results

The paper grades have different grammages and therefore the fracture toughness index and tensile strength index is used to compare them. For comparing the handsheets this is not necessary, because the handsheets all have a grammage of about 80 g/m².

In this chapter the following color code was used for the different paper grades:

Table 5-1: Color code used for the analysis of the results.

Color code		***Paper grades***
	Reference paper	Office paper
		Woodfree base paper
		Kraftliner
		Glassine white
		Glassine yellow
		Glassine orange
	Industrial refining	WT = 0 kWh/t
		WT = 40 kWh/t
		WT = 80 kWh/t
		WT = 120 kWh/t
	Lab PFI refining	Rev = 0
		Rev = 600
		Rev = 1200
		Rev = 1700
	Filler content	Filler content = 0 %
		Filler content = 5 %
		Filler content = 10 %
		Filler content = 20 %
		Filler content = 25 %
		Filler content = 30 %

5.1 Reference-measurements

To facilitate a comparison of the handsheets a reference-measurement with six representative paper grades was conducted. Therefore, an office paper, a woodfree base paper, a kraft liner and three different grammages of glassines were used. The three different glassines also were base papers. The woodfree base paper as well as the kraft liner were organized from Omya GmbH and the three distinct glassines by Mercer.

Table 5-2: Paper grades used in experiments.

Paper grades	***Grammage [g/m²]***
Office paper	80
Woodfree base paper	58
Kraft liner	140
Glassine white	59
Glassine yellow	56
Glassine orange	48

The reference-measurement were also made to obtain a wider range of paper grades for comparison between tear-, tensile and fracture toughness measurements. For comparison fracture toughness measurements of 60 strips in MD and 60 strips in CD were measured. To compare the different paper grades with different grammages the fracture toughness index in *Jm/kg* was used. In Figure 5-1 can be seen that the fracture toughness index in CD is significantly higher than in MD. This is remarkable, as other paper strength properties are always showing a higher strength in MD, i.e., in the direction of fiber orientation. Kraftliner and the three glassines have in MD and CD a higher fracture toughness index than office paper and woodfree base paper.

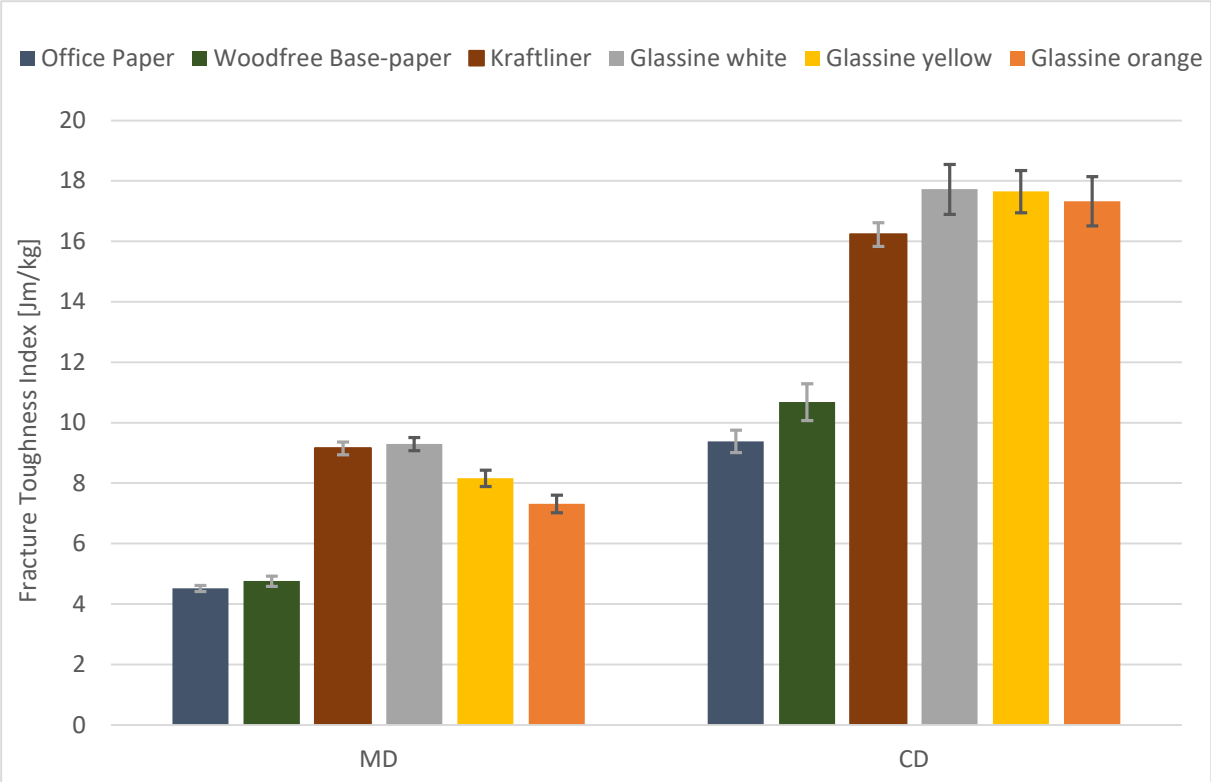

Figure 5-1: Representative paper grades

5.2 Reproducibility-measurement

For the reproducibility-measurement for every paper grade the confidence interval width *CIW* was determined, which is specified in chapter 3.4. Therefore, Equation (3-40) is used to determine the *CIW* for several numbers of samples from 0 to 100. The reproducibility-measurement was performed for the fracture toughness index and the tensile strength index.

According to the ISO standards for both, tensile and fracture toughness [16] a minimum of 10 samples has to be tested to get a good accuracy. In Figure 5-2 we see that 10 samples are way too little to get a *CIW* of 5 %. For almost every paper grade the number of samples must be over 80. Only for kraftliner, office paper and glassine white it needs in any case more than 50 samples to get a *CIW* of 5 %, for many papers even more than 100. If the *CIW* would be increased to 10 % the number of samples would be half the number as for 5 %.

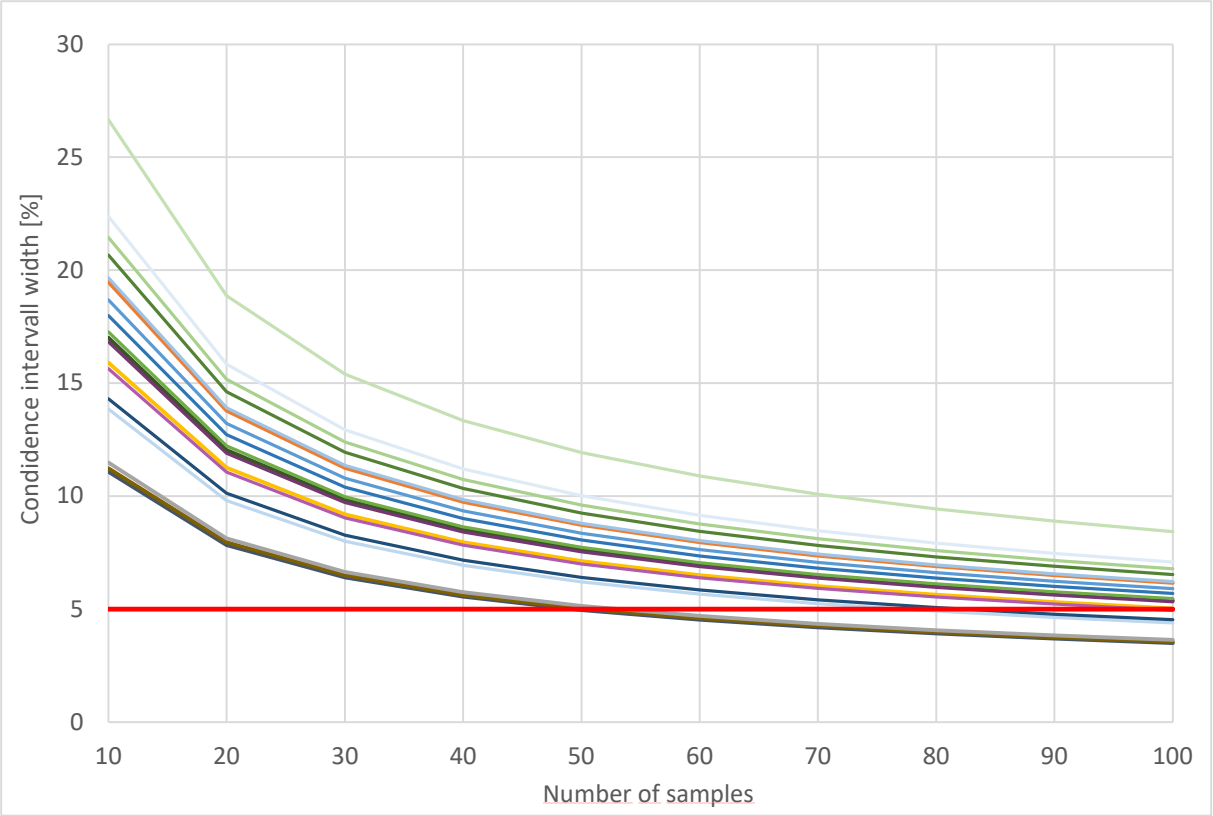

Figure 5-2: Reproducibility-measurement for the fracture toughness index [Jm/kg]

For the tensile strength index the standardized minimum of samples is also 10. For most paper grades this number is too little. But, as it can be seen in Figure 5-3, compared to the fracture toughness index much less samples must be tested to get the same accuracy. A *CIW* of 5 % can be achieved by using at maximum 25 of samples, at minimum less than 10. In fact, it needs 7-9 times less samples to get the same accuracy for tensile strength index.

It can be concluded that measuring fracture toughness requires a much higher effort than measuring tensile strength. First, the test itself requires two measurements (tensile and notched tensile test) and thus much more testing work and sample material (the notched test strips are also about 3 times wider than the tensile test strips). On top of that the measurement uncertainty is about 3 times higher for the fracture toughness measurement, meaning that 7-9 times more samples must be measured to obtain the same precision of the result.

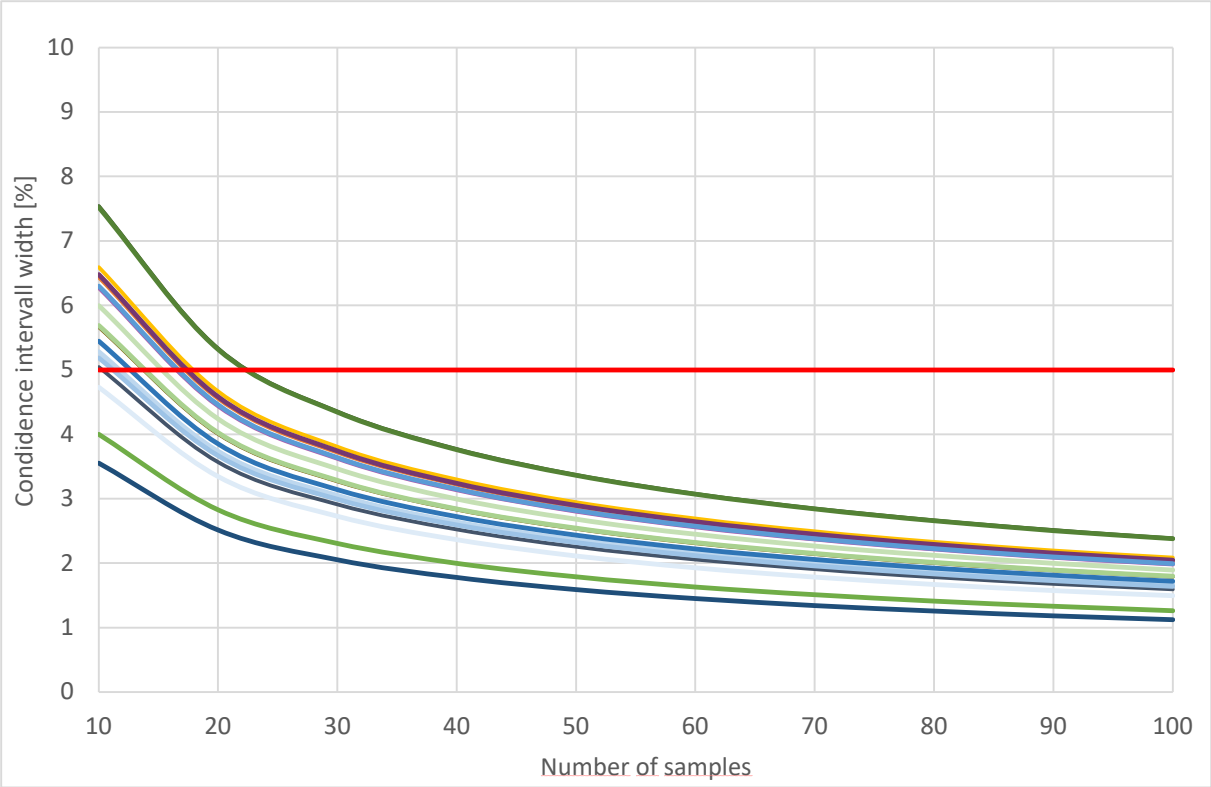

Figure 5-3: Reproducibility-measurement for tensile strength index [Nm/kg]

5.3 Impact of refining

To see the impact of refining two different refining methods were performed. The industrial refining was carried out at Mercer Stendal and the lab PFI refining was carried out at the laboratory at TU Graz. For both a pulp mixture of 70 % BHKP and 30 % BSKP was used to form handsheets with 2,4 g mass and a grammage of about 80 g/m².

With the handsheets the tensile test, notched tensile test and tearing resistance test were performed. From these tests the tensile strength, fracture toughness, and tear are received. These three mechanical properties were then compared to each other, and the results are described in this chapter.

5.3.1 Industrial refining

The industrial refining was performed at Mercer Stendal and was then extracted and carried to Graz to form the handsheets with a pulp mixture of 70 % BHKP and 30 % BSKP. For this, the BHKP was kept constant and the BSKP was varied. The pulp was refined at the following specific refining energies:

Table 5-3: Specific refining energy [kWh/t] for BHKP and BSKP

Specific refining energy [kWh/t]				
BSKP (Referenz)				*BHKP (Eucalyptus)*
0	40	80	120	60

These specific refining energies were defined before the experiments started. In Figure 5-4 the mean values from the industrial refining experiment are given. It can be seen that fracture toughness and tear behave similarly. They both have a local maximum at 40 kWh/t. Tensile strength in contrast increases continuously with increasing specific refining energy.

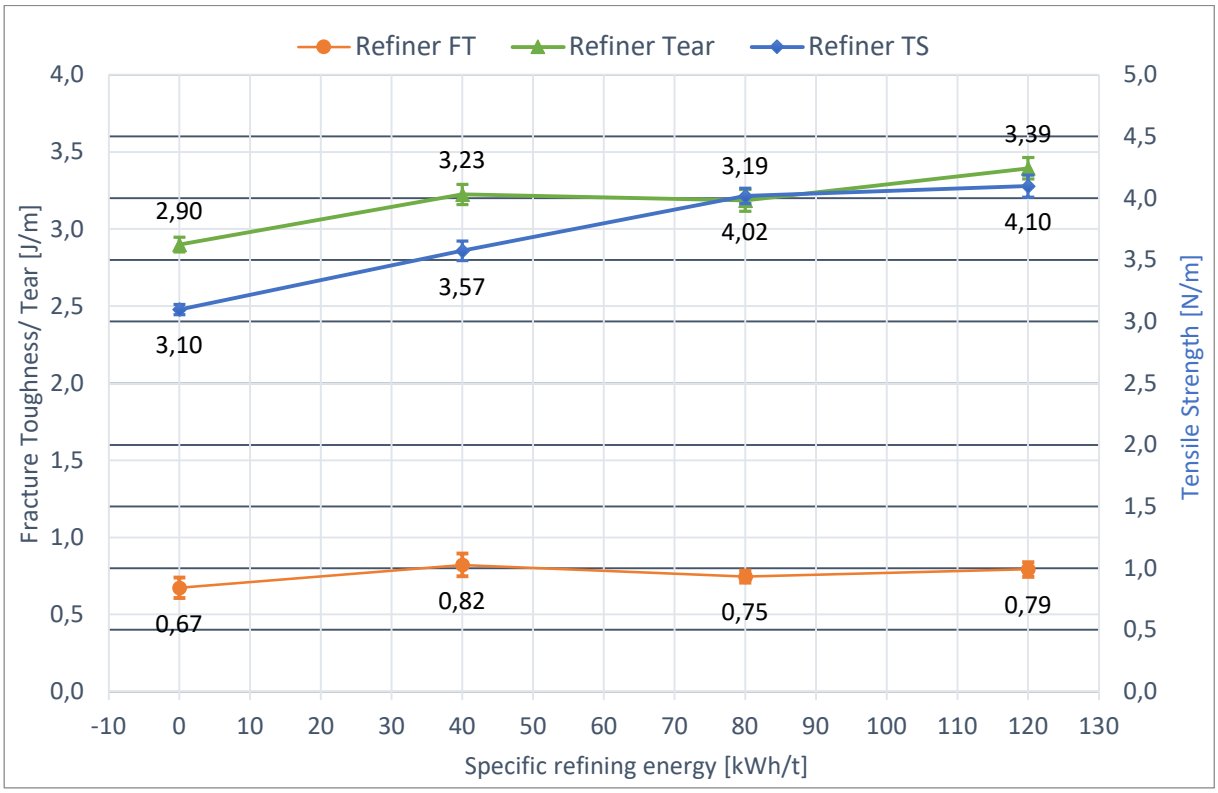

Figure 5-4: Fracture toughness, tear, and tensile strength of industrial refining

The next three figures show the mean values of fracture toughness compared to tear-, and tensile strength, and in Figure 5-7 the mean values of notched tensile strength are compared to tensile strength of the industrial refining experiment.

In Figure 5-5 the mean values of fracture toughness and tear are shown. The highest value for fracture toughness of 0,82 J/m occurs at 40 kWh/t. At this specific refining energy also the tear value of 3,23 N is higher than for 80 kWh/t with a tear value of 3,19 N. This shows the same behavior seen in Figure 5-4. Also, in the middle range of fracture toughness, around 0,75 - 0,8 J/m, tear values between 3,2 N and 3,4 N can be measured – for the various levels of tear there are not extremely high differences in fracture toughness.

For tensile strength (Figure 5-6) in the middle range of fracture toughness the same behavior can be seen. For various levels of tensile strength (3,6 - 4,2 N/m] are not very high differences in fracture toughness. As seen in Figure 5-4 the tensile strength increases with increasing specific refining energy.

What is very interesting is, that the notched tensile strength, from the notched tensile test, correlates very well with the tensile strength, see Figure 5-7. Still the relationship is not linear. This means that the differences between tensile strength and fracture toughness are NOT descending from a difference in material strength in the notched and un-notched test. On the contrary, the strength of the material in the notched case can be well predicted from the un-notched case.

Different to fracture toughness vs. tear and fracture toughness vs. tensile strength both the notched tensile strength and tensile strength varies more. Only for the specific refining energy of 80 and 120 kWh/t have almost identical values for notched tensile strength and tensile strength.

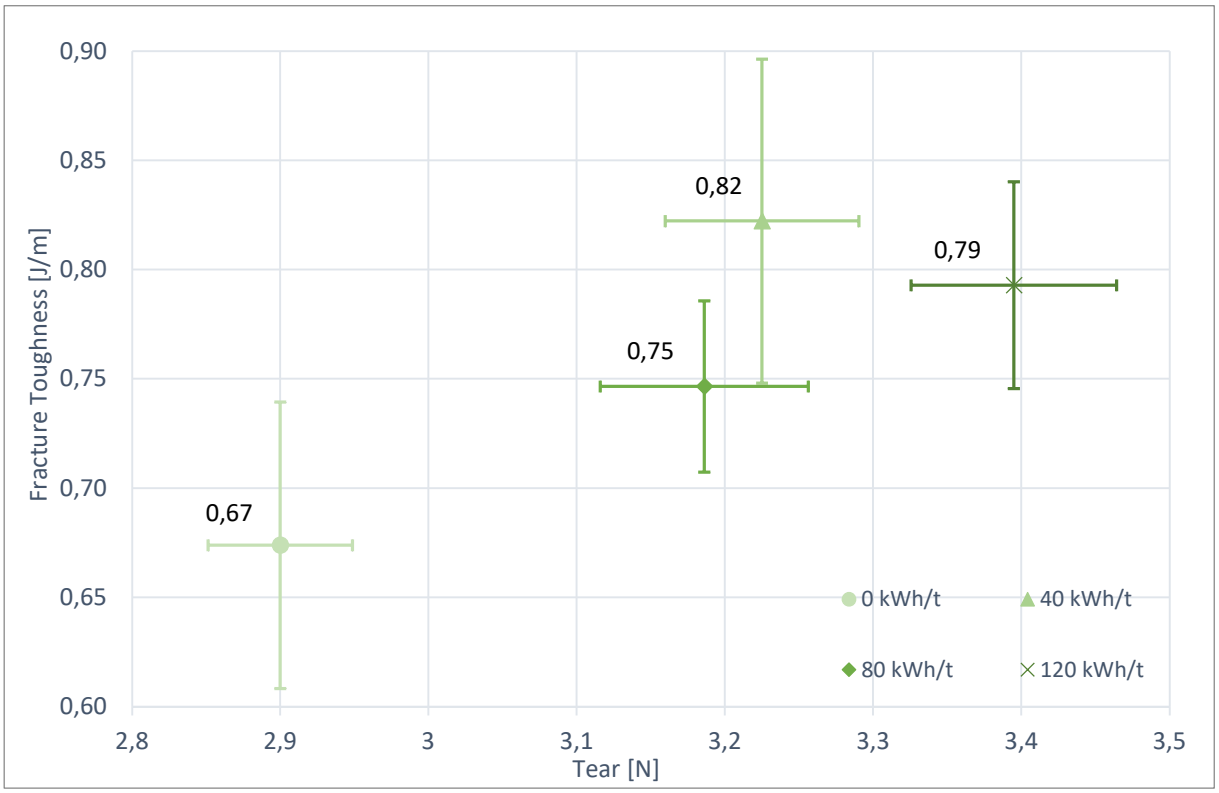

Figure 5-5: Fracture toughness vs. tear for industrial refining

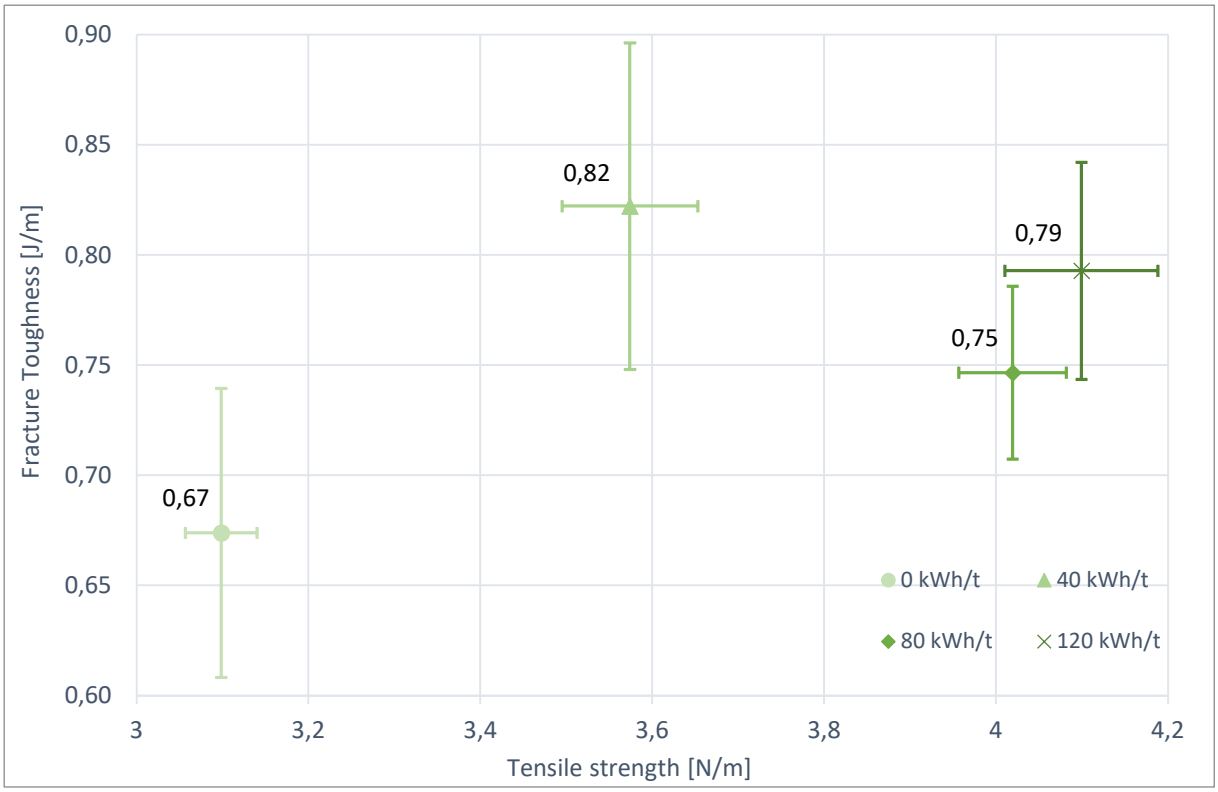

Figure 5-6: Fracture toughness vs. tensile strength for industrial refining

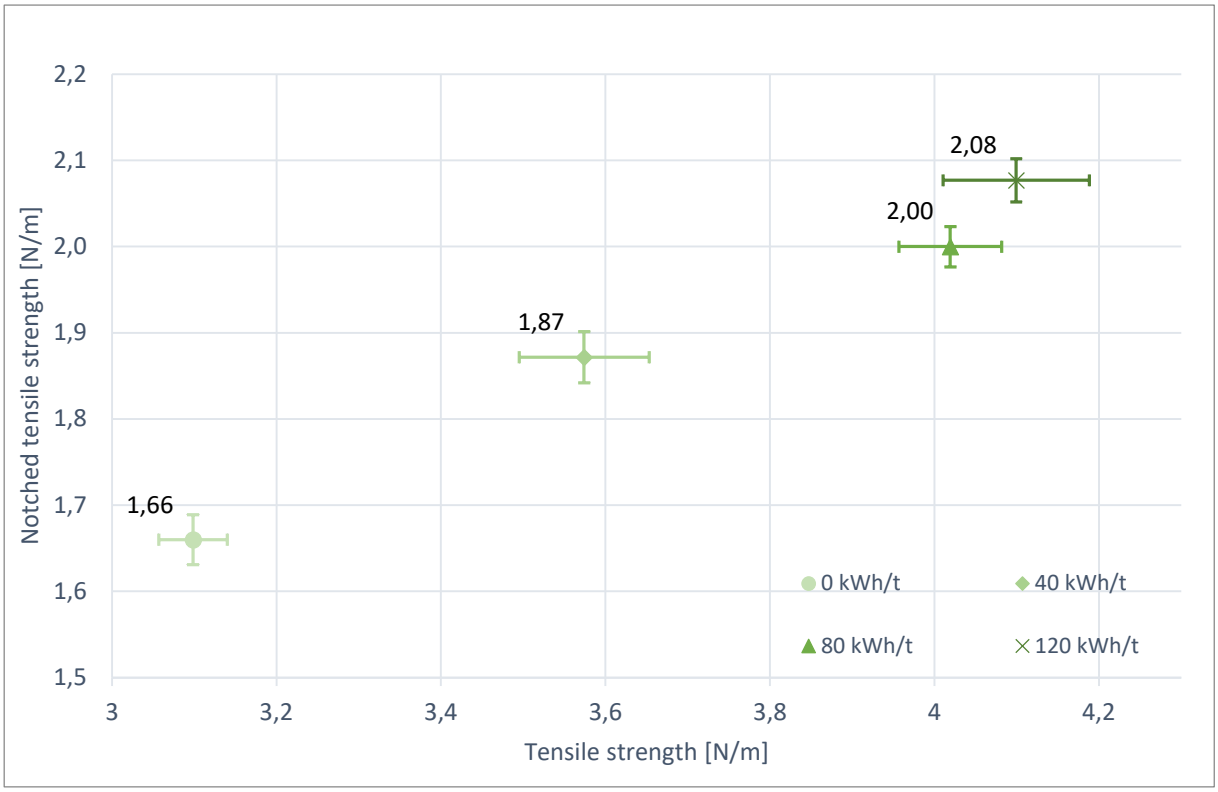

Figure 5-7: Notched tensile strength vs. tensile strength for industrial refining

5.3.2 Lab PFI refining

The lab PFI refining was performed at TU Graz with the pulp provided from Mercer Stendal. To compare the industrial refining with the lab PFI refining a pre-trial was carried out.

Pre-trial

Aim of the pre-trial was to get the same tensile strength index by refining with a PFI mill as by industrial refining. The pulp was refined with the following revolutions. Then, handsheets were formed from this pulp.

Table 5-4: Revolutions for the pre-trial for BHKP and BSKP

BHKP (Eucalyptus)	400 rev	700 rev	1000 rev	1300 rev	1500 rev
BSKP (Referenz)	400 rev	700 rev	1000 rev	2000 rev	3000 rev

With the handsheets a standard ISO test was performed and the tensile strength index for every refining point was determined. The mean values of the tensile strength index were then plotted over the revolutions and the specific refining energy, Figure 5-8. The revolutions for the main trial were determined by intersecting a horizontal line from the industrial refining point with the curve from the PFI refining, compare arrows in Figure 5-8:

Table 5-5: Revolutions for the main-trial for BHKP and BSKP

BHKP (Eucalyptus)	700 rev		
BSKP (Referenz)	600 rev	1200 rev	1700 rev

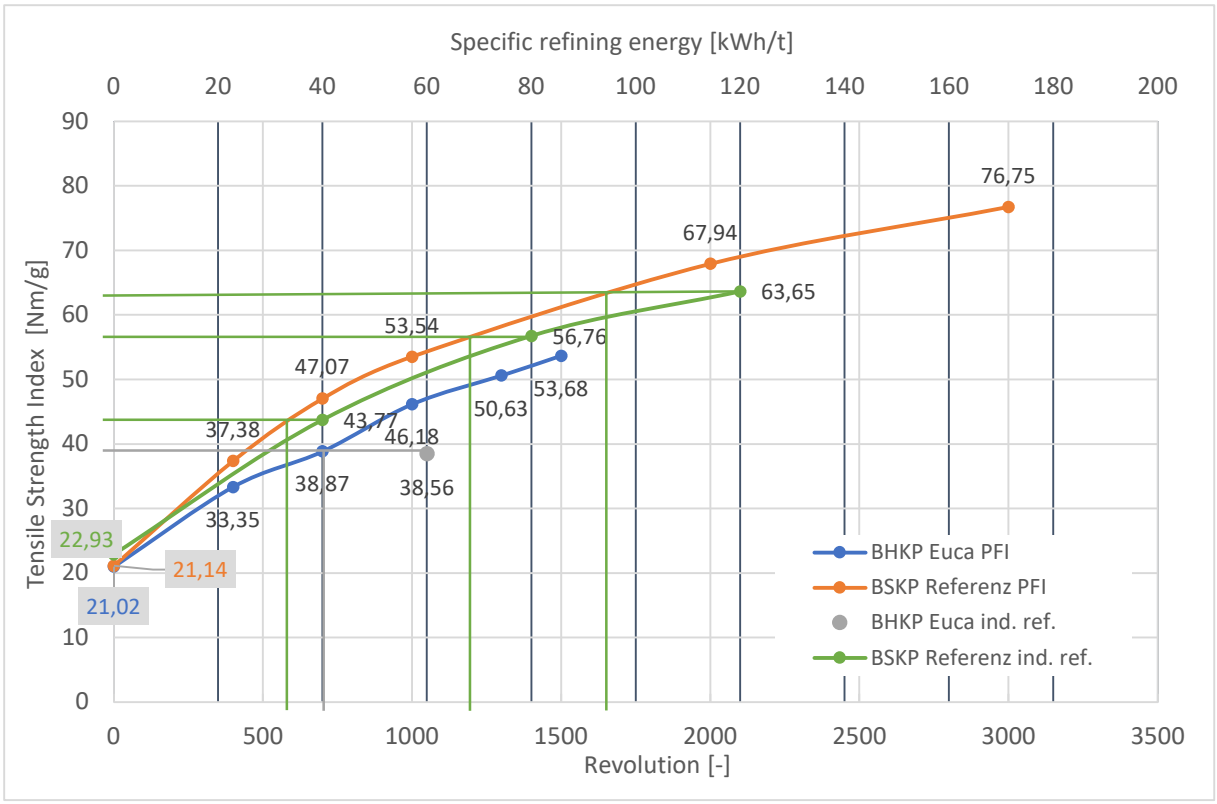

Figure 5-8: Tensile strength index lab PFI refining vs. industrial refining.

Main-trial

For the main-trial a pulp mixture of 70 % BHKP and 30 % BSKP was used to form handsheets. The revolutions for BHKP were constant for every refining point and the revolutions for BSKP varied (Table 5-5). With the handsheets a tensile test, a notched tensile test and a tear resistance test were performed.

Figure 5-9 shows the mean values from fracture toughness, tear, and tensile strength for the lab PFI refining. For the lab PFI refining only fracture toughness shows a local maximum at 600 revolutions. This refining point is comparable to the industrial refining at 40 kWh/t. Tear and tensile strength both continuously increase with increasing revolutions.

The mean values for fracture toughness, tear, tensile strength and notched tensile strength are plotted in Figure 5-10 - Figure 5-12.

Fracture toughness compared to tear (Figure 5-10) shows the same local maximum at 40 kWh/t than for industrial refining. However, the same behavior in the middle range of fracture toughness as for industrial refining can be seen, at 0,44 J/m a tear between 2,7 N to 3,1 N can be found. The same behavior can be seen for tensile strength in the middle range of fracture toughness (Figure 5-11).

The values of fracture toughness do not vary very much for the laboratory refining. The lowest value is 0,41 J/m and the highest 0,50 J/m. This is a change of only 0,09 J/m for increasing revolutions.

In Figure 5-12 again an excellent relationship between notched tensile strength and tensile strength is shown, the relation is also quite linear. In fact, the notched tensile strength is about ½ of the tensile strength. Also, the values for notched tensile strength and tensile strength are varying more, e.g., for low revolutions the value for both the notched tensile strength and tensile strength is in the lower range.

Summarizing the findings from the industrial- and lab refining trials a moderate correlation between fracture toughness and tear/tensile strength can be found. It is interesting that at low refining intensities (40 kWh/t and 600 rev.) a nonlinear increase in fracture toughness shows.

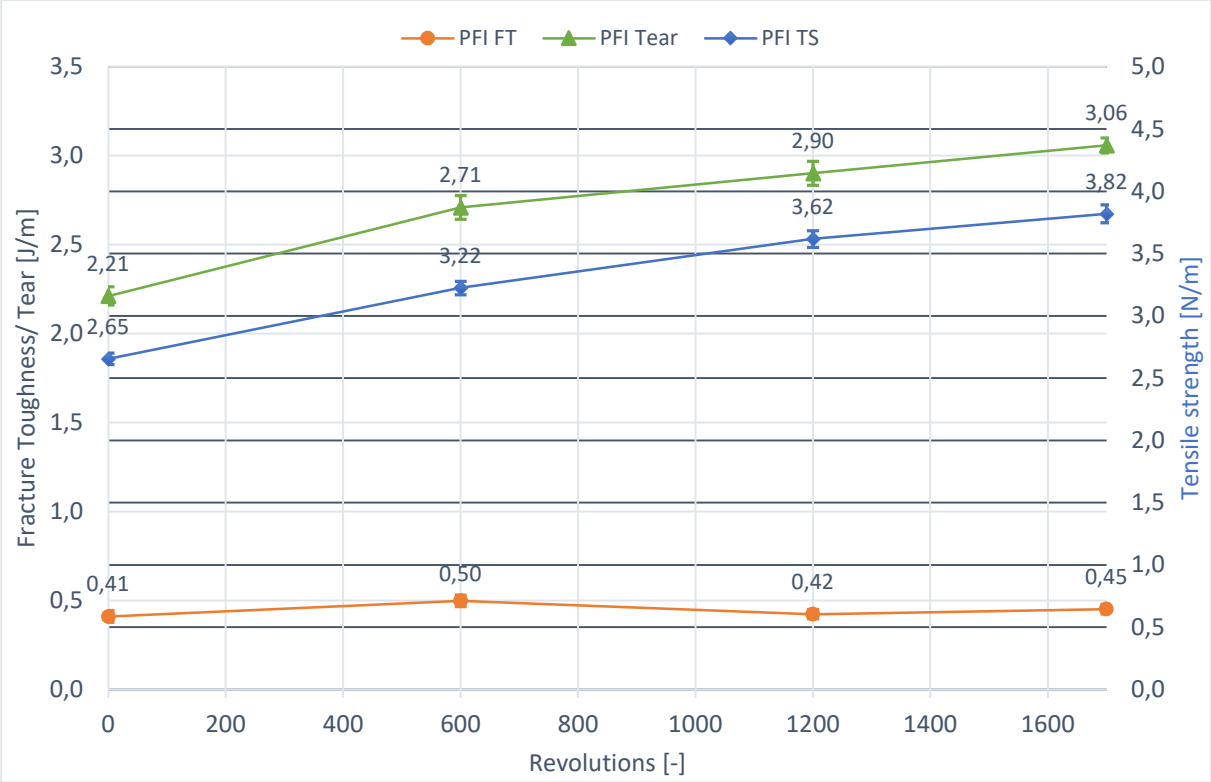

Figure 5-9: Fracture toughness, tear, and tensile strength of lab PFI refining

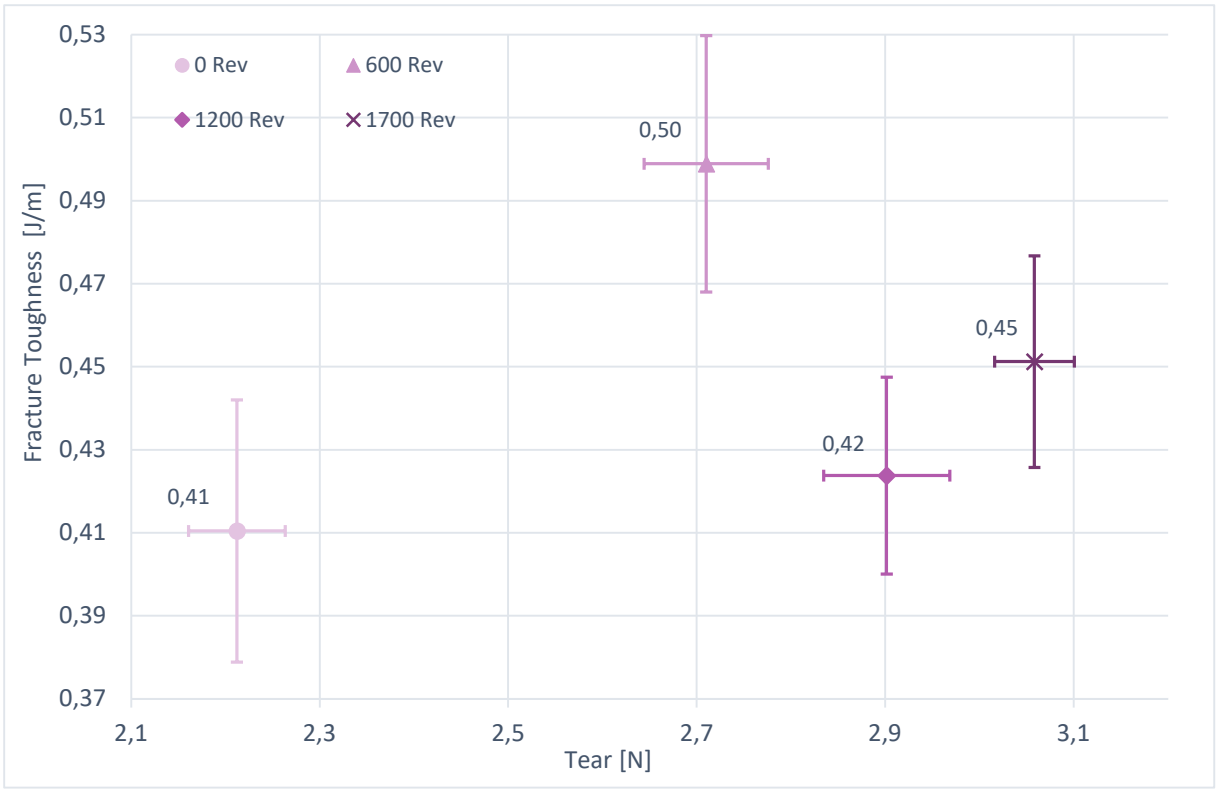

Figure 5-10: Fracture toughness vs. tear for lab PFI refining

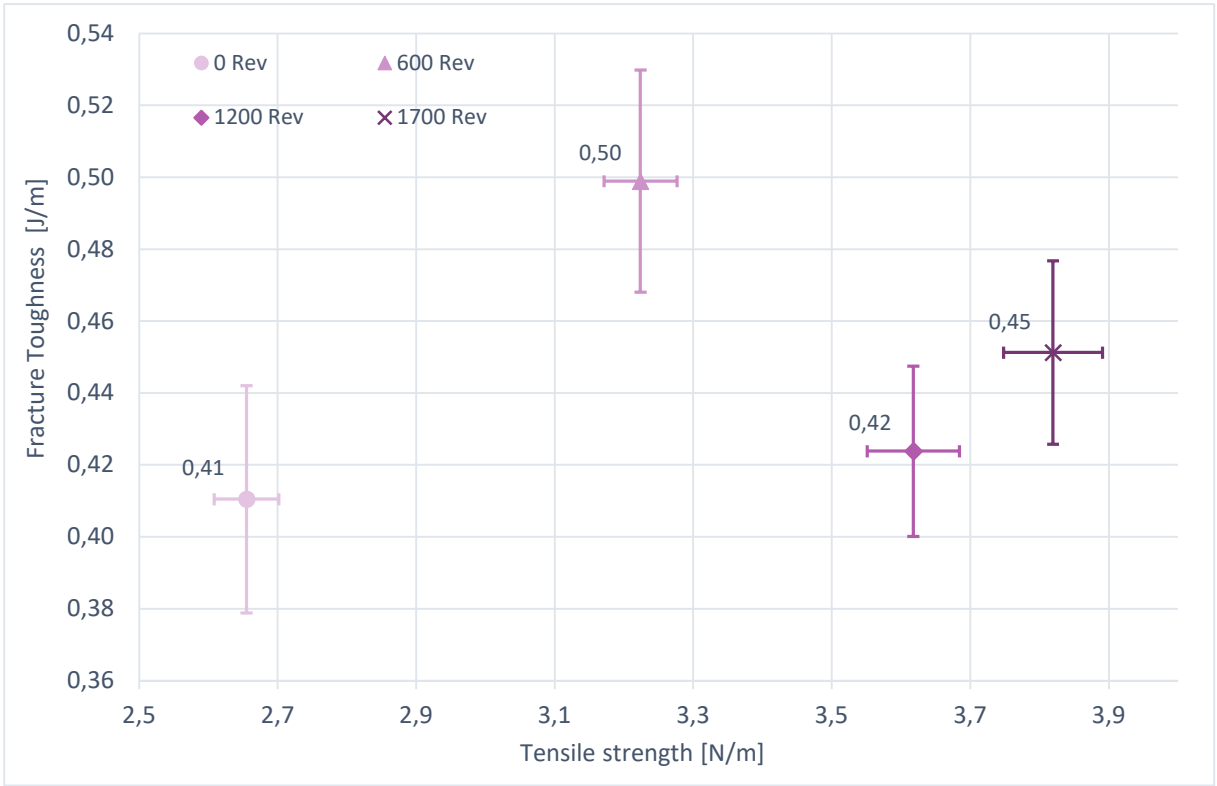

Figure 5-11: Fracture toughness vs. tensile strength for lab PFI refining

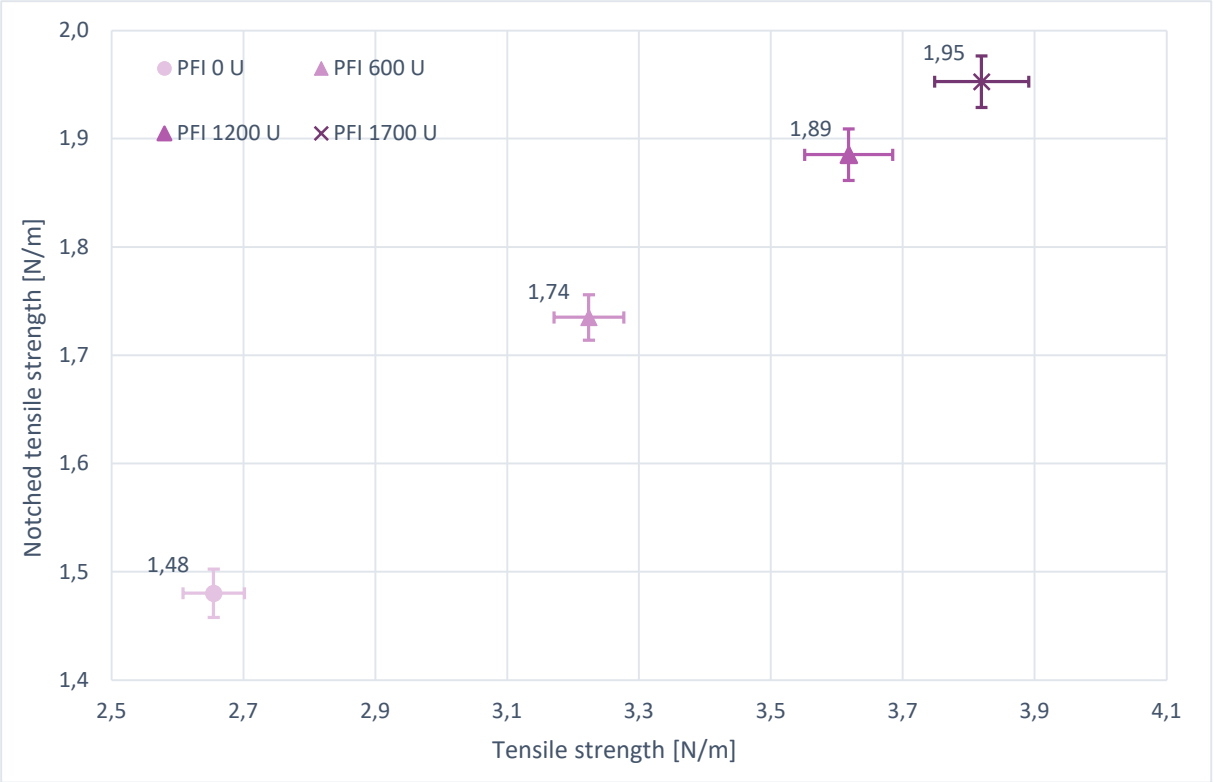

Figure 5-12: Notched tensile strength vs. tensile strength for lab PFI refining

5.4 Impact of filler

The motivation for this experiment was to see if fracture toughness, tear or tensile strength are behaving similar or differently with increasing filler content.

The pulp for the experiment was provided from Mercer Stendal with a specific refining energy of 60 kWh/t for BHKP and 80 kWh/t for BSKP. Omya GmbH provided the filler and the retention agent. The handsheets were formed with a pulp mixture of 70 % BHKP and 30 % BSKP. The filler and the retention agent were added separately for every handsheet. For the right retention agent dosage, a pre-trial was performed.

5.4.1 Pre-trial

The aim of the pre-trial was to determine the amount of filler necessary to achieve a 20 % filler content in the sheets and the ideal retention agent dosage used for the main-trial. This trial was conducted without the use of a retention agent and then repeated with retention agent.

Without retention agent

For the first attempt a retention of 50 % was presumed which leads to a filler amount of 0,937 g and a sheet weight of 1,916 g. Based on the dry content of the filler material, the initial weight was calculated. However, the initial amount of filler material was insufficient, and the filler

material was increased until the sheet attained a weight of approximately 2,4 g. To achieve the target sheet weight, the filler content had to be raised to 30,039 g and was obtained on the 10th trial, as illustrated in blue in Figure 5-13. This resulted in a sheet weight of 2,393 g.

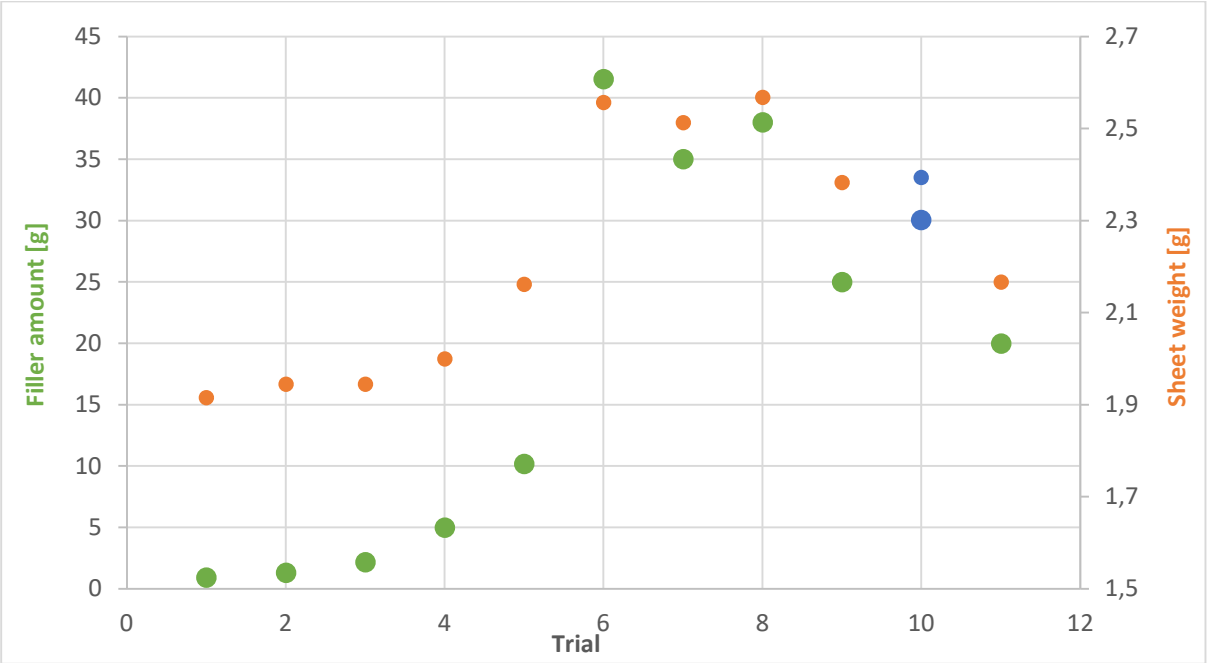

Figure 5-13: Filler amount to get 20 % filler content.

With retention agent

The purpose of this pre-trial was to determine the appropriate dosage of retention agent for the main trial by varying the retention agent and the filler content from one attempt to another. The 7th attempt resulted in a sheet weight of 2,398 g with a filler material application of 0,769 g and a retention agent application of 1,875 ml. Thus, for the main-trial 1,875 ml of the retention agent was applied. It must be noted that this amount of retention agent was added to all handsheets, 0 % filler to 30 % filler. In this way a possible influence of the retention agent on the results has been eliminated.

Table 5-6: Retention agent dosage for the main-trial

	Application filler [g]	***Application retention agent [ml]***	***Output weight after drying chamber [g]***
R1	0,616	1,500	2,266
R2	0,616	1,625	2,237
R3	0,615	1,750	2,264
R4	0,613	1,875	2,335
R5	0,614	2,500	2,274
R6	0,769	1,875	2,331
R7	0,898	1,875	2,398

5.4.2 Main-trial

The handsheets with filler and retention agent were analyzed and the tensile test, notched tensile test and tearing resistance test were performed. From these tests the tensile strength, fracture toughness, and tear are received. Assuming a retention of 50 % leads to higher filler amounts needed in the pulp suspension. The higher the filler content gets the higher the amount of filler needed for a handsheet is. The used filler amount for the varied filler content is given in Table 4-6 and the retention agent dosage is received from the pre-trial.

The results for mean values of the mechanical properties fracture toughness, tensile strength and tear are plotted in Figure 5-14. All three mechanical properties decrease linearly with increasing filler content. Fracture toughness decreases slightly faster than tensile strength and tear. In contrast to refining, fracture toughness behaves similar like tear and tensile when adding filler. Apparently fracture toughness is developing differently from tear and tensile in refining, but not when changing filler content.

In Figure 5-15 the mean values of fracture toughness are plotted over tear. For filler content the test series are more different than for refining. This leads to a different behavior of the relationship between fracture toughness and tear. The values for tear and fracture toughness vary over the range. For example, for a low fracture toughness a low tear value is received. The higher the filler content the lower the fracture toughness values and the tear values.

Tensile strength behaves the same as tear. With higher filler content lower tensile strength values are received. Fracture toughness vs. tensile strength is shown in Figure 5-16.

For notched tensile strength plotted over tensile strength the behavior is the same as for the test series of industrial refining and lab PFI refining. This means the relationship between notched tensile strength and tensile strength is almost linear. Notched tensile strength increases with decreasing filler content, e.g., the lowest notched tensile strength values and tensile strength values are received for a filler content of 30 %.

The behavior seen in Figure 5-14 for fracture toughness, tear and tensile strength can be verified plotting fracture toughness over tear and tensile strength (Figure 5-15, Figure 5-16). Also, the relationship of notched tensile strength and tensile strength seen for the refining trials can be verified.

In summary the correlation between fracture toughness and tear/tensile strength is much better for various levels of filler content, than for different levels of refining. It seems that fracture toughness is linearly related to filler content, but not to refining intensity.

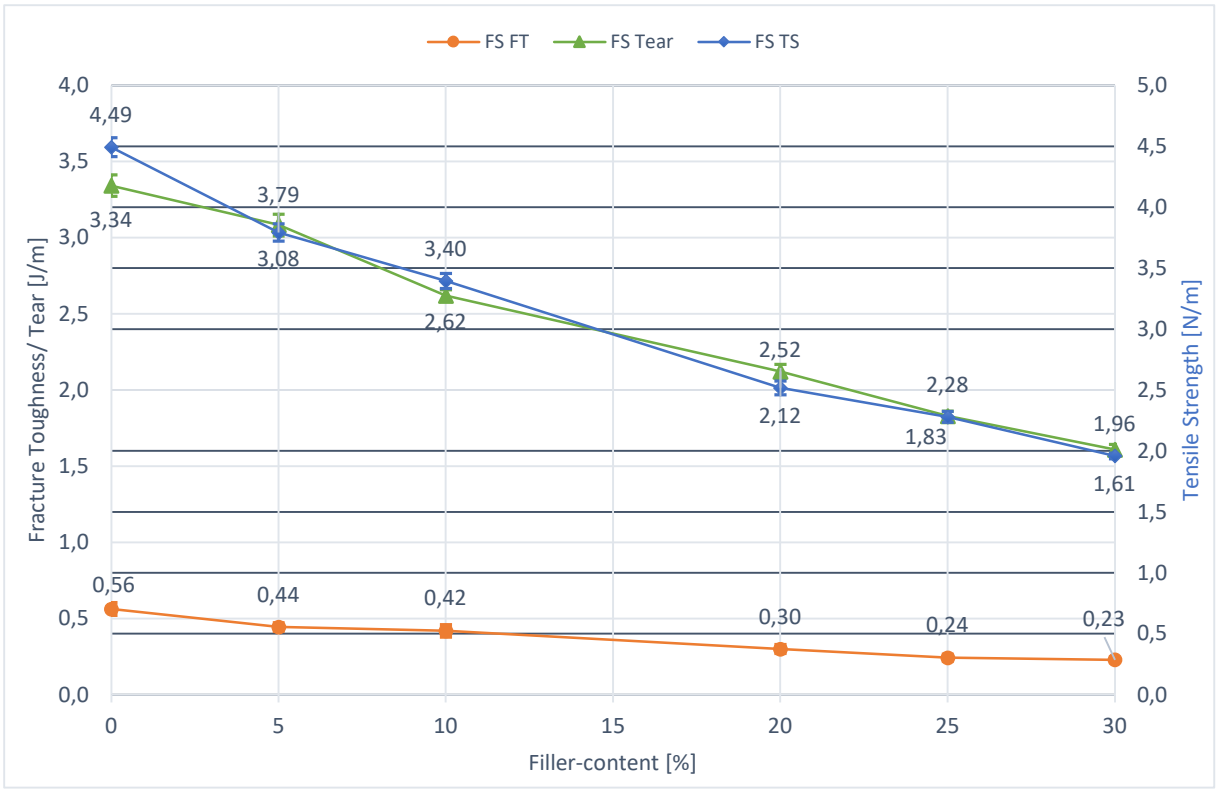

Figure 5-14: Fracture toughness, tear, and tensile strength as a function of filler content

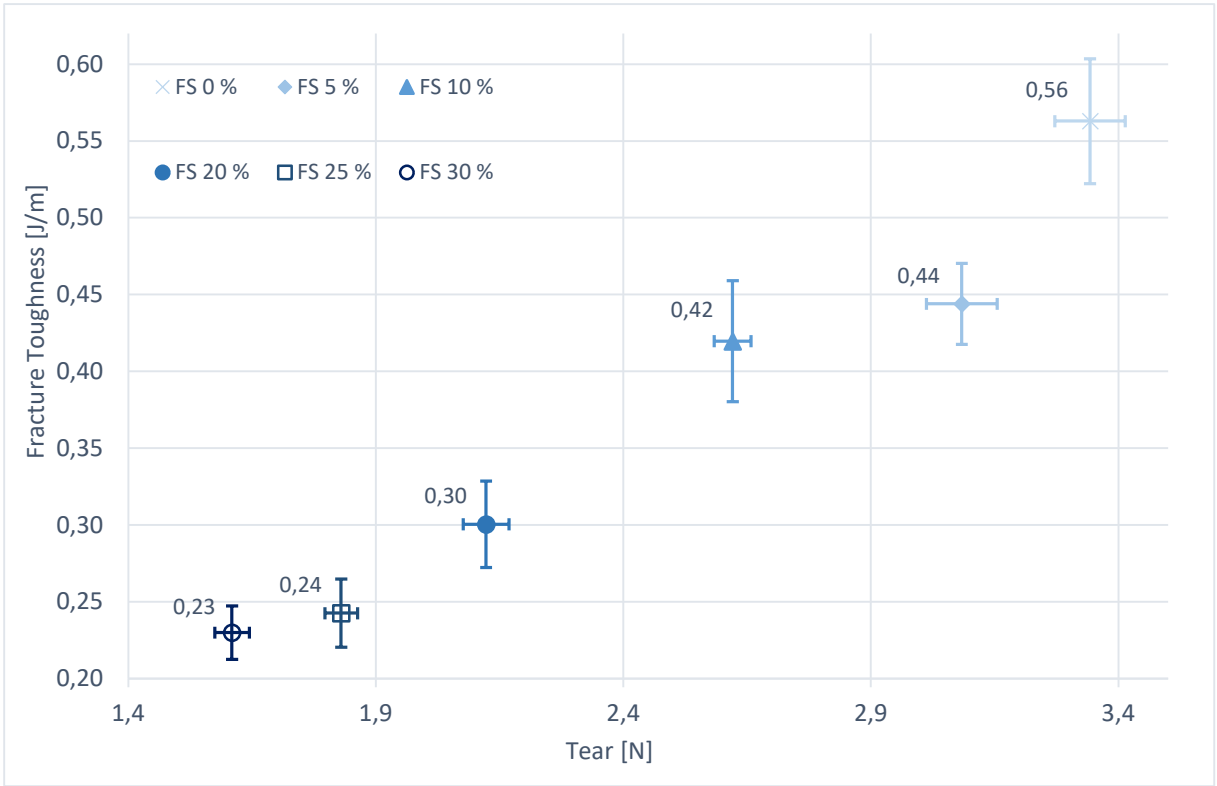

Figure 5-15: Fracture toughness vs. tear of filler content

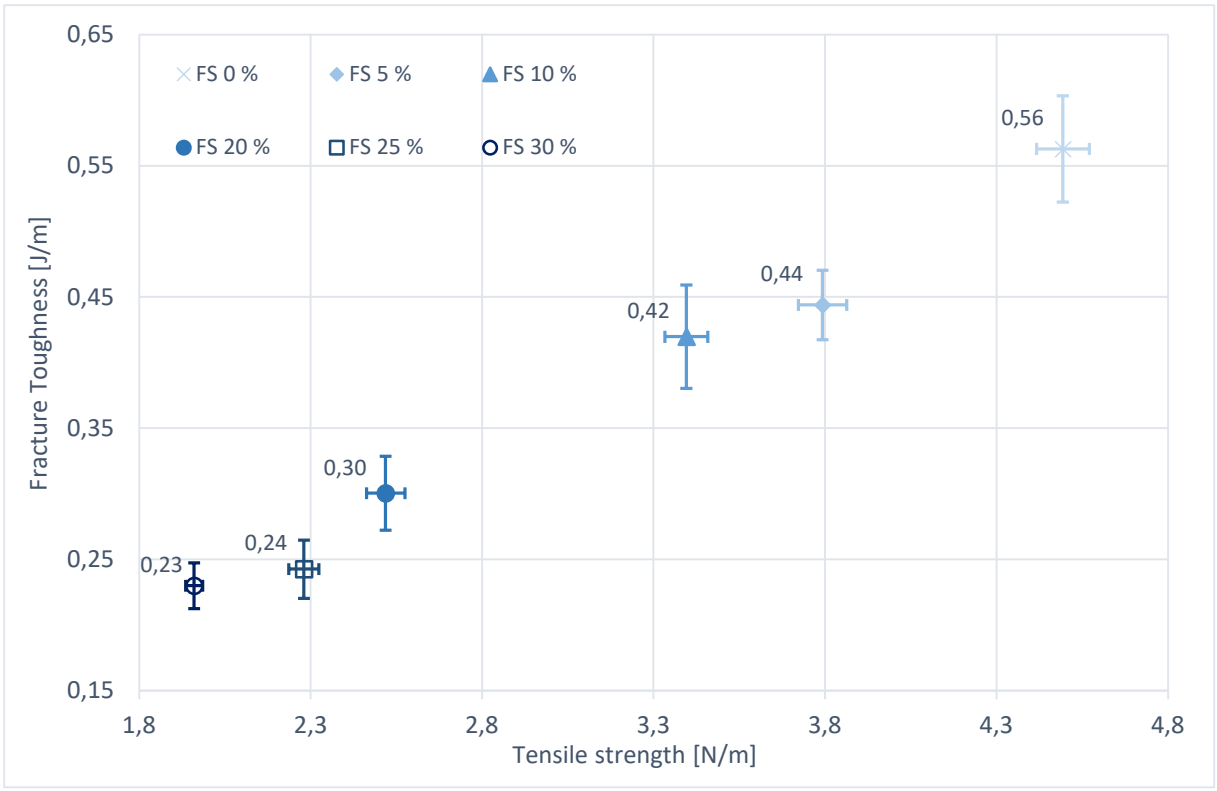

Figure 5-16: Fracture toughness vs. tensile strength for filler content

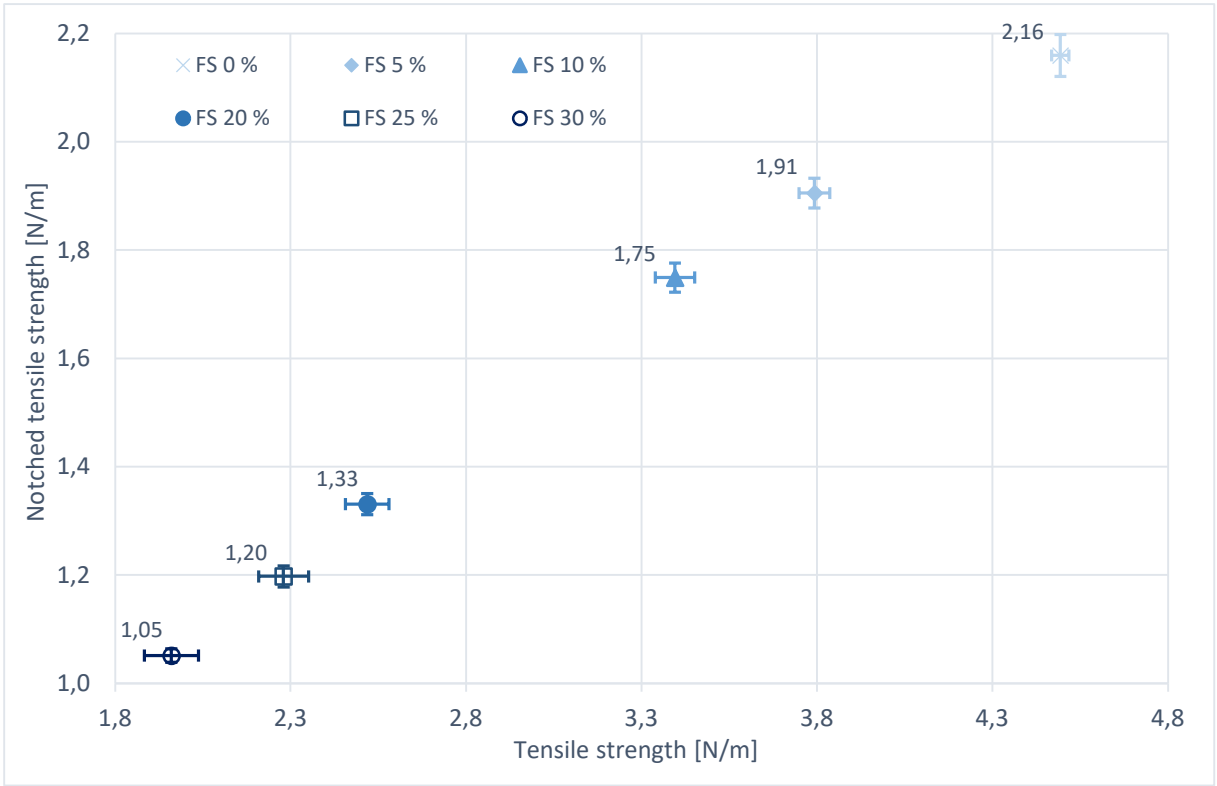

Figure 5-17: Notched tensile strength vs. tensile strength for filler content

Filler retention

After the main-trial was finished the filler content was determined. For this, pieces of the remaining handsheets were put in the oven for 5 h at a temperature of 575 °C. A perfect filler retention would result exactly in the filler content that was desired. As it can be seen in Table 5-7, for filler content 5-25 % the filler retention is lower than the desired filler content but reaches almost the desired values. Only for 30 % the filler retention is higher. It must be considered that the pulp itself has an ash content of 0,1 % to 0,3 %. This is not considered in these results.

Table 5-7: Filler-content

	5 %	***10 %***	***20%***	***25 %***	***30 %***
Initial weight [g]	4,40	4,40	4,31	4,76	4,66
Output weight [g]	0,21	0,38	0,83	1,11	1,45
Ash content [%]	4,80	8,71	19,35	23,33	31,04
Filler amount [g]	0,22	0,39	0,85	1,14	1,48
Filler content [%]	4,90	8,91	19,78	23,85	31,73

5.5 Refining individual values

To see the impact of refining for the different fiber lengths (Short fibers and long fibers), handsheets were formed with short fibers BHKP and long fibers BSKP. With these handsheets the same tests, tensile test, notched tensile test, and tear resistance test, were performed. BHKP and BSKP were refined at the following specific refining energy:

Table 5-8: Specific refining energy for refining points

Short fibers BHKP (Eucalyptus)	30 kWh/t	60 kWh/t	90 kWh/t
Long fibers BSKP (Referenz)	40 kWh/t	80 kWh/t	120 kWh/t

In Figure 5-18 the mean values of the mechanical properties are plotted over the specific refining energy. Generally, fracture toughness, tensile strength, and tear are lower for the short fibers BHKP. All three mechanical properties increase with a lower slope than for the long fibers BSKP. Fracture toughness increases for both short and long fibers with the lowest slope. The tear values for long fibers first increases to a maximum at 40 kWh/t and then decreases with increasing specific refining energy. The maximum at 40 kWh/t is the same behavior which occurs at 40 kWh/t for tear at the industrial refining with the 70/30 pulp mixture. Contrary to this, the tear value for short fibers increases with increasing specific refining energy.

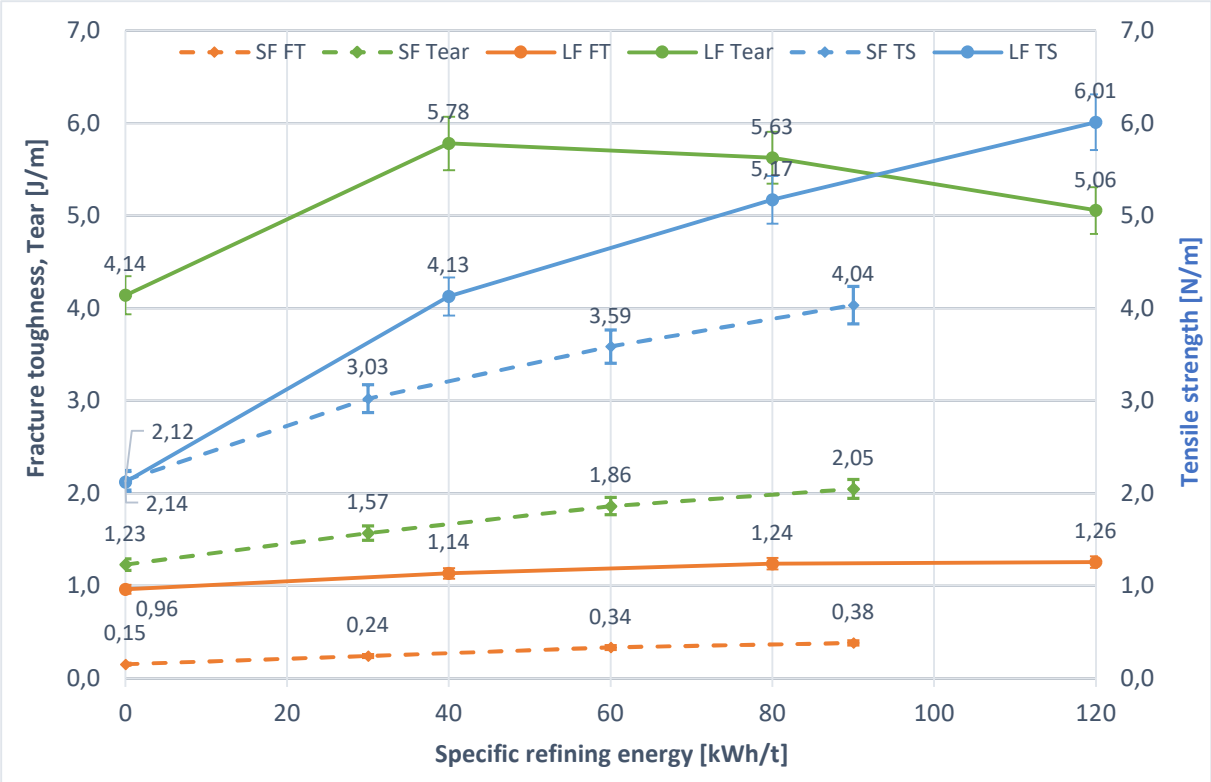

Figure 5-18: Individual values of industrial refining

5.6 Fracture toughness vs. Tear vs. Tensile strength

This chapter summarizes all mean values for all paper grades used in the experiment. Fracture toughness is compared to tear and tensile strength. Also, notched tensile strength is compared to tensile strength.

Figure 5-19 shows the mean values of fracture toughness index of the paper grades used in the experiments. For this, for the fracture toughness index of the paper grades used as reference for the handsheets the geometric mean from MD and CD was determined, because for CD, the fracture toughness index was higher than for MD. The geometric mean then can be compared to the fracture toughness index of the handsheets. The paper grade glassine white has the highest value of all, and together with glassine yellow and orange, and the kraftliner these four make the maximum. The outlier at 40 kWh/t from industrial refining can be seen. However, the outlier from lab PFI refining at 600 revolutions disappears for fracture toughness index.

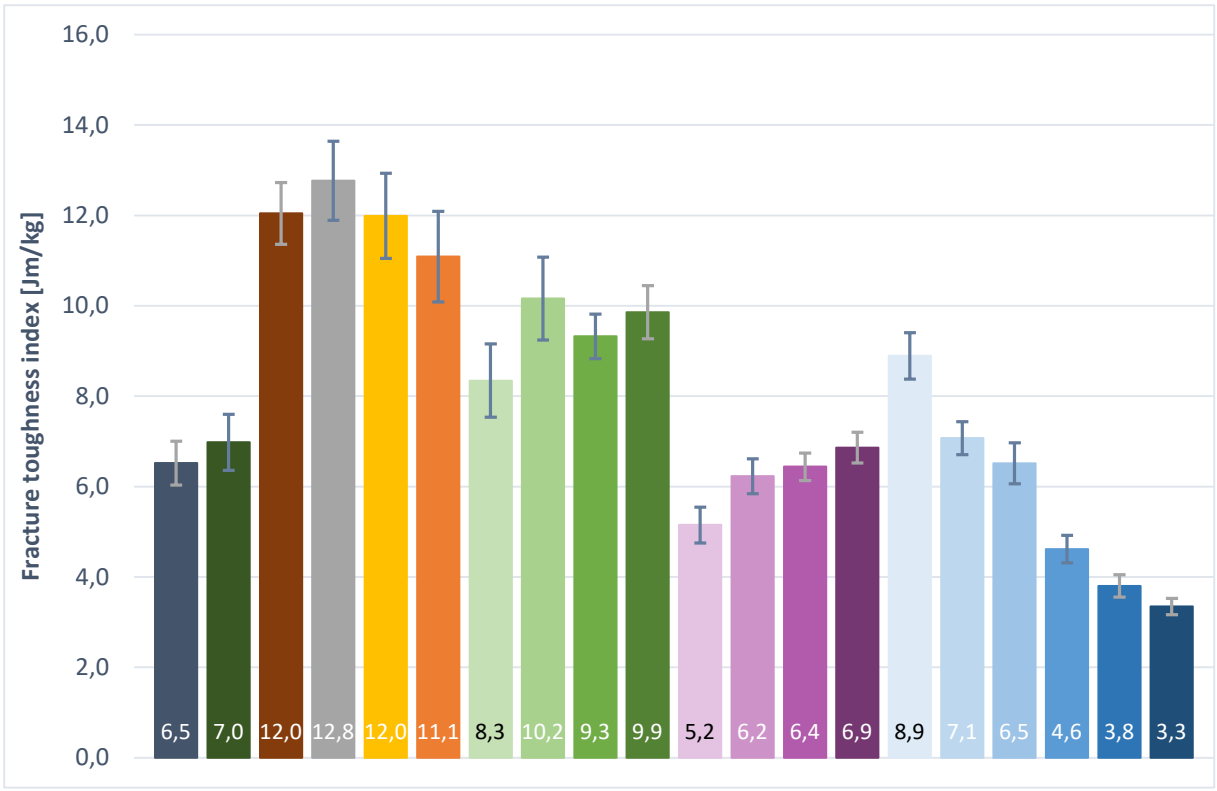

Figure 5-19: Fracture toughness index of paper grades used in the experiments.

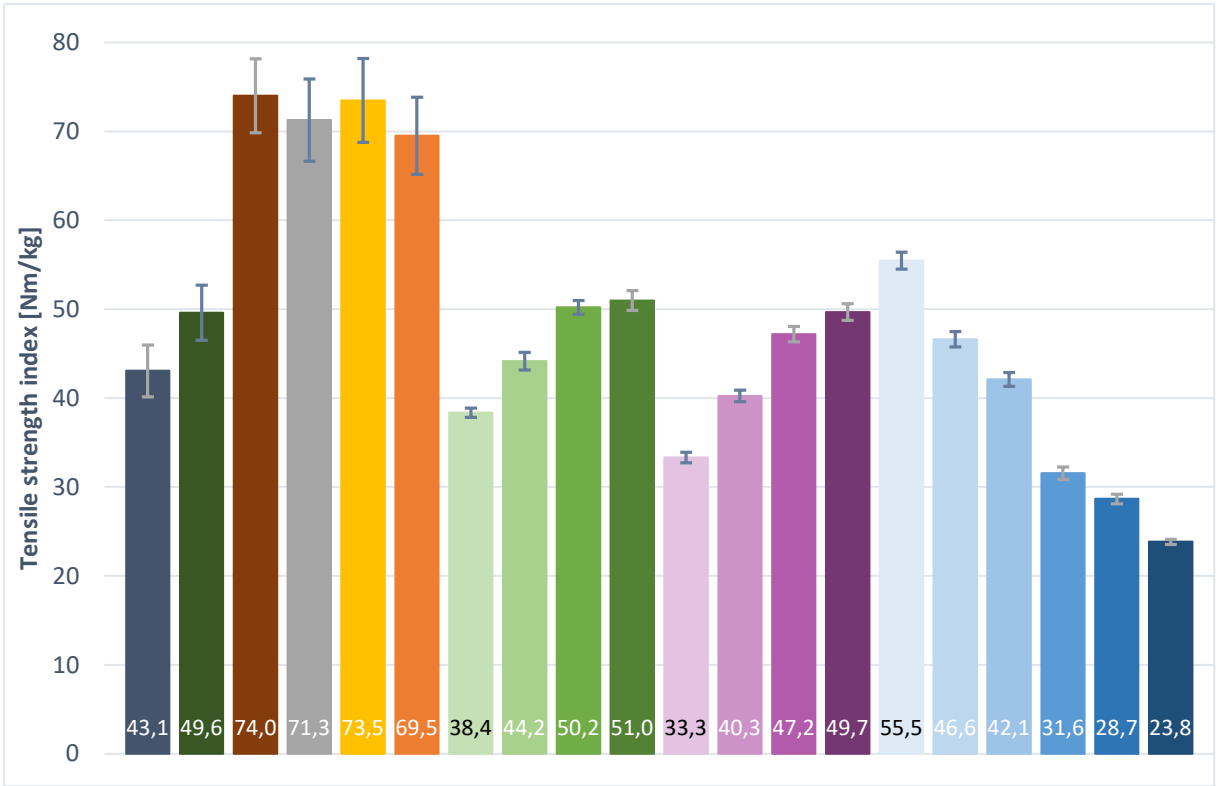

Figure 5-20: Tensile strength index of paper grades used in the experiments.

For tensile strength (Figure 5-20), kraftliner and the three different glassine make the maximum, but other than for fracture toughness the kraftliner has the highest value of all. The tensile strength for industrial refining and lab PFI refining is nearly the same. This does not occur for fracture toughness and tear.

The mean values for notched tensile strength, given in Figure 5-21, shows almost the same behavior as tensile strength. However, the confidence interval width of notched tensile strength is clearly higher than for tensile strength. Also, the values for notched tensile strength are almost ½ of tensile strength for every paper grade.

As mentioned before, the tearing resistance test was only performed for the handsheets. The tear value for industrial refining also shows the outlier at 40 kWh/t (Figure 5-22).

Fracture toughness, tensile strength, tear and notched tensile strength for the handsheets with filler does not show any unexpected behavior and are therefore not further described. For every mechanical property, the values decrease with increasing filler content.

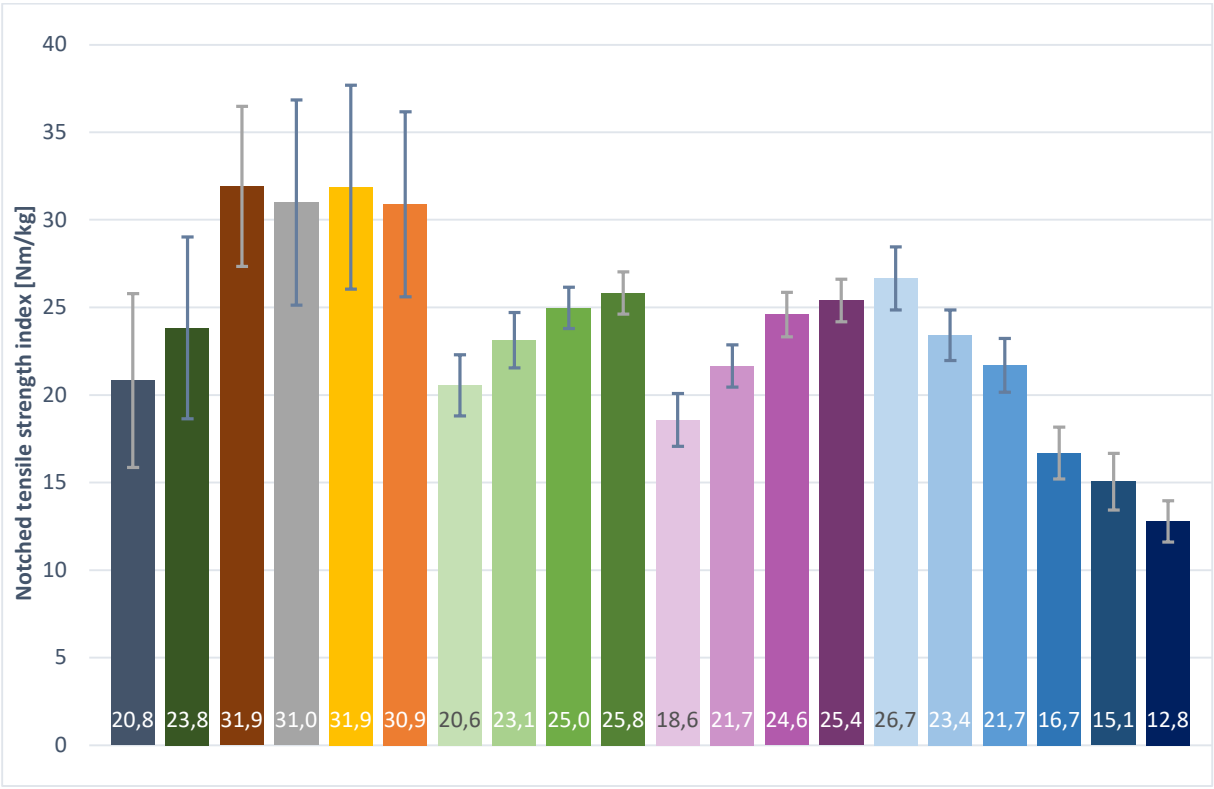

Figure 5-21: Notched tensile strength index of paper grades used in the experiments.

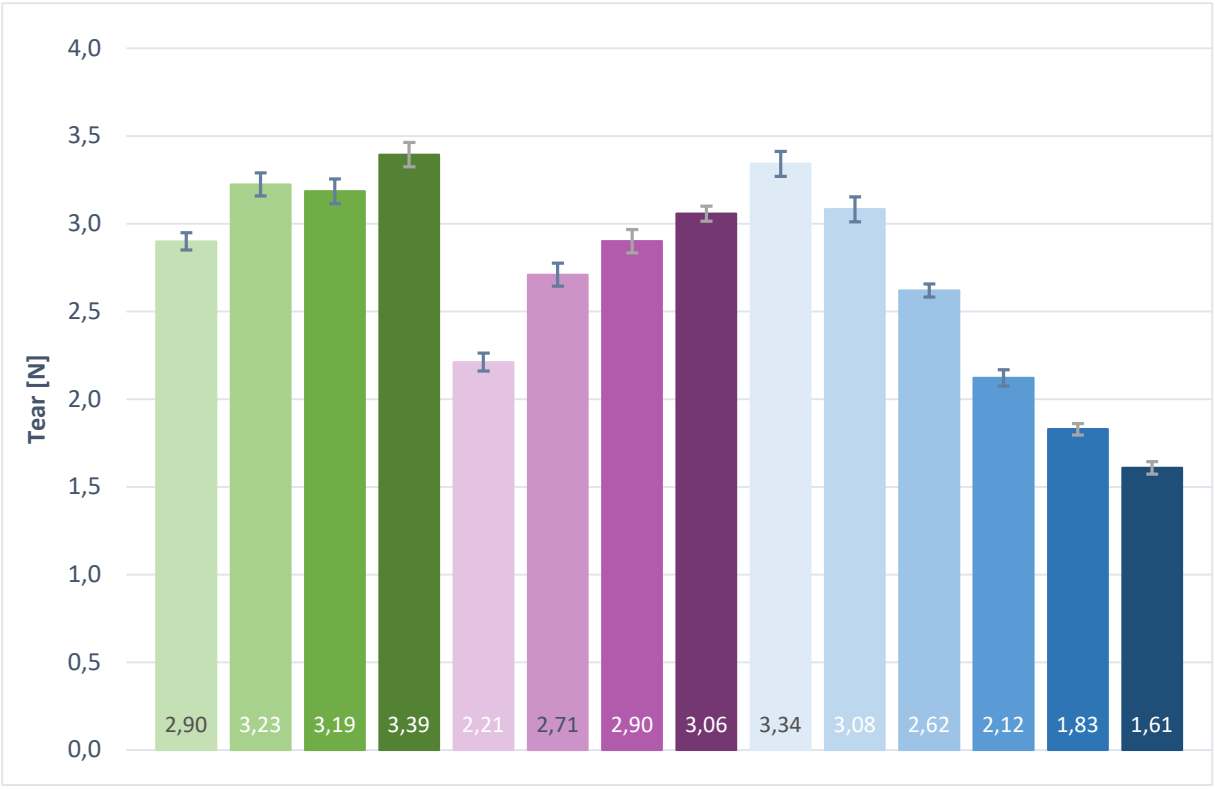

Figure 5-22: Tear of handsheets

5.6.1 Fracture toughness vs. Tear

In Figure 5-23 the mean values for fracture toughness are plotted over the tear values for the handsheets. Comparing the handsheets from the refining trials and filler trials it can be seen that the correlation between fracture toughness and tear is moderate. As seen before in Figure 5-22 and Figure 5-19 the values for fracture toughness and tear are higher for industrial refining than for lab refining and filler content. For lab refining both values are in the middle range.

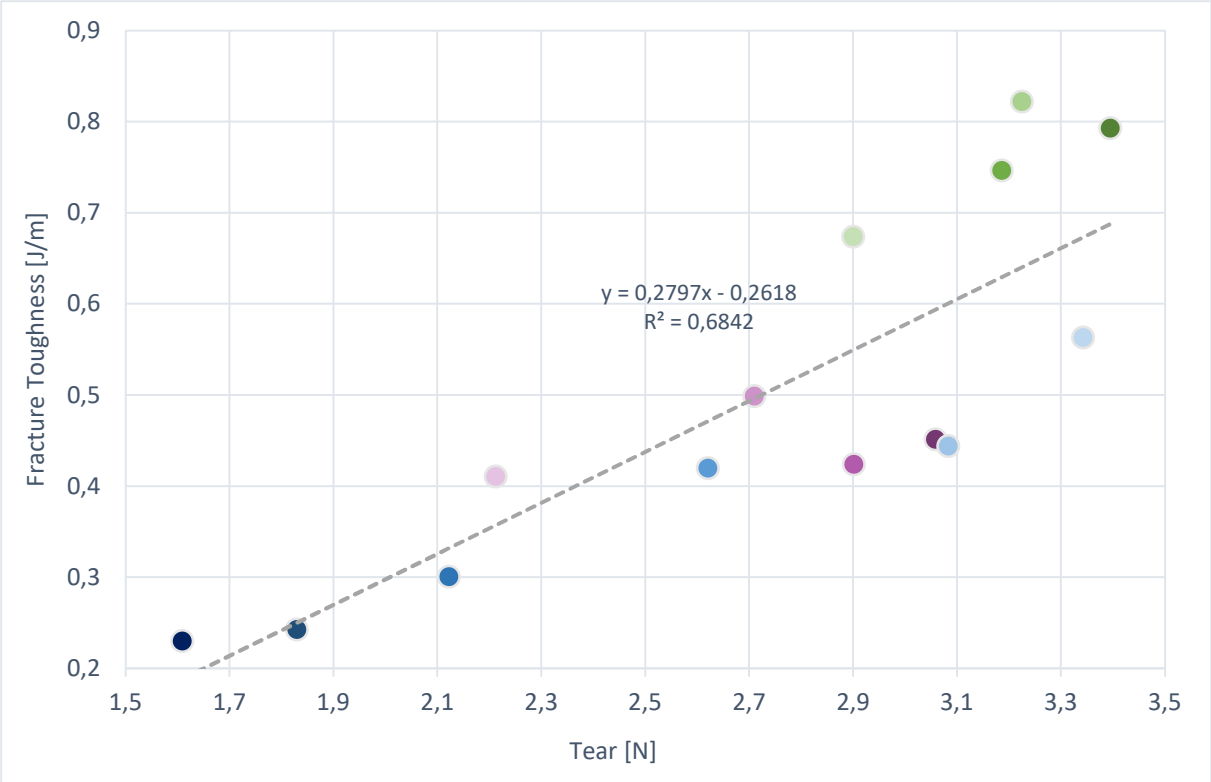

Figure 5-23: Fracture toughness vs. tear

5.6.2 Fracture toughness vs. Tensile strength

For fracture toughness and tensile strength, the reference paper grades were included (Figure 5-24). The office paper as well as the woodfree base paper are in the middle range of fracture toughness and tensile strength. However, the three different glassine and the kraftliner are in the higher range of fracture toughness and tensile strength. With these four values the correlation between fracture toughness and tensile strength in particularly good, but without them the correlation is moderate, even worse than the correlation between fracture toughness and tear. This can be seen in Figure 5-25.

Interesting to see is, that the values for filler content decreases almost on the trend line. The values for lab refining are in the middle range. For industrial refining, the tensile strength values are also in the same range. Only the fracture toughness values for industrial refining are higher than for lab refining.

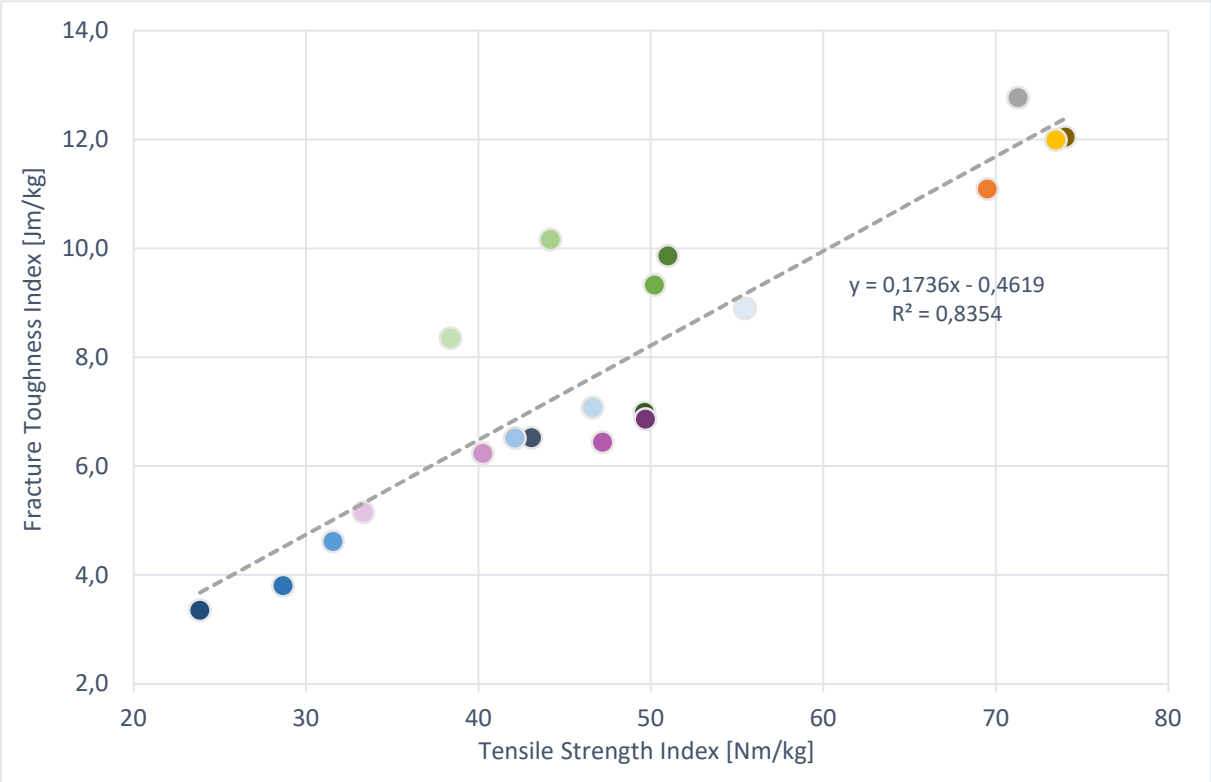

Figure 5-24: Fracture toughness vs. tensile strength

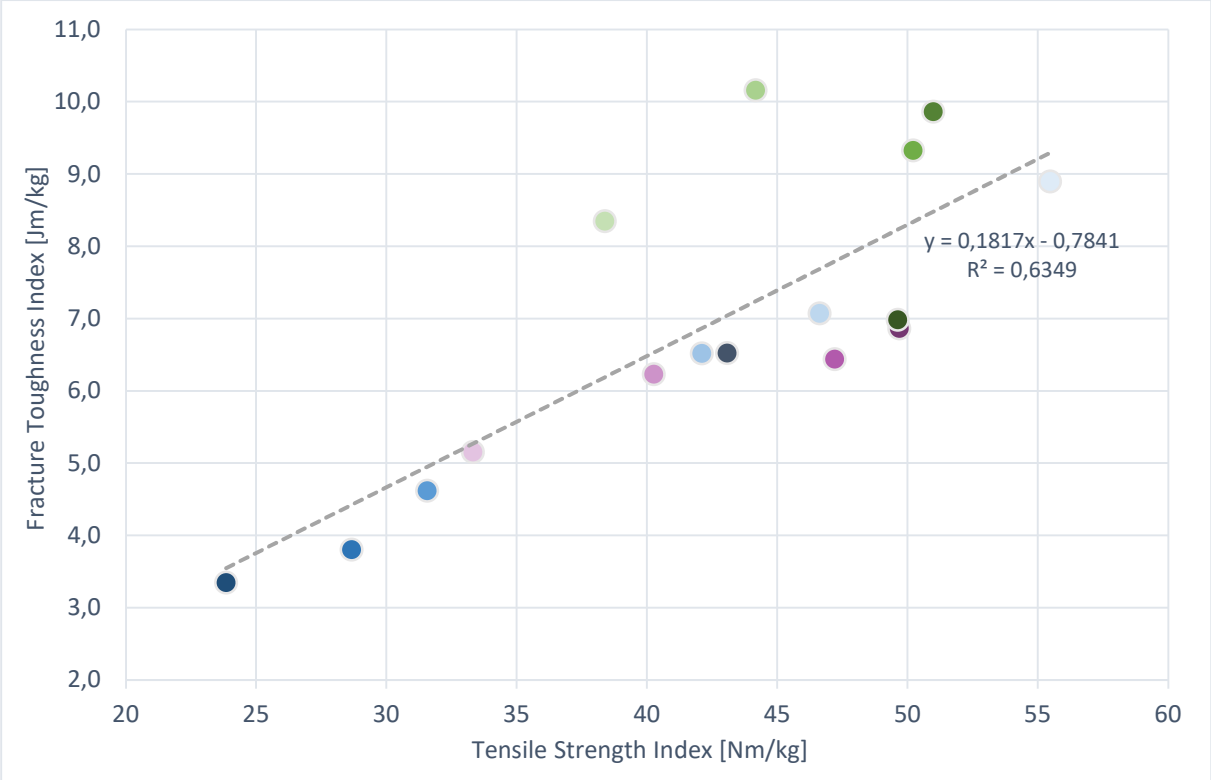

Figure 5-25: Fracture toughness vs. tensile strength without kraftliner and glassine

5.6.3 Notched tensile strength vs. Tensile strength

For notched tensile strength vs. tensile strength the three glassine as well as the kraftliner have higher values then the rest of the paper grades. However, notched tensile strength does not behave the same way as fracture toughness with tensile strength. The relationship between notched tensile strength and tensile strength is excellent with and without the three glassine and kraftliner.

The behavior seen in Figure 5-7, Figure 5-12, and Figure 5-17 can also be seen in Figure 5-26 and Figure 5-27. The values for notched tensile strength are approximately half of the values of tensile strength. This leads to the assumption mentioned before that the notch in the test strip does not affect basic mechanism that leads to the failure of the paper. It only lowers the level of force required to break the sheet.

In conclusion the fracture toughness is correlated to both, tear and tensile test. These correlations are good, but not excellent. However, notched tensile strength and normal tensile strength are extremely highly correlated. It seems that the information gained from the notched shear test is redundant to the tensile test.

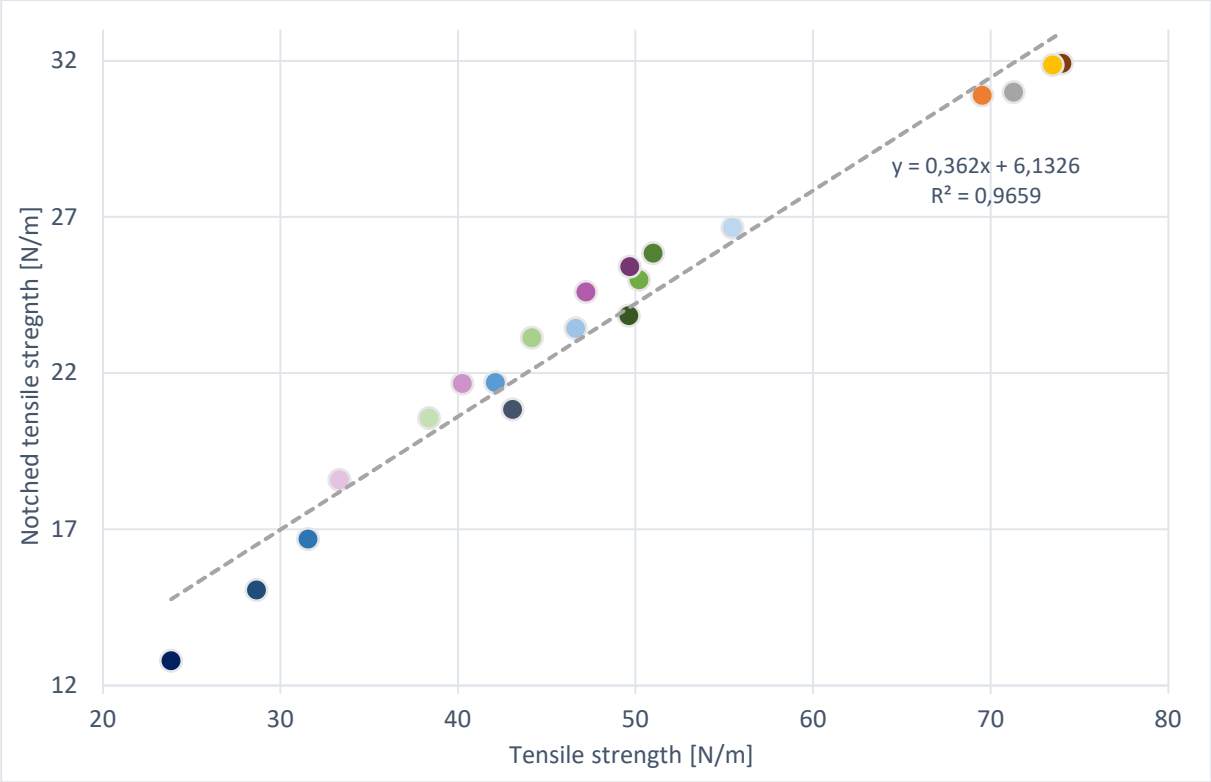

Figure 5-26: Notched tensile strength vs. tensile strength

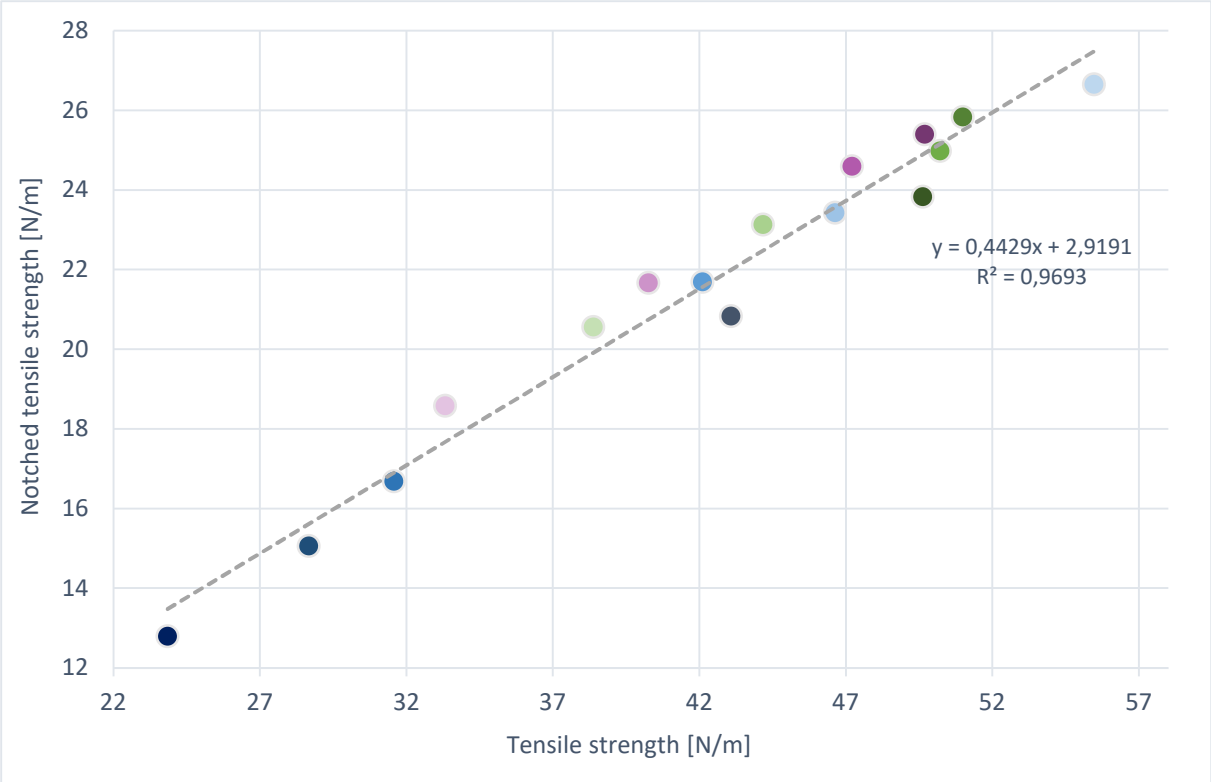

Figure 5-27: Notched tensile strength vs. tensile strength without kraftliner and glassine

5.7 Comparison of determination methods

Finally, the three different determination methods for fracture toughness were compared. The test pieces in the experiments were determined with ISO/TS 17958. From the measuring instrument the fracture toughness values according to SCAN-P 77:95 was received. Seth R. S. [2] determined fracture toughness with the simple equation using tensile strength and elongation (Equation (5-1)). The equations were extended with two different absolute terms *e* (1,08 and 0,6). Also, the absolute terms *f* and *g* are different from the two experiments performed in Seth R. S. work. This leads to four different methods to determine fracture toughness and they are plotted in Figure 5-28.

$$J_c = e\left(Tensile(N)^f \cdot Stretch(\%)^g\right) \qquad (5\text{-}1)$$

The two equations of Seth R. S. are giving very much higher values than the standardized methods. While the mean values from the determination method of Seth are between 60-180 Jm/kg, the mean values for the standardized methods are not higher than 14 Jm/kg. However, the standard ISO method correlates quite well with the two equations given by Seth R.S.

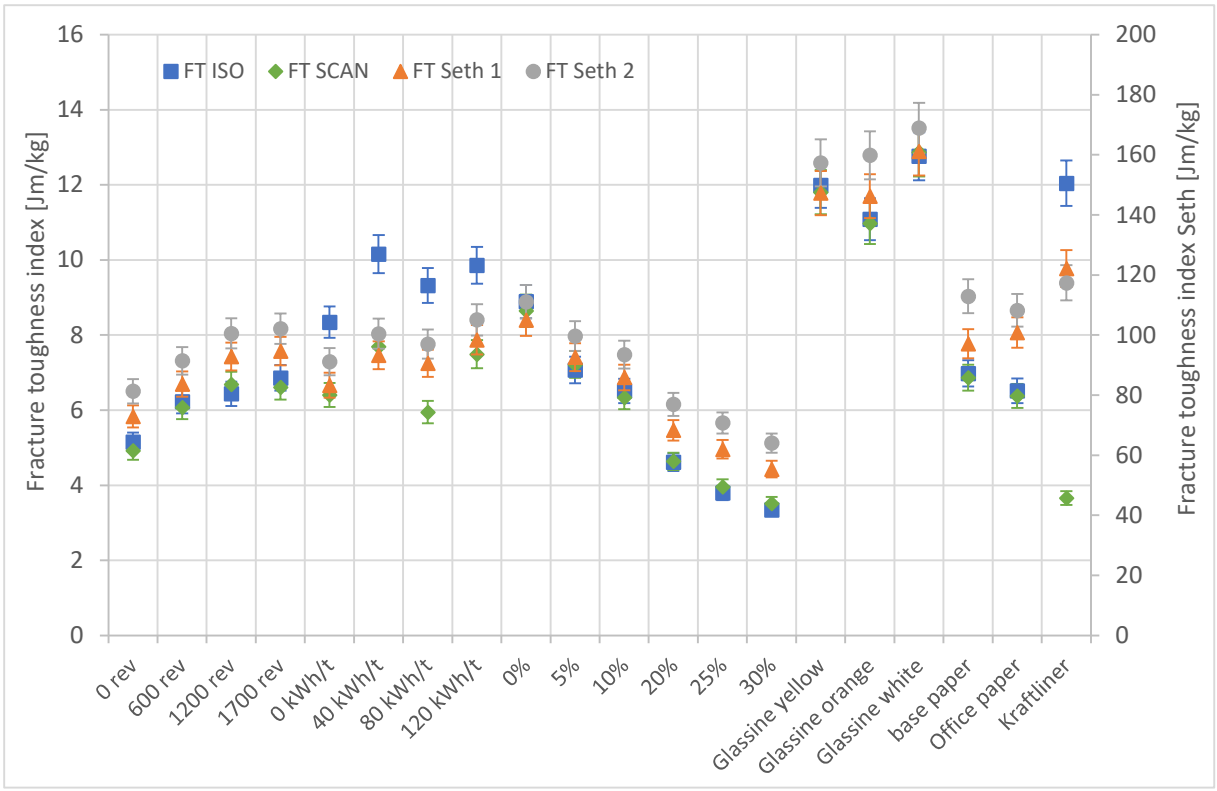

Figure 5-28: Comparison of determination methods for fracture toughness

In Figure 5-29, Figure 5-30, and Figure 5-31 the values for fracture toughness of the paper grades for the four different methods are plotted. The SCAN and both Seth methods are compared to the used ISO method.

The relationship between the ISO method and the SCAN method (Figure 5-29) is moderate. Fracture toughness determined with the ISO method for kraftliner is one of the highest values of all paper grades but determined with the SCAN method one of the lowest values. What also can be seen for the SCAN method is, that the fracture toughness values for the industrial refining is hardly increasing with increasing specific refining energy.

The two different Seth methods (Figure 5-30, and Figure 5-31) have almost the same relationship to the ISO method. The biggest difference is that the first method Seth 1 has lower fracture toughness values then the second method Seth 2. The handsheets behave almost identical. Another difference is the value for kraftliner. The value does not alternate like the other paper grades.

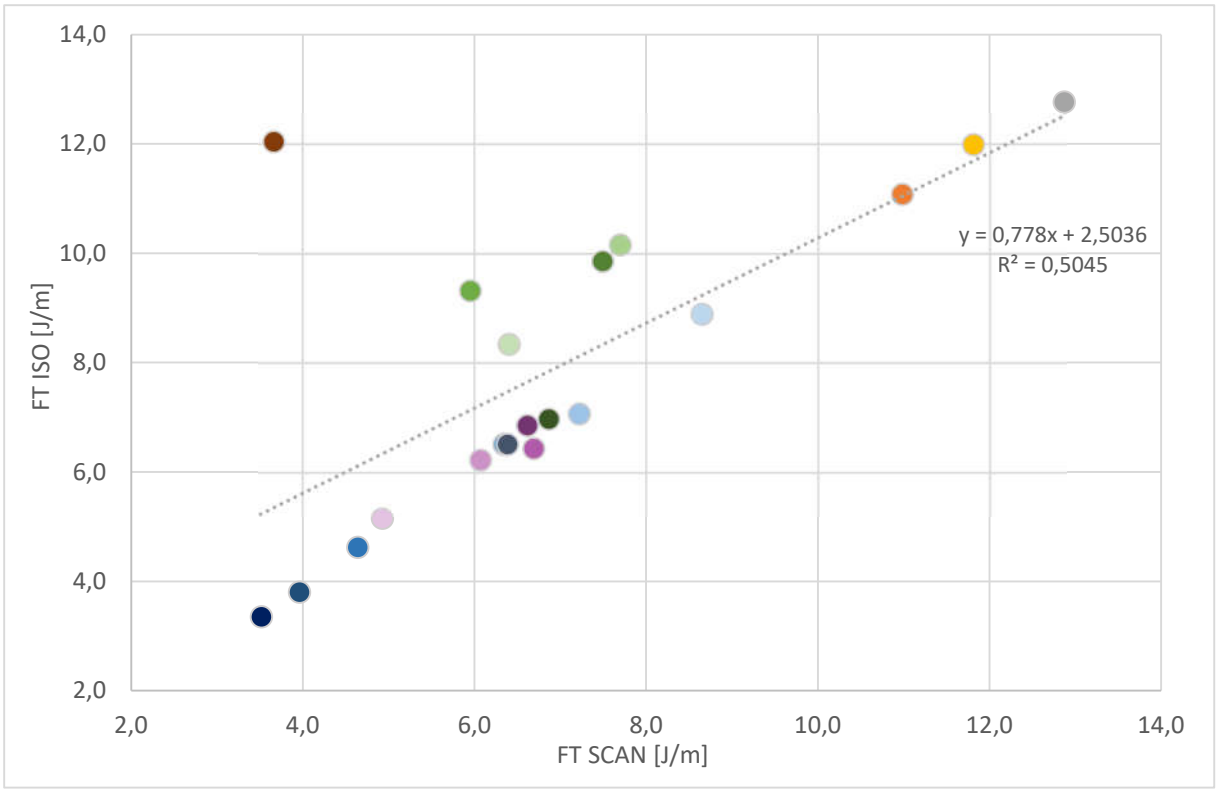

Figure 5-29: ISO-Method vs. SCAN-Method

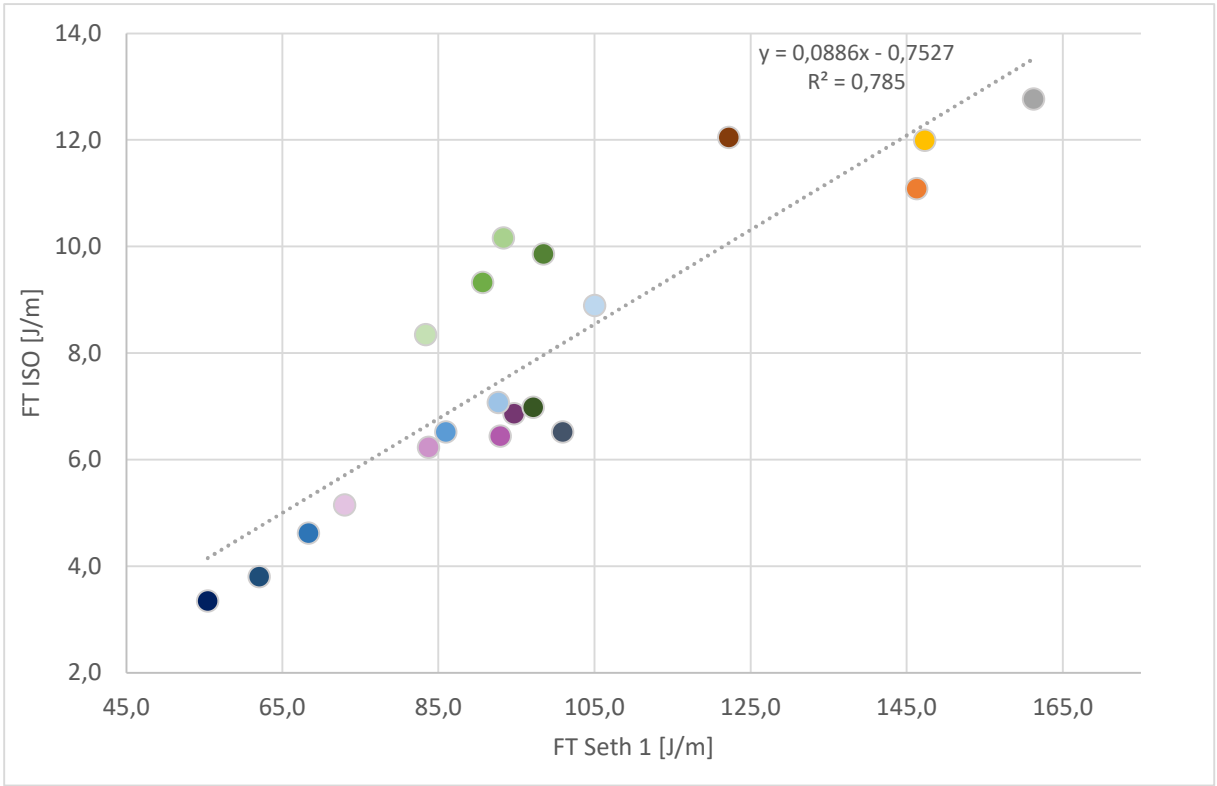

Figure 5-30: ISO-Method vs. Seth Method 1

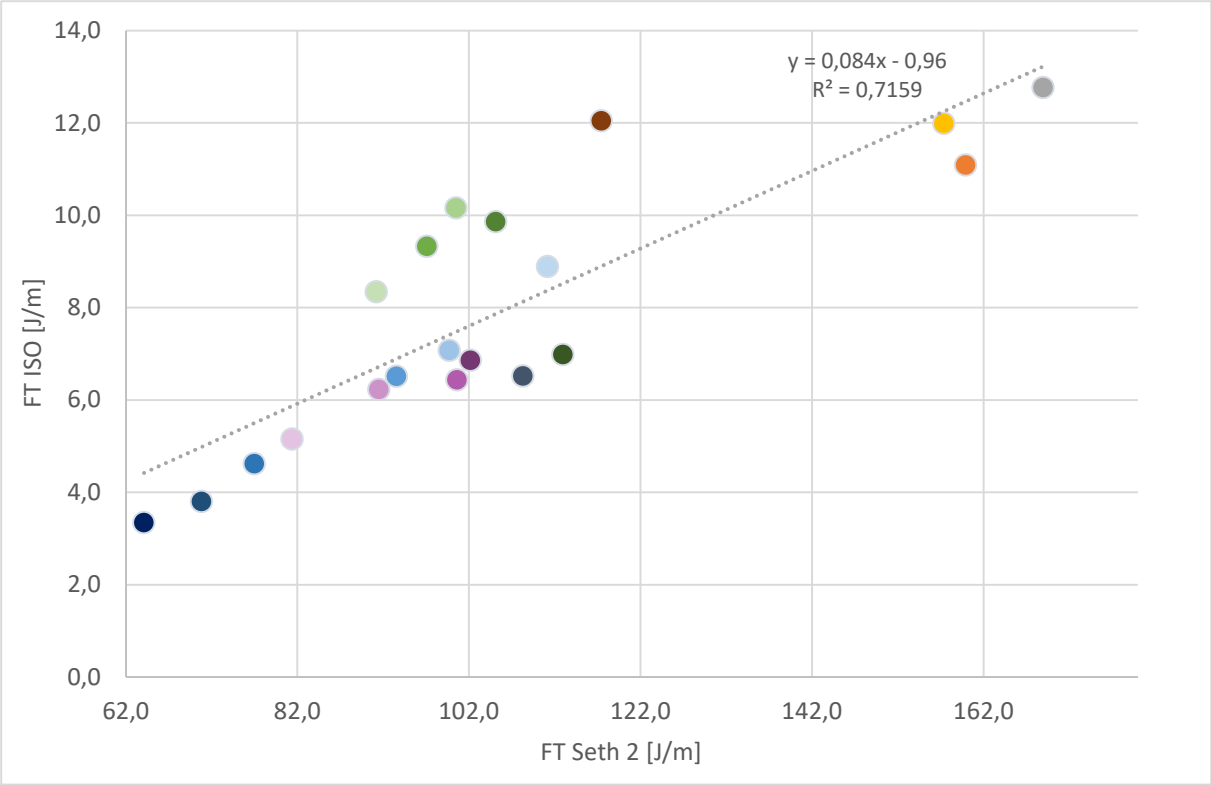

Figure 5-31: ISO-Method vs. Seth Method 2

6 Conclusion

It was surprising to find that the fracture toughness was consistently higher in CD than in MD. The results for the industrial reference papers have shown this difference. This behavior is different to any other strength property of paper. In fact, fracture toughness in MD is almost half of fracture toughness in CD.

The repeatability of the fracture toughness measurement was checked by evaluating the coefficient of variation of the results and calculating the 95 % confidence level for the mean. As mentioned before, the standard ISO method only suggests a minimum of 10 samples. This is clearly too little. For a confidence interval width of 5 % there must be over 80 samples tested. Compared to the tensile test, this is 7 times higher for the example of 5 % filler content. An explanation for this could be that the test pieces for the notched tensile test always rip apart at the center notch, while the test pieces for the tensile test rip apart at the weakest spot.

For industrial refining, tear and fracture toughness have a local maximum at 40 kWh/t which could lead to the assumption that these two parameters are highly correlated. For lab PFI refining the local maximum at 600 revolutions, which can be compared to 40 kWh/t, also can be seen. Overall, for the refining trials only a moderate correlation to tear- and tensile results

was found. For the experiment with filler that was different. Fracture toughness, tear and tensile strength decrease with increasing filler content. For fracture toughness as well as for tensile strength the values vary stronger than for the refining experiments. The correlation of fracture toughness to tear/tensile strength thus remains unconclusive: it is very good for different levels of filler, moderate for different levels of refining, and even inverse when looking at industrial samples measured in MD and CD.

Notched tensile strength and tensile strength show an almost linear relationship (R^2=0,96), where notched tensile strength is ½ of tensile strength. This behavior was not expected, it seems that the general failure mechanism is the same for notched and un-notched paper strips.

Comparing the different determination methods shows that the two different method Seth R. S. cannot be used to determine the absolute values of fracture toughness. They are clearly higher and cannot be compared to the standardized method. Even though the correlation between the standardized ISO method and the two Seth methods is good. For a simple and fast determination this method could be used.

Overall, it can be said that fracture toughness is in fact a different mechanical parameter than tear or tensile strength. But because of the much higher effort in terms of testing (normal plus notched tensile strength, larger confidence interval) compared to tensile tests it is not recommended to add the notched tensile test to the standard paper testing. For decreasing the web break fracture toughness could be a new point of view because of the center notch in the test piece, it considers more of the material behavior than the tensile test.

List of figures

List of tables

References

[1] R. S. Seth, “Plane stress fracture toughness and its measurements for paper,” *Prod. Papermak. Trans 10th Fund Res Symp Ed CF Bak.*, vol. 3, no. 25, pp. 1529–1552, 1993, doi: 10.15376/frc.1993.3.1529.

[2] R. S. Seth, “Optimizing reinforcement pulps by fracture toughness,” *Tappi J.*, vol. 79, no. 1, pp. 170–178, Jan. 1996.

[3] P. Wellmar, C. Fellers, and L. Delhage, “Fracture toughness of paper - development of a test method,” *Nord. Pulp Pap. Res. J.*, vol. 12, no. 3, pp. 189–195, Aug. 1997, doi: 10.3183/npprj-1997-12-03-p189-195.

[4] P. Wellmar, C. Fellers, F. Nilsson, and L. Delage, “Crack-Tip Characterization in Paper,” *J. Pulp Pap. Sci.*, vol. 23, no. 6, pp. J269–J275, Jun. 1997.

[5] S. Östlund and K. Niskanen, Eds., “Fracture properties,” in *Mechanics of paper products*, in De Gruyter graduate. Berlin ; Boston: De Gruyter, 2021, pp. 68–89.

[6] R. Mark, C. Jr. Habeger, J. Borch, and B. M. Lyne, *Handbook of Physical Testing of Paper*, Second Edition., vol. 1. New York, Basel: Marcel Dekker, Inc., 2002.
[7] T. Uesaka, “Web breaks in pressroom - a review,” *FSCN-Fibre-Based Mater. Technol.*, no. R-04-58, pp. 1–25, Oct. 2004.
[8] T. Uesaka, “Principal factors controlling web breaks in pressrooms - Quantitative evaluation,” *Appita Technol. Innov. Manuf. Environ.*, vol. 58, no. 6, pp. 425–432, Nov. 2005.
[9] G. Sear, R. Tyler, and C. Denzer, “Shives in newsprint: The role of shives in paper web breaks,” *Pulp and Paper Magazine Canada*, vol. 66. Jg., no. 7, pp. T351–T360, 1995.
[10] L. Larsson, “What happens in the press to cause web breaks?,” *Pulp and Paper Magazine Canada*, vol. 85, no. 9, pp. 55–59, 1984.
[11] P. Wellmar, Ø. W. Gregersen, and C. Fellers, “Prediction of crack growth initiation in paper structures using a J-integral criterion,” *Nord. Pulp Pap. Res. J.*, vol. 15, no. 1, pp. 4–11, Jan. 2000, doi: 10.3183/npprj-2000-15-01-p004-011.
[12] Scandinavian pulp, paper and board testing committee, “Fracture toughness - Constant rate of elongation method (1,7 mm/s).” Stockholm, Sweden, 1995.
[13] P. Mäkelä, H. Nordhagen, and Ø. W. Gregersen, “Validation of isotropic deformation theory of plasticity for fracture mechanics analysis of paper materials,” *Nord. Pulp Pap. Res. J.*, vol. 24, no. 4, pp. 388–394, Dec. 2009, doi: 10.3183/npprj-2009-24-04-p388-394.
[14] P. Mäkelä, “Engineering fracture mechanics analysis of paper materials,” *Nord. Pulp Pap. Res. J.*, vol. 27, no. 2, pp. 361–369, May 2012, doi: 10.3183/npprj-2012-27-02-p361-369.
[15] P. Mäkelä and C. Fellers, “An analytic procedure for determination of fracture toughness of paper materials,” *Nord. Pulp Pap. Res. J.*, vol. 27, no. 2, pp. 352–360, May 2012, doi: 10.3183/npprj-2012-27-02-p352-360.
[16] ISO copyright office, “Determination of fracture toughness - Constant rate of elongation method (1,7mm/s).” Switzerland, Apr. 15, 2013.
[17] L. Aihua, F. Mengyan, L. Yanruyu, and L. Zhidong, “Application of outlier mining in insider identification based on Boxplot method,” *Procedia Comput. Sci.*, vol. 91, pp. 245–251, Oct. 2022, doi: 10.1016/j.procs.2016.07.069.
[18] F. E. Grubbs, “Sample criteria for testing outlying observations,” *Inst. Math. Stat.*, vol. 21, no. 1, pp. 27–58, Mar. 1950.
[19] J. Bortz, *Statistik - Für Sozialwissenschaftler*, 4th ed. Springer-Verlag Berlin Heidelberg GmbH, 1993.
[20] Frank-PTI, “Lab Refiner-LR40,” presented at the Lab Refiner-LR40, Feb. 2018. Accessed: Jun. 24, 2023. [Online]. Available: www.frank-pti.com
[21] Frank-PTI, “Pulp Tester - Laboratory Refiner LR40,” vol. No. S21000. [Online]. Available: www.frank-pti.com
[22] P. K. Yasumura, M. L. O. D’almeida, and S. W. Park, “Multivariate statistical evaluation of physical properties of pulps refined in a PFI mill,” *O Pap.*, vol. 23, no. 3, pp. 59–65, Mar. 2012.
[23] A. Chakraborty, M. M. Sain, M. T. Kortschot, and S. B. Ghosh, “Modeling energy consumption for the generation of microfibres from bleached kraft pulp fibres in a PFI mill,” *BioResources*, vol. 2, no. 2, pp. 210–222, Apr. 2007, doi: 10.15376/biores.210-222.